2015

The Unfolded Protein Response And Calcium Dysregulation In Autosomal Dominant Retinitis Pigmentosa Animal Models.

Vishal Madhukar Shinde
University of Alabama at Birmingham

THE UNFOLDED PROTEIN RESPONSE AND CALCIUM DYSREGULATION IN AUTOSOMAL DOMINANT RETINITIS PIGMENTOSA ANIMAL MODELS.

by

VISHAL SHINDE

COMMITTEE MEMBERS

MARINA S. GORBATYUK
THOMAS NORTON, COMMITTEE CHAIR
ALECIA GROSS
MOHAMMAD ATHAR
SHU-ZHEN WANG

A DISSERTATION

Submitted to the graduate faculty of the University of Alabama at Birmingham,
in partial fulfillment of the requirements for the degree of
Doctor of Philosophy

BIRMINGHAM, ALABAMA
2015

THE UNFOLDED PROTEIN RESPONSE AND CALCIUM DYSREGULATION IN AUTOSOMAL DOMINANT RETINITIS PIGMENTOSA ANIMAL MODELS.

VISHAL SHINDE

SCHOOL OF OPTOMETRY – VISION SCIENCE

ABSTRACT

The photoreceptor cell death in autosomal dominant retinitis pigmentosa (ADRP) is associated with molecular changes that occur due to mutations in a specific gene. S334ter RHO and P23H RHO are two ADRP rat models expressing mutant rhodopsin. The unfolded protein response (UPR) is a cellular stress response involved in the pathophysiology of several retinal disorders including P23H RHO rats. Considering our previous findings, we started our investigation by examining the status of UPR in S334ter RHO rats. As UPR tightly regulates several signaling pathways, we further studied whether UPR activation in S334ter and P23H RHO retina is accompanied by the changes in other cellular pathways such as autophagy, inflammation, calcium signaling and mitochondria dependent and independent apoptosis.

By gene and protein expression profiling in S334ter RHO retina, we demonstrated the activation of UPR at postnatal day (P) 15. We have also noticed that activated UPR in S334ter RHO is accompanied with alterations in the expression of BCL2 family genes, oxidative stress associated genes and caspases.

In P23H RHO retina we examined the changes in autophagy, mTOR/AKT and BCL2 family proteins. Our data demonstrated that P23H RHO retina experiences significant decline in the expression of autophagy associated proteins whereas marked overproduction

in mTOR, which is a negative regulator of autophagy. We have observed a delay in retinal degeneration in P23H rats upon the modulation of mTOR with rapamycin.

The UPR and calcium dysregulation are tightly linked mechanisms, therefore we validated whether both the ADRP model retinas experience a dysregulation in calcium homeostasis. Through retinal calcium imaging we noticed an elevated cytoplasmic Ca^{2+} in both ADRP model retinas together with calpain activation. After examining the activity of several calcium sensing proteins and calcium channels, we validated that UPR induced ER Ca^{2+} depletion plays a significant role in the progression of retinal degeneration in S334ter and P23H RHO retinas. In a series of experiments in both ADRP model retinas, we have also found disrupted mitochondrial permeability, which can trigger apoptotic events.

Our study has revealed several novel potential therapeutic targets from UPR, apoptotic and calcium regulatory pathways. Modulation of these molecular targets could potentially reduce the rate of retinal degeneration.

Keywords – Retinitis pigmentosa, unfolded protein response, and calcium induced apoptosis.

DEDICATION

Dedicated to my parents Usha and Madhukar Shinde who inspired and guided me throughout my life.

ACKNOWLEDGEMENTS

I would like to thank Dr. Marina Gorbatyuk from the bottom of my heart for being a terrific mentor to me for past the five years. During my PhD training, she always inspired me to conduct meaningful scientific research and supported me throughout my failures. I would specially thank her for believing in me and giving me a great degree of freedom to achieve my research goals. I greatly appreciate her patient mentorship which not only trained me as a scientific thinker but also helped me a lot to be a goal oriented researcher. I feel fortunate to have had such a wonderful and motivating mentor.

I would like to thank my amazing committee members Dr. Athar, Dr. Gross, Dr. Norton and Dr. Wang. My committee members have always been a great support system for me, guiding me towards right scientific direction. My committee members have not only contributed significantly to my experimental designs but also helped me improve my presentation skills. I am thankful for their key suggestions which led to interesting research findings.

I greatly appreciate the mentoring of Dr. Vincenzo Guarcello which strengthened my research at each stage of my graduate study. My sincere thanks to vision science program director, coordinator and faculty members for providing very pleasant and exciting environment in the graduate program. Also I am greatly thankful to Dr. Vinayak Khattar for helping me to improve my scientific writing skills.

I would also like to thank all the members of Dr. Gorbatyuk's lab for assisting me in my experiments and for always being there and making my stay pleasant in the lab. I sincerely thank all my friends in Birmingham, Fort Worth and Ruston for always being with me and for giving me the everlasting beautiful memories.

I always feel fortunate for having a lovely supporting family. The unconditional love, hard work and sacrifices of my parents always inspired me to achieve my goals. I will always be grateful to my elder brothers Vivek (dada) and Nayan (bhaiyya) for supporting and motivating me throughout my life. Words cannot express how thankful I am to my family for being there for me which sustained me thus far.

TABLE OF CONTENTS

Page

LIST OF FIGURES

ER STRESS IN RETINAL DEGENERATION IN S334TER Rho RATS

MODULATION OF CELLULAR SIGNALING PATHWAYS IN P23H RHODOPSIN PHOTORECEPTORS

LIST OF ABBREVIATIONS

1. UPR- Unfolded protein response
2. ADRP- Autosomal Dominant Retinitis Pigmentosa
3. RP- Retinitis Pigmentosa
4. RHO- Rhodopsin
5. RPE- Retinal Pigment Epithelium
6. ER – Endoplasmic Reticulum
7. ERG- Electroretinography
8. OCT- Optical Coherence Tomography
9. OS- Outer Segment
10. IS- Inner Segment
11. ONL- Outer Nuclear Layer
12. WT- Wild Type
13. SD- Sprague Dawley
14. H&E- Haemotoxylin and Eosin
15. Tn- Tunicamycin
16. Tg-Thapsigargin

CHAPTER 1

GENERAL INTRODUCTION

Retinitis Pigmentosa

Retinitis Pigmentosa (RP) is a heterogeneous group of inherited retinal dystrophies characterized by progressive photoreceptor cell death with a prevalence of 1 in 4000 individuals affected in a general population [1]. The function of photoreceptor cells is to capture and process light (photons) which ultimately translates into a visual impulse. In most cases symptoms of RP usually manifest during childhood and/or young adults, with progressive deterioration of photoreceptors in adult life. Degeneration of the retina begins in the midperiphery of the fundus and then gradually advances towards the macula and fovea. There are two main types of photoreceptors, rods and cones. While cones are primarily required for daytime vision, rods primarily function during less intense light. Typical RP is described as rod-cone dystrophy, affecting rod photoreceptors at the initial phase in which night blindness is the first symptom, followed by peripheral vision loss. On the other hand, cone-rod dystrophy is another form of RP affecting central vision first [1-3]

Symptoms

In an early stage of RP, night blindness is the main symptom; nevertheless, patient still has a relatively normal life. At this stage it is difficult to establish the diagnosis since fundus examination and optic disc seems to be normal. Obvious night blindness with difficulties

to drive and walk during night are prominent symptoms of mid stage RP. Clinical picture is clear at this stage as fundus examination reveals bone spicule shaped pigment deposits in the retina along with changes in the optic disc and narrowing of retinal blood vessels. Patient can no longer move autonomously because of complete loss of peripheral vision (tunnel vision) at the later stage of RP. Fundus examination at this stage shows widespread pigment deposits all over the retina. Reading is difficult and magnifying glasses are necessary. Reading becomes impossible once central vision is affected [1,2].

Genetics

RP is a genetic disorder inherited in autosomal dominant, autosomal recessive or X linked manner [4]. Majority of the genes associated with RP are expressed either in photoreceptors or retinal pigment epithelium (RPE). These known genes can be grouped into several functional classes: 1) RHO, PDE6alpha, PDE6beta, CNGA1 genes involved in the visual cascade 2) RPE65, ABCA4, RBP4 genes participating in the visual cycle 3) RDS and ROM1 genes encoding cell-surface proteins from tetraspanins family 4) NRL and CRX photoreceptor transcription factors 5) and genes involved in mitochondrial metabolism [3].

Diagnosis

Preliminary diagnosis of RP is based on the presence of night blindness, peripheral visual field defects, and lesions in the fundus and progressive elevation in these signs over the time. Full field Electroretinography (ERG) is a key diagnostic test, especially when patients are asymptomatic. A definitive clinical diagnosis requires a diagnostic test one or two years after first signs of symptoms. Due to huge heterogeneity of the disease, usually, a systemic

molecular diagnosis is not routinely performed, however, few laboratories perform molecular diagnostic tests and search for mutations in the most frequently involved genes.

Treatment

Presently there is no recognized treatment for RP, except for some very limited success that has been observed with vitamin A supplements. Due to lack of definitive diagnostic procedures and effective treatment, RP disease progression is an area of active biomedical research. Currently there are several therapeutic modalities under intense investigation, which primarily utilize data gathered from the research on different animal models of the disease. The potential treatment options include gene therapy, neurotropic factors, antiapoptotic agents and dietary supplements. Significant technological advances have been achieved in the area of stem cell therapy, retinal transplants and retinal implants which have a potential to prevent the progression of RP.

Rhodopsin

There are multiple genetic mutations which can cause RP phenotype. The autosomal dominant form of RP (ADRP) is associated with mutations in at least 14 different genes. Mutations in the rhodopsin gene (RHO, OMIM 180380, accession ID U49742) are the most prevalent mutations identified to date resulting in 30% to 40% of all ADRP cases [5]. Rhodopsin (RHO) is a G protein coupled receptor protein that functions as a light sensor in photoreceptor. Over 120 mutations in RHO have been detected which can cause RP phenotype [6].

Rhodopsin is a transmembrane photopigment consisting of protein moiety opsin and reversibly bound chromophore retinal located in the stack of disc membrane present in the

outer segment of rod cells. Morphologically, rod cells have two distinct regions – an outer and inner segment. The outer segment of rods, which is responsible for photo-transduction, houses the rhodopsin molecule. The inner segment of the rods is connected to the outer segment through ciliary processes that contain the metabolic machinery necessary for rod cell homeostasis [7].

Rhodopsin is synthesized in ER and transported to the outer segment through Golgi [7]. It is an integral membrane protein consisting of the extracellular surface domain, the membrane embedded domain and intracellular surface domain [8]. The extracellular domain is important for proper folding of the receptor which allows cellular processing and chromophore binding [9]. The intracellular domain is responsible for rhodopsin sorting and targeting. The membrane embedded domain is made up of seven transmembrane alpha helical segments which contain the binding site for the chromophore, retinal [8].

When light hits a rhodopsin protein from rod cell, a photon get absorbed which results in isomerization of 11-cis retinal to all-trans retinal. This triggers change in the rhodopsin conformation which activates transducing, resulting in closure of ion channels from outer segment. This in turn hyperpolarizes the plasma membrane and initiates a signaling of second order neurons. Activation of a single rhodopsin molecule by a single photon is capable of preventing the entry of 10^7 cations into the rod cell. During this phototransduction event 11-cis retinal isomerizes to all-trans retinal and dissociates from opsin moiety. The all-trans retinal is converted to cis-retinal through a series of enzymatic reactions, which binds to opsin and rhodopsin is regenerated.

Several point mutations in an extracellular or cytoplasmic domains of rhodopsin can cause RP phenotype and are linked to autosomal dominant retinitis pigmentosa (ADRP).

Classification of rhodopsin mutations has been done based on their *in vitro* properties when expressed in cultured epithelial cells [10] [11]. The mutant rhodopsin is classified as class 1 and class 2 mutants. Class 1 mutants resemble wild-type rhodopsin in expression levels, folding properties and form a functional photopigment whereas class 2 mutants exhibits low expression level, less stability and varied functional characteristics, and inefficient transport to the plasma membrane. Class 2 mutants also tend to misfold and are retained in the ER.

P23H and S334ter RHO Rat Models

P23H rhodopsin is a classic example of class 2 mutant which is a leading cause of RP in the North America and the first ADRP mutation to be identified [12]. The P23H RHO exhibits characteristic of toxic gain of function and dominant negative mutation [13]. In P23H RHO, proline at position 23 of N-terminal is replaced by histidine. In wild type rhodopsin, Pro-23 interacts with tyrosine at position 102, an interaction that is necessary to maintain a proper orientation of rhodopsin structure. Several studies suggest that the pathogenicity of P23H RHO is associated with visual transduction because P23H RHO traffics normally to the outer segment of photoreceptors [14] [15]. Few other studies suggest that misfolding of P23H RHO is a major cause of retinal cell death since *in vitro* expression of P23H RHO affects normal protein degradation, which results in the formation of aggresomes in cells [16] [17]. Furthermore, some investigations have also shown that misfolded P23H RHO can disrupt outer segment disc formation [18] [19]. In cultured cells, P23H RHO is retained in ER which induces the activation of the unfolded protein response (UPR) and apoptosis [18,20,21]. P23H RHO also affects the trafficking of wild type rhodopsin which implies a classic dominant negative effect. Several

conflicting interpretations of P23H RHO localization in retina have been reported claiming the accumulation of P23H RHO at photoreceptor nerve terminal and photoreceptor outer segment [14] [22].

The carboxyl terminal domain of rhodopsin is necessary for its transport to rod outer segment containing post Golgi trafficking signal of rhodopsin and phosphorylation sites for rhodopsin kinase. The C- terminal point mutations in rhodopsin include P347L, P347R, P347S and V345M. S334ter and Q334ter mutations in rhodopsin result in a C-terminal truncation. Similarly, intron splice mutation (N88) is thought to remove the entire C-terminal of rhodopsin [11,23]. S334ter RHO mutation results in the expression of a rhodopsin protein that lacks the 15 C-terminal amino acids that are involved in rhodopsin trafficking to the photoreceptor outer segments and in the deactivation of the rhodopsin protein after light absorption. A previous study conducted using this rat model expressing S334ter RHO demonstrated that the nature of the rhodopsin sorting defect, but not the constitutive activation of the phototransduction cascade, contributes significantly to apoptosis [24].

The transgenic rats, expressing mutant P23H RHO or S334ter RHO shows gradual retinal cell death and decline in the retinal function which can be easily tracked by electroretinography (ERG). This fact makes them particularly useful models to investigate the molecular mechanism involved in the pathogenesis and progression of ADRP. Several complex molecular pathways regulate the retinal cell death during the progression of RP. It seems clear that the multiple cellular pathways such as ER stress, oxidative stress, inflammation, autophagy, and mitochondria dependent and independent apoptosis drive the retinal cell death in RP. However, the relationship between the genetic defects which

cause RP and the corresponding activated cellular mechanisms have not been investigated. Here we have studied the involvement of several molecular pathways in photoreceptor cell death of S334ter and P23H RHO retinas.

Aberrant protein conformation is a leading cause of RP progression, and endoplasmic reticulum (ER) monitors the protein conformation, which makes ER a very interesting organelle to investigate molecular mechanisms in RP. It has been shown that ER retention of P23H RHO activates unfolded protein response (UPR) [18,20,21] and the modulation of UPR can restore the visual function in P23H RHO rat retinas [25]. Interestingly, several studies have also demonstrated the involvement of UPR in retinal degeneration [26,27]. In Chapter 2, we have investigated whether UPR-associated signaling is activated during S334ter RHO photoreceptor degeneration and assessed the involvement of additional cellular pathways such as mitochondria induces apoptosis, oxidative stress and ERAD associated pathway.

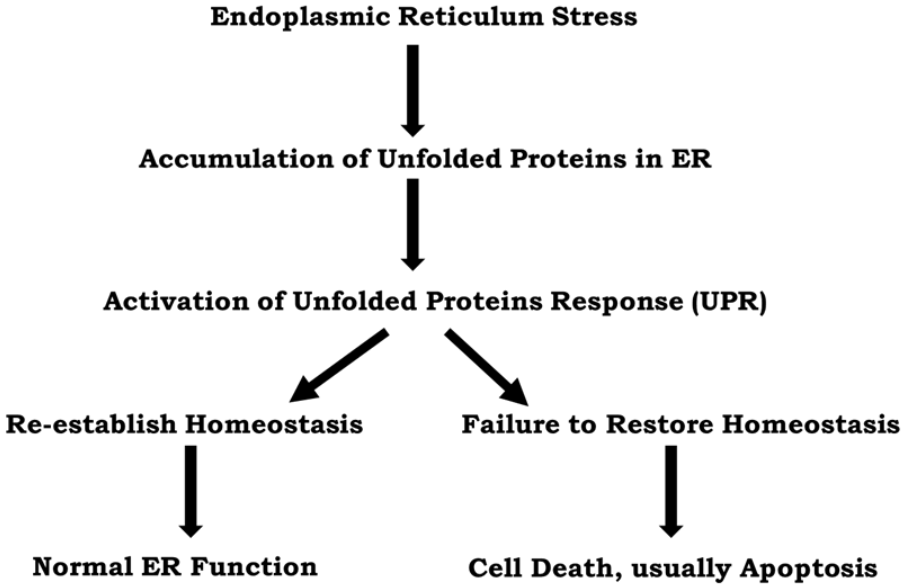

UPR Activation Schematic.

The primary purpose of UPR activation is to reestablish cellular homeostasis and resolve the cellular stress. A failure to restore this homeostasis can redirect UPR towards cellular apoptosis. UPR functions to resolve cellular stress through the activation of pro–survival autophagy pathway. In the 3rd chapter, we have investigated whether UPR activation in P23H RHO retinas is accompanied by changes in autophagy and mTOR/AKT signaling. We have also investigated if the alteration of mTOR/AKT could prevent the rate of retinal degeneration in P23H RHO rats. While investigating the role of autophagy in both ADRP rat models we found that autophagy signaling has been altered in P23H RHO retinas but not in S334ter RHO.

It is known that the ER serves as the primary store of the calcium in the cell. The secondary messenger Ca^{2+} is known to participate in a wide variety of physiological functions, including signal transduction, muscle contraction, protein and hormone secretion. The normal ER functions to regulate intracellular Ca^{2+}, protein synthesis, gene expression, secretion, metabolism, and apoptosis [28]. The ER disturbance results in extra release of ER Ca^{2+} into the cytosol, after which free Ca^{2+} can either be transported to the mitochondria or directly activate cytotoxic cellular pathways [29]. Previously, in both the ADRP rat models, we have investigated the activation of UPR, which is a sign of the malfunctioning of ER. In Chapter 4, we have deciphered the role of ER Ca^{2+} depletion during the progression of RP in S334ter and P23H RHO retinas. Here we have successfully demonstrated that activated UPR significantly contributes to cytoplasmic Ca^{2+} overload which can drive photoreceptor cell death in ADRP retinas.

REFERENCES

1. Hamel, C., Retinitis pigmentosa. Orphanet J Rare Dis, 2006. **1**: p. 40.
2. Musarella, M.A. and I.M. Macdonald, Current concepts in the treatment of retinitis pigmentosa. J Ophthalmol, 2011. **2011**: p. 753547.
3. Phelan, J.K. and D. Bok, A brief review of retinitis pigmentosa and the identified retinitis pigmentosa genes. Mol Vis, 2000. **6**: p. 116-24.
4. Daiger, S.P., S.J. Bowne, and L.S. Sullivan, Perspective on genes and mutations causing retinitis pigmentosa. Arch Ophthalmol, 2007. **125**(2): p. 151-8.
5. Hernan, I., et al., Cellular expression and siRNA-mediated interference of rhodopsin cis-acting splicing mutants associated with autosomal dominant retinitis pigmentosa. Invest Ophthalmol Vis Sci, 2011. **52**(6): p. 3723-9.
6. Briscoe, A.D., C. Gaur, and S. Kumar, The spectrum of human rhodopsin disease mutations through the lens of interspecific variation. Gene, 2004. **332**: p. 107-18.
7. Hargrave, P.A., Rhodopsin structure, function, and topography the Friedenwald lecture. Invest Ophthalmol Vis Sci, 2001. **42**(1): p. 3-9.
8. Menon, S.T., M. Han, and T.P. Sakmar, Rhodopsin: structural basis of molecular physiology. Physiol Rev, 2001. **81**(4): p. 1659-88.
9. Doi, T., R.S. Molday, and H.G. Khorana, Role of the intradiscal domain in rhodopsin assembly and function. Proc Natl Acad Sci U S A, 1990. **87**(13): p. 4991-5.
10. Sung, C.H., C.M. Davenport, and J. Nathans, Rhodopsin mutations responsible for autosomal dominant retinitis pigmentosa. Clustering of functional classes along the polypeptide chain. J Biol Chem, 1993. **268**(35): p. 26645-9.
11. Sung, C.H., et al., Functional heterogeneity of mutant rhodopsins responsible for autosomal dominant retinitis pigmentosa. Proc Natl Acad Sci U S A, 1991. **88**(19): p. 8840-4.
12. Dryja, T.P., et al., Mutation spectrum of the rhodopsin gene among patients with autosomal dominant retinitis pigmentosa. Proc Natl Acad Sci U S A, 1991. **88**(20): p. 9370-4.
13. Mendes, H.F., et al., Mechanisms of cell death in rhodopsin retinitis pigmentosa: implications for therapy. Trends Mol Med, 2005. **11**(4): p. 177-85.

14. Olsson, J.E., et al., Transgenic mice with a rhodopsin mutation (Pro23His): a mouse model of autosomal dominant retinitis pigmentosa. Neuron, 1992. **9**(5): p. 815-30.

15. Roof, D.J., M. Adamian, and A. Hayes, Rhodopsin accumulation at abnormal sites in retinas of mice with a human P23H rhodopsin transgene. Invest Ophthalmol Vis Sci, 1994. **35**(12): p. 4049-62.

16. Illing, M.E., et al., A rhodopsin mutant linked to autosomal dominant retinitis pigmentosa is prone to aggregate and interacts with the ubiquitin proteasome system. J Biol Chem, 2002. **277**(37): p. 34150-60.

17. Saliba, R.S., et al., The cellular fate of mutant rhodopsin: quality control, degradation and aggresome formation. J Cell Sci, 2002. **115**(Pt 14): p. 2907-18.

18. Frederick, J.M., et al., Mutant rhodopsin transgene expression on a null background. Invest Ophthalmol Vis Sci, 2001. **42**(3): p. 826-33.

19. Liu, X., et al., Defective phototransductive disk membrane morphogenesis in transgenic mice expressing opsin with a mutated N-terminal domain. J Cell Sci, 1997. **110** (Pt 20): p. 2589-97.

20. Leonard, K.C., et al., XIAP protection of photoreceptors in animal models of retinitis pigmentosa. PLoS One, 2007. **2**(3): p. e314.

21. Lin, J.H., et al., IRE1 signaling affects cell fate during the unfolded protein response. Science, 2007. **318**(5852): p. 944-9.

22. Goto, Y., et al., Functional abnormalities in transgenic mice expressing a mutant rhodopsin gene. Invest Ophthalmol Vis Sci, 1995. **36**(1): p. 62-71.

23. Jacobson, S.G., et al., Phenotypes of stop codon and splice site rhodopsin mutations causing retinitis pigmentosa. Invest Ophthalmol Vis Sci, 1994. **35**(5): p. 2521-34.

24. Green, E.S., et al., Characterization of rhodopsin mis-sorting and constitutive activation in a transgenic rat model of retinitis pigmentosa. Invest Ophthalmol Vis Sci, 2000. **41**(6): p. 1546-53.

25. Gorbatyuk, M.S., et al., Restoration of visual function in P23H rhodopsin transgenic rats by gene delivery of BiP/Grp78. Proc Natl Acad Sci U S A, 2010. **107**(13): p. 5961-6.

26. Wu, L.M., et al., [Endoplasmic reticulum stress proteins are activated in rd retinal degeneration]. Zhonghua Yan Ke Za Zhi, 2008. **44**(9): p. 807-12.

27. Ryoo, H.D., et al., Unfolded protein response in a Drosophila model for retinal degeneration. Embo j, 2007. **26**(1): p. 242-52.

28. Bravo, R., et al., Endoplasmic reticulum and the unfolded protein response: dynamics and metabolic integration. Int Rev Cell Mol Biol, 2013. **301**: p. 215-90.

29. Kaufman, R.J. and J.D. Malhotra, Calcium trafficking integrates endoplasmic reticulum function with mitochondrial bioenergetics. Biochim Biophys Acta, 2014. **1843**(10): p. 2233-9.

CHAPTER 2

ER STRESS IN RETINAL DEGENERATION IN S334TER RHO RATS

by

VISHAL SHINDE, OLGA SIZOVA, JONATHAN H. LIN, MATHEW M. LAVAIL and MARINA S. GORBATYUK.

Plos One

Abstract

The S334ter rhodopsin (RHO) rat (line 4) bears the rhodopsin gene with an early termination codon at residue 334 that is a model for several such mutations found in human patients with autosomal dominant retinitis pigmentosa (ADRP). The Unfolded Protein Response (UPR) is implicated in the pathophysiology of several retinal disorders including ADRP in P23H Rho rats. The aim of this study was to determine if UPR is activated in ADRP animal models and to investigate how the activation of UPR molecules leads to the final demise of S334ter RHO photoreceptors. RT-PCR was performed to evaluate the gene expression profiles at postnatal day (P) 10, P12, P15, and P21 in S334ter Rho photoreceptors. We demonstrated that during P12–P15 period, ER stress-related genes were strongly upregulated in transgenic retinas, resulting in the activation of the UPR which was confirmed using western blot analysis. The activation of UPR was associated with the elevated expression of JNK, Bik, Bim, Bid, Noxa, and Puma genes and increased calpain activity accompanied with cleavage of caspase-12. We have also demonstrated that mitochondrial permeability has been compromised in S334ter RHO retina resulting in release of AIF and cytochrome C in the cytosol.

Introduction

Retinitis pigmentosa (RP) is an inherited retinal disorder that is caused by the progressive loss of rod and cone photoreceptors with clinical hallmarks that include sensitivity to dim light, abnormal visual function and characteristic bone spicule deposits of pigment in the retina [1]. This disease affects approximately 1 in 3200, and an estimated 1.5 million people are affected worldwide. The autosomal dominant form of RP (ADRP) is associated with mutations in at least 14 different genes; however, mutations in the rhodopsin gene (RHO, OMIM 180380, accession ID U49742) are the most prevalent mutation identified to date resulting in 30% to 40% of all ADRP cases [2], [3].

S334ter rhodopsin (RHO) rats (line 4) express rhodopsin gene containing an early termination codon at residue 334 and is a model of a number of RHO truncation mutations in human RP patients (http://www.ask.com/wiki/Retinal_Degeneration (Rhodopsin_Mutation). This mutation results in the expression of a rhodopsin protein that lacks the 15 C-terminal amino acids that are involved in rhodopsin trafficking to the photoreceptor outer segments and in the deactivation of the rhodopsin protein after light absorption. A previous study conducted using this rat model demonstrated that the nature of the rhodopsin sorting defect, but not the constitutive activation of the phototransduction cascade, contributes significantly to apoptosis by interfering with the normal cellular machinery in the post-Golgi transport pathway or in the plasma membrane [4]. The study also revealed a correlation between the severity of mis-sorting of the truncated rhodopsin protein and the rate of cell death in these animals. Although the primary cause of

degeneration in the S334ter-4 RHO photoreceptors has been identified, the precise mechanism responsible for triggering the apoptotic cascade remains unknown.

The apoptotic death of photoreceptor cell is the cornerstone of the pathophysiological process in RP [5], [6]. Although the role of caspases in the execution of apoptosis in retinal degeneration has been demonstrated, the process has not been fully investigated. Moreover, conflicting data has been published regarding the pro-apoptotic cellular signals that lead to the deterioration of photoreceptor cells. These studies indicate that diverse cellular pathways are involved in the demise of photoreceptor cells; for example, two independent caspase activation pathways (the cellular stress response and the death receptor pathway) have been identified in the rd mouse model [7]. However, a separate study of the rd mouse suggests that cell death occurs through the caspase-independent pathway, and the DNA cleavage originates independently of caspase-9, -8, -7, -3, and -2 activation and cytochrome C release [8]. Another study demonstrates that in S334ter-4 Rho retinas, apoptosis contributes to the progression of retinal degeneration. [9], [10].

Recently, it has been proposed that the death of RP photoreceptors may involve multiple mechanisms, including caspase-dependent and caspase-independent pathways. Due to their energy production and calcium homeostasis properties and their ability to compartmentalize cell death activators, mitochondria play a central regulatory role in this process [11], [12]. In addition, the activation and translocation of AIF (apoptosis-inducing factor) from the mitochondria and the translocation of caspase-12 (ER stress-associated caspase) to the nucleus in dying photoreceptors suggests that there is a link between the

mitochondrial caspase-independent pathway and the endoplasmic reticulum (ER) stress signal in the cytoplasm [12]. These studies suggest that the ER stress response is involved in the pathological events of ADRP photoreceptors. Therefore, it will be important to determine if mislocalized truncated proteins, as compared to misfolded truncated proteins, are involved in the retinal pathology of S334ter-4 RHO rats.

Recently, many studies have examined the involvement of the ER stress response or the unfolded protein response (UPR) in retinal degeneration [13], [14], [15], [16], [17]. In a previous study, we suggested that the UPR is involved in ADRP progression in P23H RHO-3 transgenic rats and that over-expression of the Bip/Grp78 protein reprograms the UPR and protects the P23H RHO photoreceptors from degeneration [16]. The activation of the UPR in the S334ter-4 RHO rat model has never been analyzed in detail therefore we investigated how the UPR contributes to the degeneration of S334ter-4 RHO photoreceptors. Our interest has been fueled by a previous study in S334ter-4 RHO rats demonstrating that the truncated S334ter-4 rhodopsin protein is retained in the cytoplasm or is associated with the cell membrane [4]. In addition, we are interested to determine if the activation of the ER stress signal in this model initiates apoptosis and if there is a dynamic link between the activation of the UPR and mitochondria-induced apoptosis.

Materials and Methods

Ethics statement

The animal protocol was carried out with approval from the Review Board for Animal Studies at the University of North Texas Health Science Center (Approval Number # 2009/10-46-AO5) and in accordance with the guidelines of the Association for Research in Vision and Ophthalmology Statement for the Use of Animals in Ophthalmic and Vision Research. All efforts were made to minimize the number and the suffering of the animals used.

Animal model

Homozygous S334ter rhodopsin transgenic rats (line 4) were maintained in the UNTHSC housing facility and were bred with WT Sprague-Dawley (SD) rats to generate heterozygous S334ter-4 rhodopsin rats. Therefore, the SD rats were used as WT controls in our experiments. The animals were sacrificed on P10, P12, P15, P18 and P21 for RNA and protein analyses. All rats were maintained in specific pathogen-free (SPF) conditions with a 12-hour light and 12-hour dark daily cycle.

RNA preparation and Real-Time PCR Analysis

Retinas from SD and S334ter-4 rats at P10, P12, P15, P18 and P21 of development were isolated. Total RNA was isolated from the individual retinas from each strain using an RNeasy Mini kit (Qiagen, Valencia, CA) (P10, N = 4; P 12, N = 6; P15, N = 5, P18 N = 6;

P21, N = 6). Using individual retinal extracts of SD and S334ter-4 Rho retinas and a high capacity cDNA Reverse transcription Kit (Applied Biosystems); two cDNAs were prepared from each RNA sample. Each cDNA (10 ng) was subjected to qRT-PCR using Applied Biosystems TaqMan assays on 96-well plates (validated for each selected gene) on a One Step Plus instrument (Applied Biosystems, Foster City, CA) to compare the number of cycles (Ct) needed to reach the midpoint of the linear phase. All observations were normalized to the GAPDH housekeeping gene. The replicated RQs (Relative Quantity) values for each biological sample was average. Biological samples from each strain were used for the qPCR data analysis. A semi-quantitative RT-PCR analysis of spliced Xbp1 was performed as described [70]. Quantification of the spliced portion of the XbP1 cDNA was performed by obtaining ratio of spliced Xbp1 to normalized unspliced Xbp1.

Retinal protein extract for Western blot analysis

Retinal protein extracts were obtained from dissected retinas by sonication in a buffer containing 25 mM sucrose, 100 mM Tris-HCl, pH = 7.8, and a mixture of protease inhibitors (PMSF, TLCK, aprotinin, leupeptin, and pepstatin). The total protein concentration in right and left retinas from individual rat pups was measured using a Biorad protein assay, and 40 µg of total protein was used to detect individual proteins. The detection of proteins was performed using an infrared secondary antibody and an Odyssey infrared imager (Li-Cor, Inc.). Antibodies that detect the stress-induced phosphorylated proteins pPERK, pEIF2α, were from Cell Signaling (1:1000). Antibody detected pATF6 (full land cleaved form) was from Imgenex (1:1000). Anti-Grp78 and anti-CHOP (1:1,000) were from Santa-Cruz Biotechnology; the anti-AIf1 and anti-caspase-12 antibodies

(1:1,000) were from Abcam and cytochrome *C* was from Santa-Cruz. β-actin was used as an internal control and was detected by the application of anti-β-actin antibody (Sigma-Aldrich).

Isolation of cytoplasm and mitochondria from S334ter-4 RHO retinas

The isolation of the cytosolic fraction from the individual retinas of five SD and five transgenic rats was performed using the Mitochondria Isolation Kit for Tissues (Thermo Scientific). The mitochondria were separated from the cytoplasm using the Dounce stroke method as recommended by the Termo Scientific manufacturer. The protein concentration of each fraction was determined using a Biorad protein assay. To confirm the absence of mitochondrial contamination in the cytoplasmic fractions, a western blot was probed with CoxIV antibody (Abcam).

Calpain activity assay

The detection of calpain activity was performed using the Calpain Activity Assay kit from BioVision in accordance with the manufacturer's recommendations and compared the activation of calpains in S334ter-4 Rho and SD retinal tissues. The detection of the cleavage substrate Ac-LLY-AFC was performed in a fluorometer that was equipped with a 400-nm excitation filter and 505-emission filter.

Statistical analysis

All data were evaluated and plotted using GraphPad Prism5 software. We analyzed the results using Student's *t*-test for unpaired samples or a two-way ANOVA analysis of

variance. All data are represented as the mean ± SEM. The P values that indicated statistical significance in experiments are "*" ($P<0.05$), "**"($P<0.01$), and "***" ($P<0.001$).

Results

The retinal degeneration in S334ter-4 rats has been described previously [4], [18], [19], http://www.ucsfeye.net/mlavailRDratmodels.shtml. Photoreceptor degeneration begins at about postnatal day (P) 13 [4] and about 25% of the photoreceptors are lost by P30, 50% by P60 [19] and about 65% by P120. In addition, high resolution light microscopy has demonstrated that at P4, P6, P8 and P10 the S334ter-4 retinas are indistinguishable from age-matched wild-type controls and this is reflected in a normal ONL thickness at P10. A very few pyknotic nuclei are observed at P12 resulting in the ONL thinning only beginning at P21 (LaVail, unpublished observations). Therefore, we choose P10 as the first time point to observe the kinetics of the gene expression involved in the UPR and UPR-associated signaling pathways.

Previous studies have demonstrated the cytoplasmic localization of the S334ter-4 rhodopsin protein in the retina [20] of the transgenic lines 3 and 5. In our study of S334ter-4 RHO, we confirmed the mislocalization and retention of truncated rhodopsin in the cytoplasm of S334ter-4 RHO photoreceptors (data not shown). Therefore, we were interested to determine if mis-trafficking of the S334ter-4 RHO protein provokes the ER stress and ER stress associated signaling.

Expression of genes associated with oxidative stress is elevated in S334ter-4 RHO retinas

ER homeostasis is a fragile equilibrium that is modulated by dysregulation of the calcium or oxidative/reductive balance. Recently, it has been demonstrated that two processes, UPR oxidative stress are linked [21-23]. Therefore, we analyzed the relative expression of genes that are sensitive to an oxidative/reductive environment.

To further assess the effect of the mislocalized truncated rhodopsin protein on oxidative stress, we examined the expression level of hypoxia-inducible factor α (Hif1αa), superoxide dismutase (Sod1) and the nuclear factor kappa-light-chain-enhancer of activated B cells (Nf-kB) genes. Figure 1 shows the relative expression of these genes in S334ter-4 RHO and SD (Sprague Dawley) rats on P10, P12, P15 and P21.

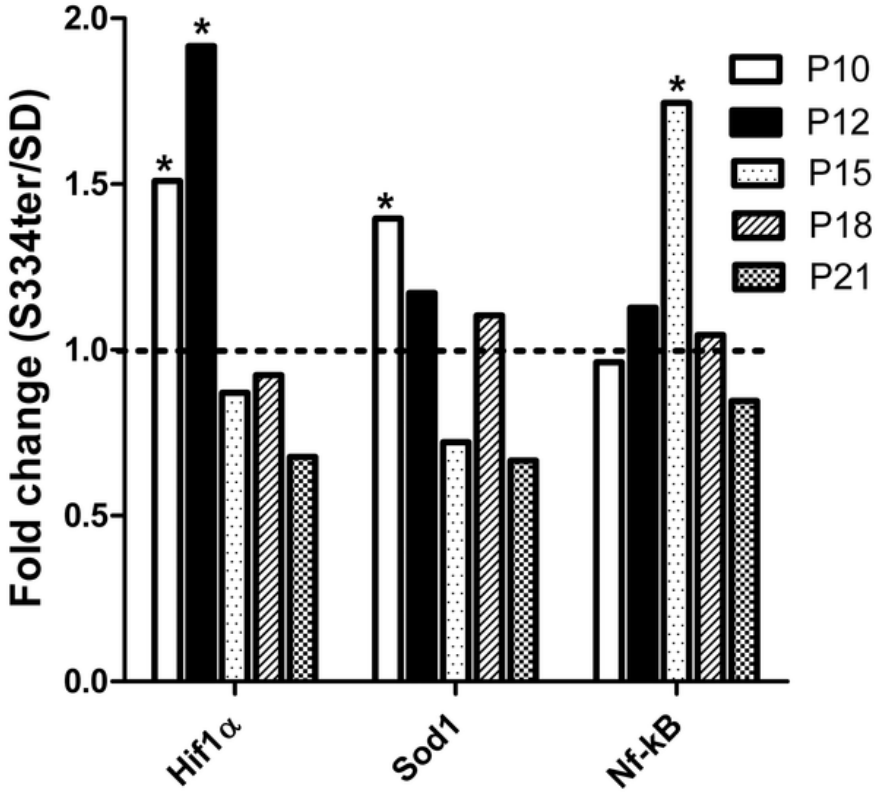

Figure 1. Relative expression of the oxygen stress-induced Hif1a, Sod1 and Nf-kB genes in S334ter-4 RHO retinas at different ages. Relative gene expression in S334ter-4 RHO retina was measured on P10, P12, P15, P18 and P21 and a fold change was expressed as a ratio of S334ter-4 RHO relative expression to SD relative expression. Expression of the Hif1α and Sod1 genes was significantly induced in P10 S334ter-4 Rho compared to SD retinas (1.5- and 1.4-fold, respectively, $P<0.05$, *). On P12, increased Hif1a expression was still evident (1.9-fold, $P<0.05$,*); however, the Sod1 expression was decreased compared to P10. When compared with Hif1a and Sod1 mRNA, the relative accumulation of Nf-kB mRNA in S334ter-4 Rho retinas exhibited alternate dynamics: a 1.7-fold increase in Nf-kB expression was observed on P15 only ($P<0.05$,*), whereas the Hif1α and Sod1 expression was diminished on P15.

Our data demonstrated that Hif1α gene expression was upregulated 1.5- and 1.9-fold on P10 and P12, respectively (0.93±0.06 in SD vs. 1.4±0.17 in S334ter-4 RHO and 0.62±0.09 in SD vs. 1.2±0.14 in S334ter-4 Rho, respectively, $P<0.05$).

On P15, the expression level of Hif1α dropped dramatically compared with that observed in the SD retina. The expression of Sod1 also increased dramatically (1.4-fold) (0.69±0.04

in SD vs. 1.334±0.1 in S334ter-4 RHO, $P<0.05$), but this increase occurred at P10. SOD1 expression subsequently declined to the level of the SD over time. In contrast, Nf-kB gene expression increased 1.7-fold (0.9±0.18 in SD vs. 1.6±0.2 in S334ter-4 Rho, $P<0.05$) only on P15. At other time points, the Nf-kB gene expression was comparable to that in the wild-type (WT) retinas.

Comparative analysis of ER stress and ERAD-associated genes in S334ter-4 RHO and SD retinas.

Figure 2 demonstrates the results of RT-PCR analysis of the genes involved in the activation of ER stress signaling in S334ter-4 RHO rats. At P10 in transgenic retinas, calnexin (Cnx) and ATF4 gene expression was significantly upregulated 1.6- and 1.5-fold, respectively (0.9±0.05 in SD vs. 1.4±0.2 in S334ter-4 RHO and 0.9±0.04 in SD vs. 1.3±0.1 in S334ter-4 RHO, respectively, $P<0.05$ in both cases). Furthermore, Ero1 gene expression was downregulated 2-fold (1.2±0.18 in SD vs. 0.6±0.18 in S334ter-4 RHO, $P<0.05$). At P12, the number of genes involved in the ER stress response was extended and included the following: Cnx (2.1-fold increase; 0.62±0.09 in SD vs. 1.3±0.16 in S334ter-4 RHO, $P<0.05$), Hsp40/Dnajc10 (1.8-fold increase; 0.65±0.1 I SD vs. 1.21±0.18 in S334ter-4 RHO, $P<0.05$), Ero1 (1.8-fold increase; 0.8±0.13 in SD vs. 1.5±0.2 in S334ter-4 RHO), Bip (1.7-fold increase; 0.7±0.01 in SD vs. 1.2±0.1 in S334ter-4 RHO, $P<0.05$), eiF2a (1.9-fold increase; 0.80±0.13 in SD vs. 1.50±±0.2 in S334ter-4 RHO, $P<0.01$), Xbp1 (1.6-fold increase; 0.72±0.08 in SD vs. 1.17±0.13 in transgenic rats, $P<0.05$), Atf6 (1.8-fold increase; 0.64±0.09 in SD vs. 1.15±0.13 in S334ter-4 RHO, $P<0.05$) and Chop (1.5-fold increase; 0.8±0.05 in SD vs. 1.3±0.12 in S334ter-4 RHO, $P<0.05$). At P15, the expression of Cnx, Ero1, eIF2a and ATF4 dropped to different extents, and although in some cases,

the expression level of these genes was higher than in the SD retinas, the relative expression of CHOP protein was consistently 1.3-fold higher than in the SD retinas. At P15, the relative expression of the following genes was significantly elevated: Hsp40/Dnajc10 (2-fold increase; 0.6±0.12 in SD vs. 1.2±0.22 in S334ter-4 RHO, $P<0.05$), Bip (2-fold increase; 0.65±0.12 in SD vs. 1.32±0.16 in S334ter-4 RHO, $P<0.01$), Xbp1 (1.5-fold increase; 0.9±0.16 in SD vs. 1.36±0.17 in S334ter-4 RHO, $P<0.05$), ATF66 (greater than 2-fold increase; 0.60±0.17 in SD vs. 1.22±0.073 in transgenic rats, $P<0.01$). At P18, the expression levels of all the genes analyzed dropped to the level of the SD retinas. The exception to this finding was the Chop gene, which exhibited upregulated expression in P18 retinas, and the Xbp1 gene, which was significantly downregulated in P18 S334ter-4 RHO retinas. Therefore, the data confirmed that the expression of ER stress-related genes, the eiF2a and Atf4 genes (the PERK pathway), the Atf6 gene (the ATF6 pathway) and the Xbp1 gene (the IRE1 pathway) were upregulated in P12–15 S334ter-4 RHO retinas.

We also examined ERAD (ER associated degradation) genes, such as Derl1 and Hrd1. Derl1 participates in the retrotranslocation of misfolded proteins into the cytosol where they are ubiquitinated and degraded by the proteasome. The Hrd1 gene is an E3 ubiquitin-protein ligase and transfers ubiquitin specifically from endoplasmic reticulum-associated UBC1 and UBC7 E2

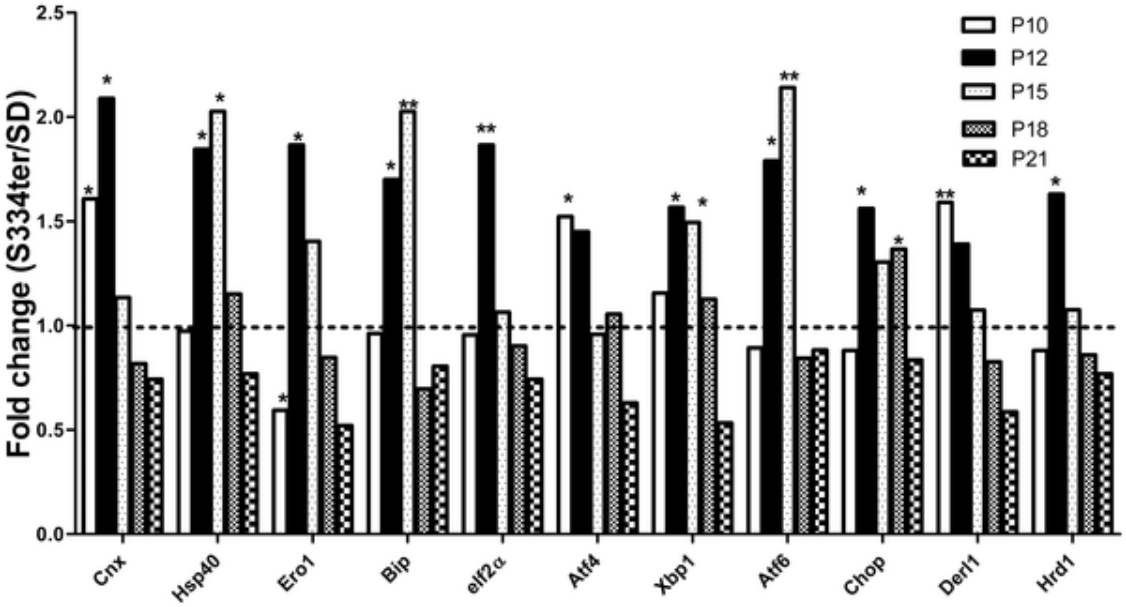

Figure 2. Relative expression of ER stress- and ERAD-related genes in S334ter-4 RHO retinas.

The UPR gene expression was altered in S334ter-4 RHO retinas. Relative gene expression in S334tr Rho retina was measured on P10, P12, P15, P18 and P21 and a fold change was expressed as a ratio of S334ter-4 RHO relative expression to SD relative expression. On P10, there was a significant reduction in the Ero1 gene expression suggesting that the ER homeostasis in S334ter-4 RHO retinas is imbalanced. The expression of this gene is decreased 2-fold ($P<0.05$, *) in S334ter-4 RHO retinas compared with SD retinas on P10. The increased expression of Calnexin (Cnx) and Atf4 genes are the first ER stress markers that respond to ER disturbance. The expression of these genes was increased 1.6- and 1.5-fold, respectively, ($P<0.05$, * in each case) on P10. On P12, the expression of other UPR upstream and downstream markers, such as Hsp40/Dnajc10, Ero1, Bip, eIf2a, Xbp1, Atf6 and Chop, were detected, which was indicated by relative increases of 1.8-, 1.8-, 1.5-, 1.9-, 1.6-, 1.8- and 1.6-fold, respectively, ($P<0.05$, * in each case with the exception of eIF2a where $P<0.01$, **). On P15, the Cnx, Ero1, eIf2a, Atf4 and Chop genes were expressed to a lesser extent or there was no significant difference in their expression levels in S334ter-4 RHO retinas compared with SD retinas. However, the Hsp40/Dnajc10, Bip, Xbp1 and ATf6 mRNAs were significantly induced on P15. Their relative expressions were 2-, 2-, 1.5- and 2-fold higher in S334ter-4 RHO retinas compared with the WT group ($P<0.01$ for Bip and Atf6, and $P<0.05$ for Hsp40/Dnajc10 and Xbp1). On P21, the expression of all genes was insignificant in the S334ter-4 RHO retinas compared with the SD retinas. Derl1 and Hrd1 gene expression was upregulated 1.5- and 1.6-fold on p10 and p12, respectively ($P<0.05$ in each case).

ligases to substrates, thereby promoting their degradation. The qRT-PCR analysis of these genes in SD and S334ter-4 RHO retinas (Figure 2) showed that both genes were transiently activated on P10 and P12. Derl1 expression increased 1.6-fold on P10 (0.9±0.03 in SD vs. 1.4±0.2 in S334ter-4 RHO, $P<0.01$) and subsequently decreased slightly over time. The expression of Hrd1 increased significantly (1.6-fold) on P12 (0.74±0.07 in SD vs. 1.24±0.17 in S334ter-4, $P<0.05$). We also examined the expression of the Edem1 and Edem2 genes and determined that there was no significant difference in the expression levels in S334ter-4 Rho retinas compared with control retinas.

We analyzed levels of the main UPR markers such as BiP, CHOP, phosphorylated protein kinase RNA-like endoplasmic reticulum kinase (pPerk), phosphorylated eIF2α (peIF2α), active ATF6 proteins and the Ire-mediated unconventional the Xbp1 mRNA splicing in S334ter-4 RHO rats (Figure 3A, B and C) using western blot analysis and a semi-quantitative RT-PCR and determined that the production of the BiP protein increased 1.5-fold in P12 S334ter-4 RHO retinas compared with SD retinas (0.047±0.008 vs. 0.071±0.005, respectively; P = 0.01. However, by P15 the difference between groups was not detected. The CHOP protein was also dramatically over-expressed (3.5-fold) (0.016±0.005 in SD vs. 0.60±0.002 S334ter-4 Rho, P = 0.0003) on P15 in S334ter-4 RHO retinas. The full length of pAtf6 protein (90 kD) (the Atf6 pathway) was significantly elevated in S334ter-4 RHO retina by 2.7-fold (0.0017±0.0011 in SD vs. 0.0048±0.0007 in S334ter-4 RHO, P = 0.04). The N-terminal of the full-length of Atf6, cleaved pAtf6 was elevated by 1.93-fold and was 0.18±0.004 in SD vs. 0.035±0.002, P = 0.004. We also observed that the peIF2α protein was significantly increased in S334ter-4 RHO retina and was 0.001±0.0005 in S334ter-4 RHO vs 0.002±0.0004, P = 0.0009.The hallmark of the

IREI pathway, the spliced Xbp1 protein was detected in S334ter-4 retina. Its level was 4.5-fold higher in transgenic retina compared to SD and was 0.022±0.003 in SD and 0.1±0.01, P = 0.001 in S334ter-4 rats. Unspliced Xbp1 protein was increased to a lesser extent (2.3-fold) in S334ter-4 rats and was 0.049±0.008 in SD and 0.13±0.001, P = 0.03 in S334ter-4. Images of western blots are shown in Fig. 3 C.

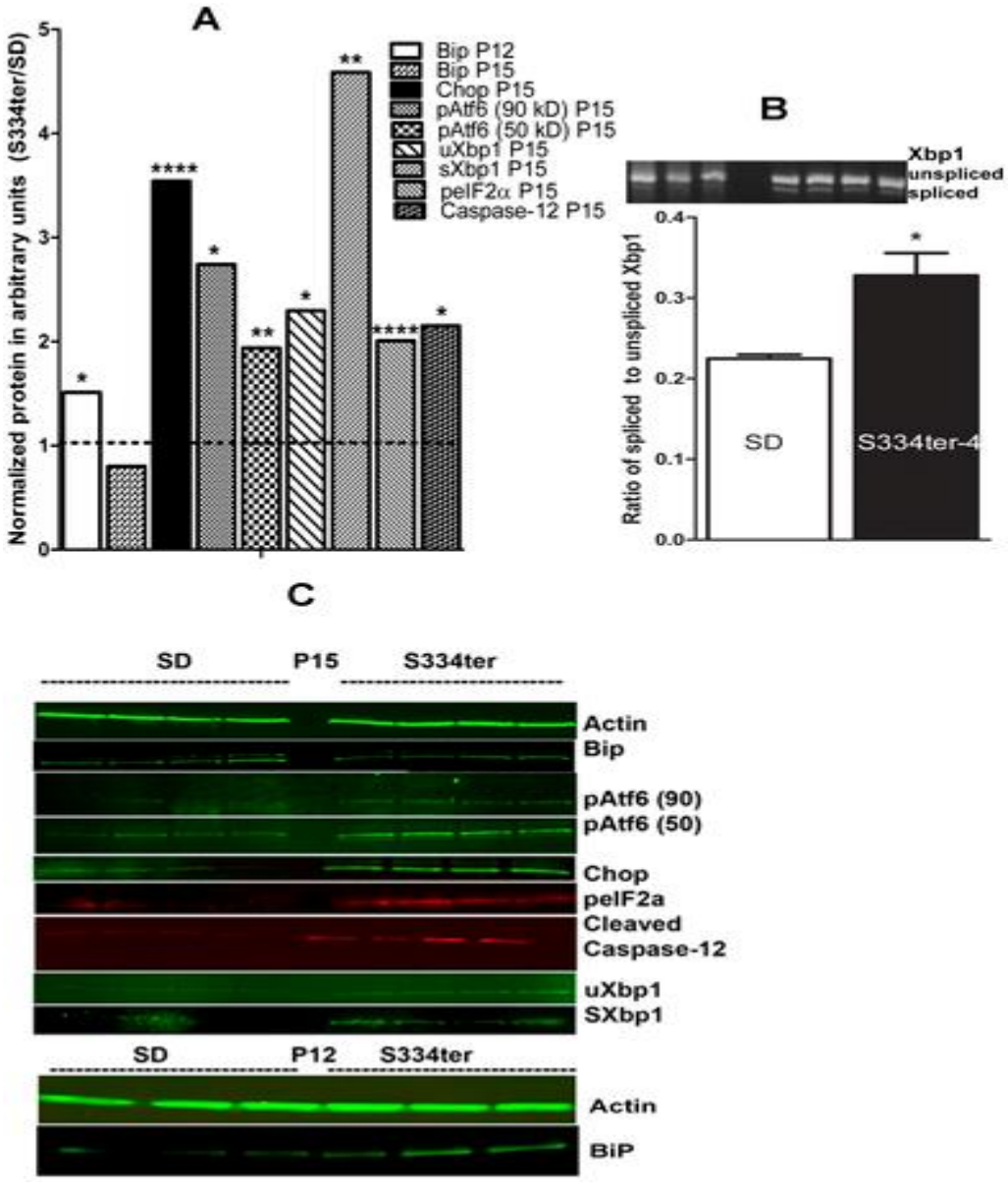

Figure 3. The ER stress markers BIP and CHOP proteins in retinas from S334ter-4 RHO rats.

A: Ratios of normalized S334ter-4 RHO BiP, CHOP, pATF6 (90), pATF6 (50), peIF2α, spliced Xbp1(sXbp1), unsliced Xbp1 (uXbp1), cleaved caspase-12 proteins to corresponding proteins in SD CHOP were used to register the alteration of protein expression. Normalization of all proteins was done by detecting β-Actin protein The ER stress markers BIP protein was a 1.5-fold upregulated in P12 S334ter-4 RHO retinas compared with SD retinas (0.047±0.008 vs. 0.071±0.005, respectively; $P = 0.01$). In P15, the level of BiP protein was significantly reduced and was not distinguishable from SD. The Chop protein was also dramatically over-expressed (3.5-fold) (0.016±0.005 in SD vs. 0.60±0.002 S334ter-4 RHO, $P = 0.0003$) on P15 in S334ter-4 RHO retinas. The full length of pAtf6 protein (90 kD) (the Atf6 pathway) was significantly elevated in S334ter-4 RHO retina by 2.7-fold (0.0017±0.0011 in SD vs. 0.0048±0.0007 in S334ter-4 RHO, $P = 0.04$). The cleaved pAtf6 (50) was significantly elevated by 1.93-fold inS334ter-4 RHO retina (0.18±0.004 in SD vs. 0.035±0.002, $P = 0.004$). The peIF2α protein was also significantly increased in S334ter-4 RHO retina and was 0.001±0.0005 in S334ter-4 RHO vs 0.002±0.0004, $P = 0.0009$. The full length of pAtf6 protein (90 kD) (the Atf6 pathway) was significantly elevated in S334ter-4 RHO retina by 2.7-fold (0.0017±0.0011 in SD vs. 0.0048±0.0007 in S334ter-4 RHO, $P = 0.04$). The N-terminal of the full-length of Atf6, cleaved pAtf6 was elevated by 1.93-fold and was 0.18±0.004 in SD vs. 0.035±0.002, $P = 0.004$. We also observed that the peIF2α protein was significantly increased in S334ter-4 RHO retina and was 0.001±0.0005 in S334ter-4 RHO vs 0.002±0.0004, $P = 0.0009$. The spliced Xbp1 protein was detected in S334ter-4 retina. Its level was a 4.5-fold higher in transgenic retina compared to SD and was 0.022±0.003 in SD and 0.1±0.01, $P = 0.001$ in S334ter-4 rats. Unspliced Xbp1 protein was increased to a lesser extent (2.3-fold) in S334ter-4 rats and was 0.049±0.008 in SD and 0.13±0.001, $P = 0.034$ in S334ter-4. Increase in active caspase-12 was observed in S334ter-4 RHO retina. The level of cleaved caspase-12 (20 kD) was elevated in S334ter-4 RHO rats on P15 compared to control over 2-fold and was 0.05±0.007 in SD vs. 0.12±0.02 in S334ter-4 RHO, $P = 0.014$ on P15. B: Upper panel: Quantification of spliced form of the Xbp1 mRNA (the IRE signaling) detected by RT-PCR reaction. We observed 1.45-fold increased in the spliced form of Xbp1 mRNA in S334ter-4 RHO retina. The ratio of spliced Xbp1 to normalized unspliced Xbp1 mRNA was 0.22±0.0006 in SD vs. 0.033±0.031 in S334ter-4 RHO retina, $P = 0.025$). Image of the agarose gel loaded with RT-PCR product obtained with Xbp1 specific primers is shown in a lower panel. C: Images of western blots treated with anti-Actin, Bip, CHOP, peIf2α, pATF6, Xbp1 antibodies and detected with secondary antibodies and infrared imaging scanner are presented. The spliced form of the Xbp1 mRNA was increased in S334ter-4 RHO rats as well. The ratio of spliced Xbp1 to normalized unspliced Xbp1 mRNA was 1.45 (0.22±0.0006 in SD vs. 0.033±0.031 in S334ter-4 RHO retina, P = 0.025). An image of an agarose gel loaded with RT-PCR product obtained with Xbp1 specific primers is shown in Fig. 3B.

Autophagy is involved in retinal degeneration of S334ter-4 RHO photoreceptors

Knowing that the ERAD genes Derl1 and Hrd1 are transiently upregulated in P10 and P12 retinas, we became interested in investigating the activity of another protein degradation system, autophagy. We examined the relative expression of autophagy hallmark genes, such as Atg5 and Atg7, which are involved in autophagosome formation, and the lysosomal-associated membrane protein 2 (Lamp2). Figure 4 demonstrates that in developing S334ter-4 RHO retinas, the relative expression of Atg5 and Atg7 was not significantly different from that observed in the SD samples. However, the relative expression of the Lamp2 gene was transiently upregulated 1.8-fold on P10 in S334ter-4 RHO retinas (0.86±0.07 in SD vs. 1.5±0.16 in S334ter-4 Rho, $P<0.01$). The expression of this gene subsequently decreased with time. The results of the comparative qRT-PCR analyses are shown in Figure 4.

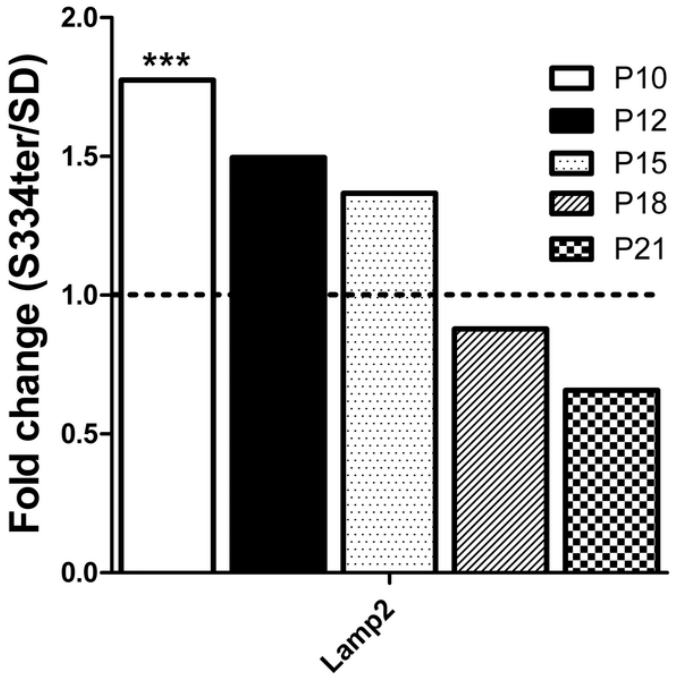

Figure 4. Relative expression of Lamp2 in S334ter-4 RHO retinas.

Relative gene expression in S334tr RHO retina was measured on P10, P12, P15, P18 and P21 and a fold change was expressed as a ratio of S334ter-4Rho relative expression to SD relative expression. The Lamp2 gene expression was upregulated in P10-P15 S334ter-4 Rho retinas. In P10, the relative expression of this gene increased 1.7-fold in S334ter-4 Rho retinas compared to that in SD retinas *(P*<0.001), and it subsequently declined in a time-dependent manner.

S334ter-4 RHO rats exhibit elevated levels of pro-apoptotic gene expression during retinal development

The ADRP photoreceptors degenerate and die through the process of apoptosis. Therefore, we examined the expression of pro-apoptotic genes belonging to the Bcl-2 family: the BH3-only interacting domain death agonist (BID), the Bcl-2-interacting killer protein (Bik), the Bcl2-like 11 apoptosis facilitator (Bim), Noxa and Puma. The results of this analysis are presented in Figure 5. We determined that the relative expression of Bik was significantly upregulated 2.3-fold in P10 S334ter-4 RHO retinas compared with P10 SD

retinas (1.24±0.14 in SD vs. 2.73±0.3 in S334ter-4 RHO, $P<0.001$). On P10, we also observed an increase in the relative expression of the Bim protein (1.7-fold; 0.83±0.05 in SD vs. 1.40±0.21 in transgenic retina, $P<0.05$). At the next two time points, Bim expression was upregulated 1.34-fold compared with controls (0.69±0.15 in SD vs 0.51±0.10 in S334ter-4 RHO, $P>0.05$) on P12 and 1.8-fold compared with controls on P15 (0.86±0.18 in SD vs. 1.54±0.11 in S334ter-4 RHO, $P<0.01$). The Noxa gene expression increased significantly in P12 and P15 S334ter-4 RHO retinas and was 2.8-fold and 2-fold higher compared to that in age-matched SD retinas, respectively (0.82±0.12 in SD vs. 2.34±0.36 in S334ter-4 RHO at P12, $P<0.0001$ and 0.88±0.24 in SD vs. 1.87±0.19 in S334ter-4 RHO at P15, $P<0.01$). On P15, the relative expression of Bid and Puma in S334ter-4 RHO retinas were increased 2.4- and 2.3-fold, respectively, compared to that in SD retinas (0.68±0.11 in SD vs. 1.62±0.23 in S334ter-4 RHO, $P<0.01$ for Bid and 1.00±0.05 in SD vs. 2.30±0.5 in S334ter-4 RHO, $P<0.001$ for Puma).

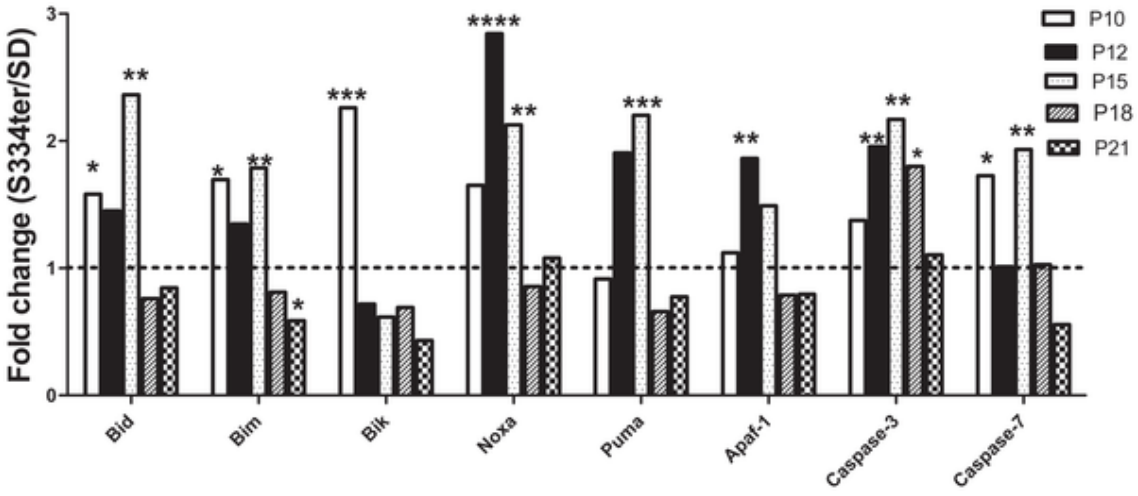

Figure 5. Relative expression of pro-apoptotic genes involved in S334ter-4 RHO retinas.

Relative gene expression in S334ter-4 RHO retina was measured on P10, P12, P15, P18 and P21 and a fold change was expressed as a ratio of S334ter-4 Rho relative expression to SD relative expression. The expression of BH3-only proteins, BID, Bim, Bik, Noxa and Puma was upregulated with different patterns in S334ter-4 RHO retinas. On P10, the expression of Bik, Bim and Bid genes increased 2.3- ($P<0.001$) 1.7- ($P<0.05$) and 1.6-fold ($P<0.05$), respectively. The expression of Bim was elevated until p15 and dropped 0.6-fold to WT levels ($P<0.05$) on P21. On P12, the Noxa gene was elevated 2.8-fold ($P<0.0001$) and remained upregulated until p15 (2-fold increase, $P<0.01$) and its expression subsequently dropped. On P15, the Puma gene appears to be upregulated 2.2-fold in S334ter-4 RHO retinas when compared to SD retinas ($P<0.001$). The Apaf1 gene expression was increased in P12 and in P15 retinas. A significant 1.9-fold upregulation Apaf1 expression was detected on P12 ($P<0.01$). The relative expression of caspase-3 was significantly upregulated during the progression of ADRP. On P12, P15 and P18, caspase-3 expression in S334ter-4 RHO retinas was elevated 1.9-fold ($P<0.01$), 2.2-fold ($P<0.01$) and 1.8-fold ($P<0.05$), respectively compared to SD retinas. The analysis of caspase-7 gene expression demonstrates a 1.7-fold ($P<0.05$) and 2-fold ($P<0.01$) increase in caspase-7 mRNA on P10 and P15, respectively.

The apoptotic protease activating factor 1 (APAF1) also induces apoptosis. Therefore, we analyzed Apaf1 gene expression during the progression of ADRP and determined that its expression was upregulated 1.9-fold in P12 transgenic retinas (0.62±0.01 in SD vs. 1.17±0.10 in S334ter-4 RHO, $P<0.01$) (Figure 5). This upregulation leads to the activation of caspase-dependent apoptosis, which was confirmed by the analysis of caspase-3 and -7 expression levels. The caspase-3 and -7 proteins are executioner caspases. We determined that the expression of caspase-3 was significantly upregulated 1.9-, 2.17- and 1.8-fold in P12, P15 and P18 S334ter-4 RHO retinas, respectively (0.7±0.1 in SD vs. 1.33±0.2 in S334ter-4 RHO, $P<0.01$, 0.69±0.21 in SD vs. 1.5±0.15 in S334ter-4 RHO, $P<0.01$ and 0.90±0.10 in SD vs. 1.63±0.22 in S334ter-4 RHO, $P<0.05$, respectively). Caspase-7 gene expression was upregulated 1.73-fold and almost 2-fold on P10 and P15, respectively

(0.82±0.04 in SD vs. 1.42±0.15 in S334ter-4 RHO, $P<0.05$ and 0.99±0.07 in SD and 1.92±0.43, $P<0.01$ in transgenic rats, respectively).

Mitogen-activated protein kinases 1 (Erk2) and 8 (Jnk) are involved in retinal degeneration in S334ter-4 RHO rats

A number of mitogen-activated kinases, such as Mapk8 (c-Jun N-terminal kinase 1) and Mapk14 (p38), play an important role in the ER stress response. Therefore, we included these and other members of the MAPK gene family, such as the extracellular signal-regulated kinases Mapk1 (Erk2) and Mapk3 (Erk1), in our study. RNA analysis of P10–P21 transgenic retinas demonstrated no significant difference in the relative expression of the Mapk3 and Mapk14 genes compared to control. In contrast, the expression of Mapk1 and Mapk8 was elevated by 1.7- and 2.3-fold, respectively, in the transgenic retinas (0.88±0.06 in SD vs. 1.5±0.20 in S334ter-4 RHO and 0.68±0.07 in SD vs. 1.60±0.3 in S334ter-4 RHO, respectively; $P<0.01$ in each case) on P10 and their expression subsequently decreased over time (Figure 6).

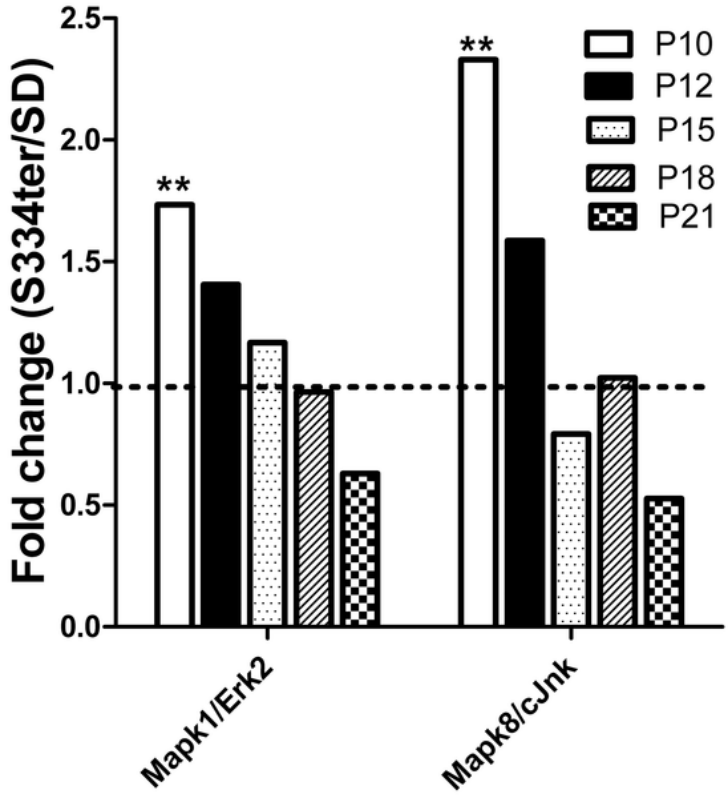

Figure 6. Relative expression of the MAPK1 (Erk2) and MAPK8 (JNK) genes in S334ter-4 RHO retinas.

Relative gene expression in S334ter-4 RHO retina was measured on P10, P12, P15, P18 and P21 and a fold change was expressed as a ratio of S334ter-4 RHO relative expression to SD relative expression. On P10, the Mapk3 (Erk1) and Mapk14 (p38) gene expression was upregulated 1.7- and 2.3-fold in S334ter-4 RHO retinas, respectively (P<0.01 for both). Starting on P12, their expression decreased with time.

pTen/Akt1 signaling is involved in retinal degeneration in S334ter-4 RHO rats

A recent study by Hu and colleagues demonstrated a critical role for the endogenous Akt and MEK1/ERK pathways in counteracting ER stress and proposed that the endogenous Akt/IAPs and MEK/ERKs control cell survival by resisting ER stress-induced cell death signaling [24]. Figure 7 shows the progressive changes in Akt1/2 gene expression in S334ter-4 RHO rats during retinal degeneration. On P12, we observed the elevation of the tumor-suppressor gene pTen that catalyzes the dephosphorylation of the Akt gene leading

to the inhibition of the Akt signaling pathway. An approximately 1.65-fold increase in the relative expression of the Pten gene (0.80±0.13 in SD vs.1.52±0.2 in S334ter-4 Rho, $P<0.05$) was observed. Subsequently, pTen expression decreased to the level of the WT samples. In contrast, the expression of the Akt1/2 genes increased after P12 and reached a peak on P15 in S334ter-4 RHO rats. The Akt1 gene expression increased by 1.65-fold (0.84±0.15 in SD vs. 1.39±0.13 in S334ter-4 Rho rats, $P<0.05$) and the Akt2 gene expression increased 1.7-fold (1.032438±0.17 in SD vs. 1.71±0.15 in S334ter-4 Rho, $P<0.01$).

ER-mitochondrial cross-talk in S334ter-4 RHO retina detected by the elevated calpain activity and release of apoptotic inducing factor 1 from mitochondria to cytosol

The physical and functional interactions between the ER and the mitochondria occur throughout their networks. The molecular foundations of this cross-talk are diverse, and Ca^{2+} is an important signal that these organelles use to communicate. A recent study by Bravo et al. [25] demonstrated that during the adaptive phase of ER stress mitochondrial events are already underway before the appearance of cell death.

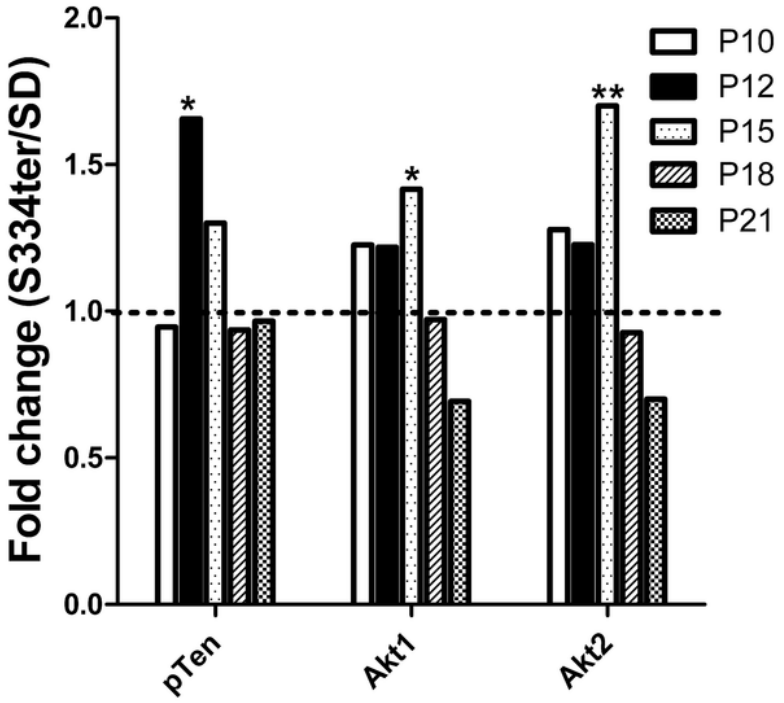

Figure 7. Relative expression of pTten, Akt1 and Akt2 genes in S334ter-4 RHO retinas.

Relative gene expression in S334ter-4 RHO retina was measured on P10, P12, P15, P18 and P21 and a fold change was expressed as a ratio of S334ter-4 RHO relative expression to SD relative expression. An approximate 1.65-fold increase in the relative expression of the pTen gene was observed (0.80±0.13 vs. 1.5±0.2, $P<0.05$) in P12 transgenic retinas. Subsequently, the expression of this gene decreased to WT levels. In contrast, the expression of the Akt1 and 2 genes increased after P12 and reached a peak on P15. The Akt1 gene expression was 0.84±0.15 in SD retinas vs. 1.40±0.13 in S334ter-4 RHO retinas, $P<0.05$. The Akt2 gene expression was 1.03±0.17 in SD vs. 1.70±0.15 in P15 S334ter-4 Rho,$P<0.01$.

The ER-induced Ca^{2+} release may facilitate the permeabilization of the mitochondrial membrane through the activation of the mitochondrial permeability transition (MPT) pore. In addition, Ca^{2+} release from the ER activates Ca^{2+}-sensitive cytosolic enzymes, which may control the distribution and activity of Bcl-2 proteins and calpains or modulate the expression of apoptosis regulatory proteins.

Therefore, we investigated calpain activation in this study. Figure 8 demonstrates that compared with SD there is a 1.4-fold and a greater than 2-fold increase in activated calpains on P15 and P30 in S334ter-4 Rho retinas (2.24±0.09 in SD vs. 3.1±0.127 in S334ter-4 RHO, $P<0.01$ and 1.287±0.27 in SD vs. 2.7±0.04 in S334ter-4 RHO, $P<0.05$, respectively). To further understand if the activation of calpains triggers mitochondria-associated apoptosis, we analyzed the mitochondrial release of the Apoptotic Inducing Factor 1 (AIF1) (Figure 9) and cytochrome *C*, which form an apoptosome with caspase-9 and apoptotic peptidase activating factor 1 (Apaf1) to activate caspase-induced apoptosis. In S334ter-4 RHO retina, we observed a 3-fold increase in the cytosolic AIF1 compared to SD. However, in P15 S334ter-4 RHO retina we did not detect any difference in the levels of cytochrome *C* compared to SD. In contrast, the relative expression of Apaf1 was upregulated (Figure 5).

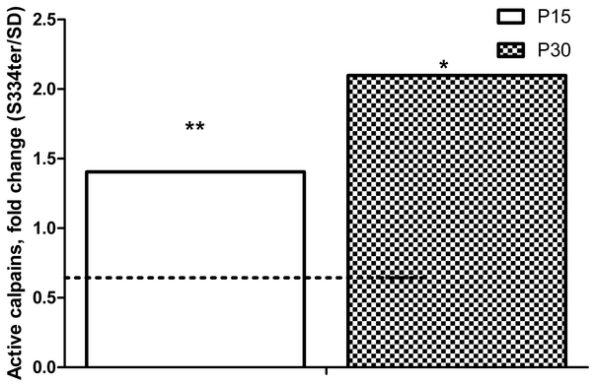

Figure 8. Activation of calpains in S334ter-4 RHO retinas.

In P15 and P30 S334ter-4 RHO retinas, we observed an activation of calpains in the cytosol measured by the fluorescence intensity emitted from the calpain substrate Ac-LLY AFC. On P15 and P30, there was a 1.4- and a greater than 2-fold increase in activated calpains in S334ter-4 RHO retinas compared with SD retinas, respectively (2.24±0.09 in SD vs. 3.1±0.127 in S334ter-4 Rho, $P<0.01$ and 1.287±0.27 in SD vs. 2.7±0.04 in S334ter-4 RHO, $P<0.05$, respectively).

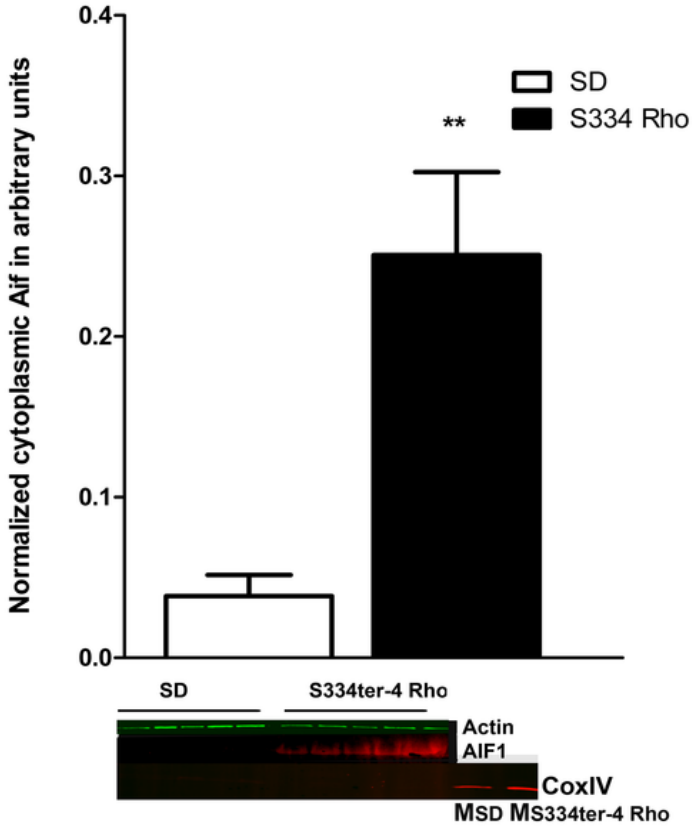

Figure 9. Release of AIF1 from S334ter-4 RHO mitochondria.

Analysis of isolated cytosolic fractions of P15 S334ter-4 RHO retinas determined that the concentration of the cleaved form of Aif1 (48 kD) was 6.5-fold higher compared with the WT cytosolic samples (0.038±0.01 in SD vs. 0.25±0.05 in S334ter-4 RHO, $P = 0.004$). Images of western blot detecting the AIF1 and COXIV proteins are shown. Detection of COXIV protein was observed only in SD (Msd) and S334ter-4 (MS s334ter-4) retinal mitochondrial fractions.

Activation of calpains provokes cleavage of caspase-12. Therefore, we analyzed caspase-12 activity in transgenic retina and found that the level of cleaved caspase-12 was elevated in S334ter-4 RHO rats on P15 compared to control over 2-fold and was 0.05±0.007 in SD vs. 0.12±0.02 in S334ter-4 RHO, $P = 0.014$ on P15. However, further analysis of S334ter-4 RHO retina by western blot and caspase-12 fluorometric activity assay showed that the activity of ER-associated caspase-12 was declined in a time-dependant manner (data not shown).

Knowing that calpains trigger the cleavage of AIF1 in the mitochondria resulting in its translocation to the cytoplasm, we analyzed the cleaved AIF1 protein (figure 9). There was a 6.5-fold increase in the levels of cleaved AIF1 in the cytoplasmic fraction of S334ter-4 RHO compared to SD photoreceptors on P15 (0.038±0.01 in SD vs. 0.25±0.05 in S334ter-4 Rho, $P = 0.004$).

Time-dependent decline of Crx and Nrl transcription factors in the S334ter-4 RHO photoreceptors

To estimate the massive loss of photoreceptor cells in S334ter-4 RHO retinas, we analyzed the relative expression of the NRL and CNX photoreceptor-specific transcription factors and determined that their expression patterns were altered during the progression of ADRP (Figure 10). The expression of the CRX gene was slightly higher in P10 and P12 S334ter-4 RHO retinas compared with SD retinas (0.95±0.04 in SD vs. 1.2±0.17 in S334ter-4 RHO, $P>0.05$ and 0.58±0.1 in SD vs. 0.70±0.12in S334ter-4 RHO, respectively). The expression of Crx decreased with time and was significantly lower in S334ter-4 Rho P21 retinas compared with SD retinas (1.10±0.11 in SD vs. 0.55±0.02 in S334ter-4 RHO, $P<0.05$). The levels of Nrl gene expression did not differ from WT levels during P10-P12. However, by P21, Nrl expression decreased dramatically in the S334ter-4 RHO retinas (1.00±0.21 in SD vs. 0.23±0.02 in S334ter-4 Rho, $P<0.05$).

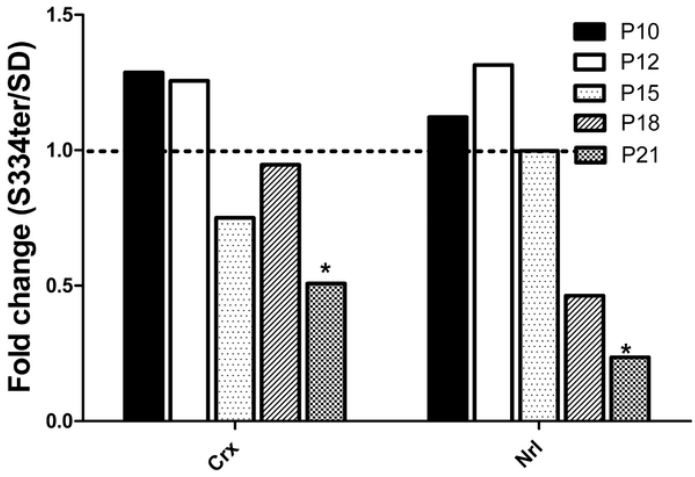

Figure 10. Relative expression of the Crx and Nrl transcription factors in S334ter-4 RHO retinas.

Relative gene expression in S334ter-4 RHO retina was measured on P10, P12, P15, P18 and P21 and a fold change was expressed as a ratio of S334ter-4Rho relative expression to SD relative expression. The qRT-PCR analysis of S334ter-4 RHO retinas revealed that the expression of the Nrl and Crx transcription factors decreased in a time-dependent manner in P10-P21 retinas. A significant reduction in the expression of both transcription factors was observed in P21 retinas, the Crx gene expression was reduced 55% ($P<0.05$), and the NRL gene expression was downregulated 23% ($P<0.05$).

Discussion

Although retinal degeneration has many etiologies, they all lead eventually to photoreceptor cell death and blindness [27]. A number of investigators have dedicated their research to the elucidation of the mechanism of retinal degeneration in ADRP, and some of these studies have focused on ADRP progression in S334ter-4 RHO rats. For example, a recent publication by Kaur et al. highlighted the contribution of mitochondria-associated apoptosis [10]. Despite the progression in our understanding of the cellular mechanisms leading to the decline of S334ter-4 RHO photoreceptors, the essential link that connects ER stress, UPR, and calpain activation with mitochondria-induced apoptosis has not been elucidated. In this study, we present a detailed investigation of the mechanisms of ER stress that lead to the activation of the UPR and apoptosis in retinas expressing mislocalized S334ter rhodopsin. We examine the status of the ER stress response and its correlation with pro-apoptotic gene expression over time (P10, P12, P15 and P21) and dissect the cellular mechanism of retinal degeneration during the development of a normal retina. Although gene expression during the maturation of WT retina is altered [28], [29], in this study, we focus on the relationship between gene expression and the progression of ADRP in transgenic rats expressing truncated S334ter rhodopsin.

The UPR is a conserved, adaptive cellular program that is activated in response to the accumulation of misfolded proteins in the ER [30]. Homeostasis in the ER may be compromised by a variety of stimuli including disturbances in redox regulation, calcium regulation, glucose deprivation, and viral infection. Oxidative protein folding depends upon the maintenance of adequate oxidizing conditions within the ER lumen and is

achieved with the help of ER oxydoreductase (ERO1). ERO1 and PDI form the main pathway for protein disulfide bond formation in the eukaryotic ER. Therefore, the modulation of ERO1 activity is a component of a homeostatic feedback system in the ER that allows the cell to rapidly adjust to fluctuations in the ER redox environment and to maintain conditions that are conducive to oxidative protein folding [31]. We analyzed the expression of the Ero1 gene during the development and progression of S334ter-4 RHO photoreceptors on P10, P12, P15 and P21 and determined that there is a deficiency in Ero1 gene expression on P10, which is followed by a rapid over-expression of the gene on P12 (nearly a 2-fold increase) in transgenic retinas (Figure 2). After P15, Ero1 expression decreased dramatically, which reflects the demand for enzymatic protein folding in the cell and the adjustment of the ER to the redox potential. For example, during hypoxia, transcription of the Ero1 gene is dramatically induced through the activation of Hif1α [32], [33], suggesting that hypoxia negatively regulates the activity of many enzymatic pathways including Ero1. Therefore, in our experiments, the modulation of Ero1 gene expression suggests that there is an alteration in physiological oxygen tension and this could be considered as a key adaptive response to a hypoxia-induced HIF-1mediated pathway (see below).

Recently, hypoxia-induced HIFf1 elevation has been studied in detail. HIF1a is a pivotal regulator of the cells' adaptation to hypoxia and is induced by hypoxia, growth factors, and oncogenes [34]. In addition, the elevated expression of HIF1a under hypoxic conditions is accompanied by the activation of ER stress genes, such as eIF2a [35], and by the increased generation of reactive oxygen species (ROS) that provide a redox signal for the induction HIF1α [36]. A number of investigators have proposed that retinal hypoxic preconditioning,

which leads to HIF1α induction, morphologically and functionally protects retinal cells against light-induced retinal degeneration [37], [38]. Others have identified HIF1α as a protein that may be required (directly or indirectly) for the normal development of the retinal vasculature [39], suggesting that hypoxia is a part of normal retinal development. In addition, oxidative stress has been identified as an important contributor to retinal degeneration in a number of studies [40]. Thus, with respect to hypoxia, it is a logical assumption that Hif1α expression levels are also modulated in transgenic rats during retinal development. Therefore, it is not surprising that the level of Hif1a expression in S334ter-4 RHO retinas correlates with Ero1 transcription, increasing 1.5- and 2-fold at P10 and P12, respectively. The expression of Hif1α has not been examined previously in S334ter-4 RHO retinas. In this study, we demonstrated that hypoxic conditions leading to oxygen deprivation persisted, at least temporarily, in the developing S334ter-4 RHO retinas. The mechanism by which the Hif1α mRNA is induced in ADRP photoreceptors appears to be adaptive response and is linked to mechanisms that maintain a homeostasis in the photoreceptor cells. In favor of this hypothesis, a rapid decline in Hif1α gene expression was observed in P15 S334ter-4 RHO retinas. Additional evidence supporting this hypothesis regarding the hypoxic status of transgenic retina comes from the analysis of the over-expression of the Nf-kB gene. Compared with Hif1α expression, Nf-kB over-expression was delayed until P15. The delay in the onset of Nf-kB over-expression may be associated at least in part with the modulation of Sod1 gene expression, which was over-expressed at P10. Recently, a direct link between the alternating expression patterns of both genes has been proposed [41].

SOD1 is a soluble protein that acts as a scavenger of superoxide converting it to molecular oxygen and hydrogen peroxide, and the SOD1 gene is considered the first line of defense against oxidative stress. The elevated expression of SOD1 has been associated with a number of neurodegenerative disorders, such as SALS and Alzheimer disease, suggesting that SOD1 upregulation is a pathological phenomenon [42]. Therefore, changes in Sod1 mRNA levels would indirectly reflect the increased accumulation of superoxide radicals in S334ter-4 RHO retinas. Although the Sod1 gene was over-expressed in P10 retinas, a dramatic drop in the expression levels of this gene was subsequently observed, which may be provoked by the induction of Nf-kB expression. The transient over-expression of Sod1 in S334ter-4 RHO retinas may be a result of the activation of the hydrogen peroxide-responsive element within the Sod1 promoter by H2O2 [42], [43], which has been shown to play a protective role in oxygen-deprived dopaminergic neurons in the rat substantia nigra [44]. Alternatively, an adaptive mechanism in S334ter-4 RHO photoreceptors that manages the stress by over-expressing a powerful antioxidant enzyme may be involved. As discussed above, the data indicate that the imbalance in ER homeostasis in S334ter-4 RHO retinas is created by hypoxic preconditions that lead to the induction of Ero1, Hif1α and Nf-kb gene expression in P10–P12. Therefore, we next investigated if the modulation of these genes provokes the activation of the UPR in S334ter-4 RHO retinas.

We analyzed the expression profiles of the following proteins: the ER resident chaperone proteins, such as calnexin (Cnx), Hsp40/Dnajc10, and Grp78/Bip; activating transcription factors Atf4, Atf6, and Xbp1; Gadd153/Chop, eIF2α (eukaryotic translation initiation factor 2α) and ERAD (ER-associated degradation) genes, such as Edem1, Edem2, Derl1, Derl2, and Hrd1 (Synovalin). The data suggest that during the development and

progression of the ADRP retina, the expression of the majority of these ER stress gene is modulated. The Cnx gene is an important component of the ER, where it is involved in the maintenance of ER protein homeostasis and participates in the folding and assembly of nascent glycoproteins and aids their transport out of the ER quality control system. Therefore, a high expression of the Cnx gene reflects a high demand for protein folding in the ER. One of these ER proteins may be an aberrant rhodopsin, which is rescued by the over-expression of the Cnx chaperone protein [45].

Further analysis of the ER chaperones Hsp40/Dnajc10, and Bip demonstrated that there is increase in the levels of Hsp40. Recently, a model of the Hsp40-mediated ERAD pathway has been proposed [46]. According to this model, the Hsp40 protein accelerates the ERAD pathway by reducing the number of incorrect disulfide bonds in misfolded glycoproteins that are recognized by EDEM1. ERAD substrates that are released from CNX are recruited by EDEM1 to the C-terminal cluster of HSP40. Therefore, an increase in Cnx suggests that there is a correlation between these synergistically working genes, which is confirmed by our experiments (Figure 2). Similar to the expression patterns of the Cnx gene, Hsp40 gene expression was also elevated 1.8- and 2-fold in P12 and P15 retinas, respectively (Figure 2), whereas the expression of Edem1 as Edem2 in the transgenic retinas (data not shown) was not significantly different from the SD retinas. This result suggests that in S334ter-4 RHO retinas, there is a high demand for the chaperoning assistance of Hsp40.

Another component of the ERAD pathway is the BIP (GRP78) protein. BIP binds to the J domain of Hsp40 in an ATP-dependent manner and transfers ERAD-targeted substrates to the retrotranslocation channel upon ATP hydrolysis [46]. In addition to participation in the ERAD system, BiP is an up-stream marker in the ER stress pathway and is the first line of

defense in a compromised ER. This protein activates three independent UPR pathways, PERK, ATF6 and IRE1. RNA analysis of the S334ter-4 RHO and SD retina samples demonstrated that the increase in Bip expression correlated with the expression of Cnx and Hsp40/Dnajc10, reaching a peak on P15 with a 2-fold increase in the S334ter-4 RHO retinas. Western blot analysis was used to confirm the increased production of the BIP protein providing proof of the elevation of the BIP protein in S334ter-4 RHO rats.

The PERK pathway is activated in P12 transgenic retinas, which was evident from the upregulation of the eIf2a and Atf4 genes and elevation of peIF2α. In P15 retinas western blot analysis demonstrated the increased production of the peIf2α protein providing proof of activation of the PERK signaling pathways in S334ter-4 RHO rats. In addition, expression of the ATF6 (the ATF6 pathway) gene was increased steadily up to P15, after which they decreased to levels that were observed in the controls. Therefore, it is not surprising that the level of full-length pAtf6 (90 kD) and its cleaved form (pAtf6-50) in P15 S334ter-4 RHO retina were significantly increased. The level of Xbp1 (the IRE1 pathway) was also steadily increased up to P15. However, later in P21 retina expression of the Xbp1 gene was significantly reduced in transgenic retinas that could be a result of a decreased catalase expression, enhanced ROS generation, and the loss of mitochondrial MPTP after H2O2 exposure in S334ter-4 RHO photoreceptors [47]. In P15 S334ter-4 Rho retina, we observed increase in a spliced and unspliced forms of Xbp1 protein suggesting that the IRE pathways is activated.

Signaling through the PERK, ATF6 and IRE1 genes triggers pro-apoptotic stimuli during prolonged ER stress. However, these genes do not directly cause cell death, but they initiate the activation of downstream molecules, such as CHOP or JNK, which further push the

cell down the path towards death. CHOP, a downstream marker in the UPR, is a pro-apoptotic protein that regulates the activity of genes including Bcl2, GADD34, ERO1 and TRB3 [48]. In our experiments, we demonstrated that Chop mRNA was elevated during ER stress in P12 S334ter-4 RHO retinas. The increase in Chop expression suggested that the adaptive phase of the UPR in the transgenic retinas initiated apoptosis, causing the S334ter-4 RHO photoreceptors to self-destruct. The over-expression of the CHOP protein was confirmed by western blot analysis suggesting that the CHOP protein is overproduced at transcriptional and translational levels. Therefore, in summary, we propose that all three UPR pathways are activated in S334ter-4 RHO retinas.

In general, the CHOP protein is post-translationally controlled by p38 MAPK (14). Although in our study, a significant difference in p38 expression was not observed, another MAPK 8 (JNK) was dramatically upregulated 1.6-fold in P10 transgenic retinas. This JNK protein is a stress-activated protein kinase that regulates apoptosis through the induction and/or post-translational modification of BH3-only proteins and plays a central role in setting the apoptotic cascade in motion. Evidently, in S334ter-4 RHO photoreceptors, the upregulation of the JNK gene is associated with the recruitment of c-JNK via the IRE1 pathway through TRAF2-c-JNK-ASK1. In support of this hypothesis, we observed the activation of the Ire1 pathways in P12 S334ter-4 Rho retinas. The expression of Xbp1 in P12 transgenic retinas was higher when compared with the control suggesting that the Xbp1 transcriptional factor is required by the elevated production of JNK. Another rationale for the increase in JNK expression is associated with the activation of Bim, Bak and Bax proteins [48].

Regarding the pro-apoptotic Bax/Bak BH3-only proteins, it is important to note that their relative expression did not change significantly in the transgenic retinas compared with the control retinas. This observation implies that the post-translational phosphorylation of BAX/BAK proteins is primarily a result of the increase in Jnk expression. In addition, in the developing WT retina, apoptosis appears to initiate the downregulation of Bax and Bak, which are key initiators of the caspase-dependent pathway [49]. The BH3-only BID protein participates in an extrinsic apoptosis that may occur in cone photoreceptor cells [50]. Because this BID protein is considered a component of caspase-8-induced apoptosis, the increase in its expression during P10-P15 may be associated with the elevated gene expression and activation of JNK that eventually cleaves BID into a novel form called tBID. This observation suggests that beginning on P10, JNK may be involved in TNF-mediated caspase-8 activation resulting in the activation of the BID protein followed by mitochondrial-associated apoptosis [51]. However, further investigation is required to confirm this hypothesis.

In general, we determined that other members of the BH3-only family of proteins are involved in retinal degeneration in S334ter-4 RHO rats. Thus, Bik (Bcl2-interacting killer) protein, which is a novel death-inducing protein, is over-expressed significantly in P10 retinas. The higher demand for the Bik protein in transgenic retinas may correlate with the changes in Bcl-xl gene expression. Again, in our study, a modulation of Bcl-xl gene expression in transgenic retinas was not observed. An alternative explanation for the increase in production of the BIK protein is that the elevated expression of the p53 gene in S334ter-4 RHO retinas promotes Bik mRNA expression [52]. In support of this hypothesis, we observed an increase in relative expression of other p53-induced proteins, such as Noxa

and Puma. In P12–P15 S334ter-4 RHO retinas, the levels of Puma and especially Noxa (3-fold increase) are dramatically increased. Following the binding to anti-apoptotic proteins and the activation of Bax/Bak, PUMA-induced apoptosis proceeds through a typical mitochondrial pathway [53]. Therefore, we assume that on P12, the over-expression of Puma associates with the mitochondria membrane permeabilization transition pore (MPTP), which eventually leads to the cleavage and release of the AIFf1 protein and to the activation of caspase (see below). In addition, the increase in Noxa expression correlates with the upregulation of the Hif1α gene, which controls the expression of Noxa, on P10 [54]. Both Bid and PUMA trigger the mitochondrial apoptotic pathway leading to cytochrome C and AIF1 release from the mitochondria as demonstrated in our study (Figure 9).

The expression of the BH3-only Bim protein was elevated from P10 to P15 in S334ter-4 RHO retinas. The BH3-only BIM protein is an important initiator and regulator of the intrinsic pathway because BIM interacts with anti-apoptotic Bcl-2 proteins and the multidomain pro-apoptotic effector proteins BAX and BAK [55]. Because Bcl-2 expression was not modified, the increase in Bim expression may be associated with the upregulation of the Jnk pathway or the downregulation of the pro-survival Erk2 pathway in transgenic retinas. Recently, links between Bim and cJnk and between Bim and Erk signaling have been established [55]. Therefore, a decline in the expression of pro-survival Erk2 in P10 to P21 could regulate the Bim gene expression in S334ter-4 RHO retinas. An additional study has revealed that the level of Bim mRNA is positively regulated by C/EBPa and CHOP following ER stress [56], and this finding is in agreement with our results demonstrating an increase in CHOP expression in S334ter-4 RHO retinas.

Proteasomal degradation and autophagy are the two main mechanisms that control protein clearance in the cell. Unlike proteasomal degradation, autophagy degrades soluble and aggregated proteins. The molecular mechanisms responsible for the regulation of autophagy have not been completely elucidated; however, a recent study has demonstrated that severe hypoxia may lead to ER stress and may induce ATF4-dependent autophagy through LC3 as a survival mechanism [57]. In a study by Wang et al., the over-expression of KDEL (ER resident) receptors also activated autophagy [58]. It is apparent that the upregulation of the UPR genes increases the expression of KDEL receptors on the ER and this could promote autophagy in S334ter-4 RHO photoreceptors. The expression of lysosomal-associated membrane protein 2 or Lamp2 was induced significantly on P10. Our results are in agreement with the study of hypoxia-induced Lamp2 activation [59] in which the authors have proposed that hypoxia induces a high turnover of autophagic generation and degradation in cells.

The activation of calpains in transgenic retinas has been demonstrated [10]. Kaur et al. have shown that in S334ter RHO line 3 (a more rapidly degenerating line), the activation of calpain 3, which was measured using an in situ enzymatic assay on unfixed cryosections reaches a peak on P12. In our study of the S334ter RHO line 4 (a slower degenerating line), we discovered that on P15 the activation of calpains (1 and 2) is already pronounced (2-fold increase) and progresses along with retinal degeneration until P30. Our finding correlates with the study by Kaur et al. proposing that the proteolytic activity of calpains persists at times when the nuclear DNA has already disintegrated [10]. In agreement with these data, we found that the caspase-12 protein was cleaved in P15 S334ter-4 RHO retina as a result of activated calpains. Later, however, its activity measured in P21 and P30

S334ter-4 retinas was diminished. Evidently, transient activation of caspase-12 in P15 retina is sufficient to trigger the ER stress-associated apoptosis to contribute to a self-destructive program in S334ter-4 RHO photoreceptors. In addition, it has been proposed that caspase-12 is not required for caspase-dependent ER stress-induced apoptosis [60].

Therefore, we proposed that active calpains, together with the BH3-only proteins, Noxa, Puma, Bik, and Bid, compromised the MPTP in S334ter-4 RHO retinas and control a mitochondria-induced apoptosis. In support of this hypothesis, we detected the translocation of cleaved AIF1 from the mitochondria to the cytosol in S334ter-4 RHO retinas on P15. This data suggests that the S334ter-4 Rho mitochondria experience MPTP events that provoke caspase-independent apoptosis. To our knowledge, this is the first demonstration of AIF1 release from S334ter-4 RHO mitochondria.

Although we did not observe the cytosolic release of cytochrome C from mitochondria, an increase in the Apaf1 gene expression was detected suggesting the caspase-dependent activation of apoptosis. It is possible that the induction of Apaf1 expression in S334ter-4 RHO retinas is related to the upregulation of the p53 gene that controls APAf1 [61], Bik, Noxa and Puma. Therefore, p53 gene expression and the translocation of p53 to the mitochondria during the progression of ADRP should be examined in S334ter-4 RHO retinas. Despite studies demonstrating that retinal degeneration in rd1 mice occurs independent of p53 [62], others have demonstrated that the p53 gene plays a role in the regulation of photoreceptor apoptosis in inherited retinal degeneration [63], [64].

The expression of photoreceptor-specific transcription factors Nrl and Crx declined steadily in S334ter-4 RHO retinas between P10 and P21 and was reduced significantly in P21 retinas. These results suggest that in addition to the progressive collapse of

photoreceptors in S334ter-4 RHO retinas, the transcriptional inhibition of Nrl and Crx may also take place. For example, it has been proposed that the over-expression of leukemia inhibitory factor (LIF), which is highly induced in developing ADRP mice retinas that express a mutant rhodopsin protein [65], reduces Crx and Nrl-dependent transcription [66]. Another explanation of the transcriptional inhibition of the Nrl and Crx transcription factors is linked to the inhibition of histone deacetylases (HDAC) that are diminished during retinal degeneration [67] and affect the RNA levels of these genes [68]. Apparently, the level of Hdac expression is modified in S334ter-4 RHO retina. In support of this hypothesis we observed the elevation in Apaf1 gene expression (Figure 5) that has been proposed to depend on the Hdac gene expression [61]. The future study of HDAC expression would also shed light on the upregulation of the Apaf1 gene in S334ter-4 RHO photoreceptors.

Our results describe mechanisms by which ER stress may be involved in the retinal pathology of S334ter-4 RHO rats, and how ER stress may be connected to mitochondrial dysfunction (Fig.S1). During hypoxia, the ER homeostasis in S334ter-4 RHO photoreceptors is compromised, which causes the activation of the UPR. The activation of UPR in S334ter-4 RHO photoreceptors leads to the upregulation of caspase-12 and BH3-only pro-apoptotic proteins that together with calpains, affect mitochondrial function. Our study and several other studies, have demonstrated that ER stress- and mitochondria-induced apoptosis culminate in the activation of caspase-3 in S334ter-4 RHO retinas. We believe that the activation of both ER stress- and mitochondria-originated apoptotic signals occur at approximately the same time (P12–P15) during retinal development in S334ter-4 RHO rats. In favor of this hypothesis, the expression of pro-apoptotic Bcl2 genes was

significantly elevated in P12. Future experiments have to be conducted to establish a direct link between activation of the UPR and mitochondrial function in S334ter-4 RHO rats. We also demonstrate that the relative expression of the UPR, pro-apoptotic, and oxidative-related genes in S334ter-4 RHO retinas have a temporal progression between P10 and P18. It is possible that cell death is executed rapidly and even the temporal expression of some genes in the P10–P15 retinas leads to apoptotic cell death. It is important to emphasize that in addition to caspase-dependent apoptosis occurring in S334ter-4 RHO photoreceptors, a caspase-independent pathway is induced by the release of AIF1 from the mitochondria. A study by Hong et al. has demonstrated a direct link between the release of the AIF1 factor from the mitochondria and the over-activation of PARP-1 [69] suggesting that our observation of AIF1 release could be considered as additional proof of a caspase-independent pathway that occurs simultaneously in photoreceptor cells. However, additional studies are needed to determine if AIF1 release contributes to the proposed non-apoptotic cell death in S334ter RHO photoreceptors [10].

Our findings indicate a number of genes that are potential therapeutic targets for ADRP gene therapy in S334ter RHO photoreceptors. This list includes but is not limited to Bik, Bim, Noxa, Puma and Bid proteins, calpains and caspase-12 proteins. Clearly, further studies are required to shed more light on the mechanisms involved in the induction of apoptosis, such as knocking down the expression of these genes in S334ter RHO retinas.

Acknowledgement

We like to thank Mansi Kunte for helping with RNA preparation and qRTPCR. MG acknowledges the support of this work by National Institute of Health (NIH), Hope for Vision and Foundation Fighting Blindness.

References

1. Bowne SJ,Humphries MM,Sullivan LS,Kenna PF,Tam LC,et al. (2011) A dominant mutation in RPE65 identified by whole-exome sequencing causes retinitis pigmentosa with choroidal involvement. Eur J Hum Genet 19(10): 1074–1081.

2. Hernan I,Gamundi MJ,Planas E,Borras E,Maseras M,et al. (2011) Cellular expression and siRNA-mediated interference of rhodopsin cis-acting splicing mutants associated with autosomal dominant retinitis pigmentosa. Invest Ophthalmol Vis Sci 52: 3723–3729.

3. Lee EH,Wu C,Lee EU,Stoute A,Hanson H,et al. (2010) Fatalities associated with the 2009 H1N1 influenza A virus in New York city. Clin Infect Dis 50: 1498–1504.

4. Green ES,Menz MD,LaVail MM,Flannery JG (2000) Characterization of rhodopsin mis-sorting and constitutive activation in a transgenic rat model of retinitis pigmentosa. Invest Ophthalmol Vis Sci 41: 1546–1553.

5. Travis GH (1998) Mechanisms of cell death in the inherited retinal degenerations. Am J Hum Genet 62: 503–508.

6. Chang GQ,Hao Y,Wong F (1993) Apoptosis: final common pathway of photoreceptor death in rd, rds, and rhodopsin mutant mice. Neuron 11: 595–605.

7. Jomary C,Neal MJ,Jones SE (2001) Characterization of cell death pathways in murine retinal neurodegeneration implicates cytochrome c release, caspase activation, and bid cleavage. Mol Cell Neurosci 18: 335–346.

8. Doonan F,Donovan M,Cotter TG (2003) Caspase-independent photoreceptor apoptosis in mouse models of retinal degeneration. J Neurosci 23: 5723–5731.

9. Liu C,Li Y,Peng M,Laties AM,Wen R (1999) Activation of caspase-3 in the retina of transgenic rats with the rhodopsin mutation s334ter during photoreceptor degeneration. J Neurosci 19: 4778–4785.

10. Kaur J,Mencl S,Sahaboglu A,Farinelli P,van Veen T,et al. (2011) Calpain and PARP Activation during Photoreceptor Cell Death in P23H and S334ter Rhodopsin Mutant Rats. PLoS One 6: e22181.

11. Doonan F,Cotter TG (2004) Apoptosis: a potential therapeutic target for retinal degenerations. Curr Neurovasc Res 1: 41–53.

12. Sanges D,Comitato A,Tammaro R,Marigo V (2006) Apoptosis in retinal degeneration involves cross-talk between apoptosis-inducing factor (AIF) and caspase-12 and is blocked by calpain inhibitors. Proc Natl Acad Sci U S A 103: 17366–17371.

13. Wu LM,Tso M,Zhu XA,Guo XJ,Yang LP (2008) [Endoplasmic reticulum stress proteins are activated in rd retinal degeneration]. Zhonghua Yan Ke Za Zhi 44: 807–812.

14. Yang LP,Wu LM,Guo XJ,Tso MO (2007) Activation of endoplasmic reticulum stress in degenerating photoreceptors of the rd1 mouse. Invest Ophthalmol Vis Sci 48: 5191–5198.

15. Lin JH,Li H,Yasumura D,Cohen HR,Zhang C,et al. (2007) IRE1 signaling affects cell fate during the unfolded protein response. Science 318: 944–949.

16. Gorbatyuk MS,Knox T,LaVail MM,Gorbatyuk OS,Noorwez SM,et al. (2010) Restoration of visual function in P23H rhodopsin transgenic rats by gene delivery of BiP/Grp78. Proc Natl Acad Sci U S A 107: 5961–5966.

17. Ryoo HD,Domingos PM,Kang MJ,Steller H (2007) Unfolded protein response in a Drosophila model for retinal degeneration. EMBO J 26: 242–252.

18. Leonard KC,Petrin D,Coupland SG,Baker AN,Leonard BC,et al. (2007) XIAP protection of photoreceptors in animal models of retinitis pigmentosa. PLoS One 2: e314.

19. Pennesi ME,Nishikawa S,Matthes MT,Yasumura D,LaVail MM (2008) The relationship of photoreceptor degeneration to retinal vascular development and loss in mutant rhodopsin transgenic and RCS rats. Exp Eye Res 87: 561–570.

20. Martinez-Navarrete G,Seiler MJ,Aramant RB,Fernandez-Sanchez L,Pinilla I,et al. (2011) Retinal degeneration in two lines of transgenic S334ter rats. Exp Eye Res 92: 227–237.

21. Yokouchi M,Hiramatsu N,Hayakawa K,Okamura M,Du S,et al. (2008) Involvement of selective reactive oxygen species upstream of proapoptotic branches of unfolded protein response. J Biol Chem 283: 4252–4260.

22. Yokouchi M,Hiramatsu N,Hayakawa K,Kasai A,Takano Y,et al. (2007) Atypical, bidirectional regulation of cadmium-induced apoptosis via distinct signaling of unfolded protein response. Cell Death Differ 14: 1467–1474.

23. Dejeans N,Tajeddine N,Beck R,Verrax J,Taper H,et al. (2010) Endoplasmic reticulum calcium release potentiates the ER stress and cell death caused by an oxidative stress in MCF-7 cells. Biochem Pharmacol 79: 1221–1230.

24. Hu P,Han Z,Couvillon AD,Exton JH (2004) Critical role of endogenous Akt/IAPs and MEK1/ERK pathways in counteracting endoplasmic reticulum stress-induced cell death. J Biol Chem 279: 49420–49429.

25. Bravo R,Vicencio JM,Parra V,Troncoso R,Munoz JP,et al. (2011) Increased ER-mitochondrial coupling promotes mitochondrial respiration and bioenergetics during early phases of ER stress. J Cell Sci 124: 2143–2152.

26. Lee W,Kim DH,Boo JH,Kim YH,Park IS,et al. (2005) ER stress-induced caspase-12 activation is inhibited by PKC in neuronal cells. Apoptosis 10: 407–415.

27. Anderson RE,Maude MB,Bok D (2001) Low docosahexaenoic acid levels in rod outer segment membranes of mice with rds/peripherin and P216L peripherin mutations. Invest Ophthalmol Vis Sci 42: 1715–1720.

28. Blackshaw S,Harpavat S,Trimarchi J,Cai L,Huang H,et al. (2004) Genomic analysis of mouse retinal development. PLoS Biol 2: E247.

29. Dorrell MI,Aguilar E,Weber C,Friedlander M (2004) Global gene expression analysis of the developing postnatal mouse retina. Invest Ophthalmol Vis Sci 45: 1009–1019.

30. Feldman DE,Chauhan V,Koong AC (2005) The unfolded protein response: a novel component of the hypoxic stress response in tumors. Mol Cancer Res 3: 597–605.

31. Sevier CS,Kaiser CA (2008) Ero1 and redox homeostasis in the endoplasmic reticulum. Biochim Biophys Acta 1783: 549–556.

32. May D,Itin A,Gal O,Kalinski H,Feinstein E,et al. (2005) Ero1-L alpha plays a key role in a HIF-1-mediated pathway to improve disulfide bond formation and VEGF secretion under hypoxia: implication for cancer. Oncogene 24: 1011–1020.

33. Gess B,Hofbauer KH,Wenger RH,Lohaus C,Meyer HE,et al. (2003) The cellular oxygen tension regulates expression of the endoplasmic oxidoreductase ERO1-Lalpha. Eur J Biochem 270: 2228–2235.

34. Rohwer N,Dame C,Haugstetter A,Wiedenmann B,Detjen K,et al. (2010) Hypoxia-inducible factor 1alpha determines gastric cancer chemosensitivity via modulation of p53 and NF-kappaB. PLoS One 5: e12038.

35. van den Beucken T,Koritzinsky M,Wouters BG (2006) Translational control of gene expression during hypoxia. Cancer Biol Ther 5: 749–755.

36. Griguer CE,Oliva CR,Kelley EE,Giles GI,Lancaster JR Jr,et al. (2006) Xanthine oxidase-dependent regulation of hypoxia-inducible factor in cancer cells. Cancer Res 66: 2257–2263.

37. Grimm C,Hermann DM,Bogdanova A,Hotop S,Kilic U,et al. (2005) Neuroprotection by hypoxic preconditioning: HIF-1 and erythropoietin protect from retinal degeneration. Semin Cell Dev Biol 16: 531–538.

38. Grimm C,Wenzel A,Groszer M,Mayser H,Seeliger M,et al. (2002) HIF-1-induced erythropoietin in the hypoxic retina protects against light-induced retinal degeneration. Nat Med 8: 718–724.

39. Caprara C,Thiersch M,Lange C,Joly S,Samardzija M,et al. (2011) HIF1A is essential for the development of the intermediate plexus of the retinal vasculature. Invest Ophthalmol Vis Sci 52: 2109–2117.

40. Komeima K,Rogers BS,Lu L,Campochiaro PA (2006) Antioxidants reduce cone cell death in a model of retinitis pigmentosa. Proc Natl Acad Sci U S A 103: 11300–11305.

41. Huang CY,Fujimura M,Noshita N,Chang YY,Chan PH (2001) SOD1 down-regulates NF-kappaB and c-Myc expression in mice after transient focal cerebral ischemia. J Cereb Blood Flow Metab 21: 163–173.

42. Milani P,Gagliardi S,Cova E,Cereda C (2011) SOD1 Transcriptional and Posttranscriptional Regulation and Its Potential Implications in ALS. Neurol Res Int 2011: 458427.

43. Yoo HY,Chang MS,Rho HM (1999) The activation of the rat copper/zinc superoxide dismutase gene by hydrogen peroxide through the hydrogen peroxide-responsive element and by paraquat and heat shock through the same heat shock element. J Biol Chem 274: 23887–23892.

44. Geracitano R,Tozzi A,Berretta N,Florenzano F,Guatteo E,et al. (2005) Protective role of hydrogen peroxide in oxygen-deprived dopaminergic neurones of the rat substantia nigra. J Physiol 568: 97–110.

45. Noorwez SM,Sama RR,Kaushal S (2009) Calnexin improves the folding efficiency of mutant rhodopsin in the presence of pharmacological chaperone 11-cis-retinal. J Biol Chem 284: 33333–33342.

46. Hagiwara M,Maegawa K,Suzuki M,Ushioda R,Araki K,et al. (2011) Structural basis of an ERAD pathway mediated by the ER-resident protein disulfide reductase ERdj5. Mol Cell 41: 432–444.

47. Liu Y,Adachi M,Zhao S,Hareyama M,Koong AC,et al. (2009) Preventing oxidative stress: a new role for XBP1. Cell Death Differ 16: 847–857.

48. Szegezdi E,Logue SE,Gorman AM,Samali A (2006) Mediators of endoplasmic reticulum stress-induced apoptosis. EMBO Rep 7: 880–885.

49. Donovan M,Doonan F,Cotter TG (2006) Decreased expression of pro-apoptotic Bcl-2 family members during retinal development and differential sensitivity to cell death. Dev Biol 291: 154–169.

50. Besirli CG,Chinskey ND,Zheng QD,Zacks DN (2010) Inhibition of retinal detachment-induced apoptosis in photoreceptors by a small peptide inhibitor of the fas receptor. Invest Ophthalmol Vis Sci 51: 2177–2184.

51. Deng Y,Ren X,Yang L,Lin Y,Wu X (2003) A JNK-dependent pathway is required for TNFalpha-induced apoptosis. Cell 115: 61–70.

52. Hur J,Bell DW,Dean KL,Coser KR,Hilario PC,et al. (2006) Regulation of expression of BIK proapoptotic protein in human breast cancer cells: p53-dependent induction of BIK mRNA by fulvestrant and proteasomal degradation of BIK protein. Cancer Res 66: 10153–10161.

53. Yu J,Zhang L (2008) PUMA, a potent killer with or without p53. Oncogene 27: Suppl 1S71–83.

54. Kim JY,Ahn HJ,Ryu JH,Suk K,Park JH (2004) BH3-only protein Noxa is a mediator of hypoxic cell death induced by hypoxia-inducible factor 1alpha. J Exp Med 199: 113–124.

55. Hughes R,Gilley J,Kristiansen M,Ham J (2011) The MEK-ERK pathway negatively regulates bim expression through the 3′ UTR in sympathetic neurons. BMC Neurosci 12: 69.

56. Chipuk JE,Moldoveanu T,Llambi F,Parsons MJ,Green DR (2010) The BCL-2 family reunion. Mol Cell 37: 299–310.

57. Rzymski T,Milani M,Pike L,Buffa F,Mellor HR,et al. (2010) Regulation of autophagy by ATF4 in response to severe hypoxia. Oncogene 29: 4424–4435.

58. Wang P,Li B,Zhou L,Fei E,Wang G (2011) The KDEL receptor induces autophagy to promote the clearance of neurodegenerative disease-related proteins. Neuroscience 190: 43–55.

59. Suzuki C,Isaka Y,Takabatake Y,Tanaka H,Koike M,et al. (2008) Participation of autophagy in renal ischemia/reperfusion injury. Biochem Biophys Res Commun 368: 100–106.

60. Obeng EA,Boise LH (2005) Caspase-12 and caspase-4 are not required for caspase-dependent endoplasmic reticulum stress-induced apoptosis. J Biol Chem 280: 29578–29587.

61. Wallace DM,Cotter TG (2009) Histone deacetylase activity in conjunction with E2F-1 and p53 regulates Apaf-1 expression in 661W cells and the retina. J Neurosci Res 87: 887–905.

62. Hopp RM,Ransom N,Hilsenbeck SG,Papermaster DS,Windle JJ (1998) Apoptosis in the murine rd1 retinal degeneration is predominantly p53-independent. Mol Vis 4: 5.

63. Liu B,Zhu X (2000) [Photoreceptor apoptosis and p53 gene expression in inherited retinal degeneration of RSC rats]. Zhonghua Yan Ke Za Zhi 36: 65–68, 69.

64. Ali RR,Reichel MB,Kanuga N,Munro PM,Alexander RA,et al. (1998) Absence of p53 delays apoptotic photoreceptor cell death in the rds mouse. Curr Eye Res 17: 917–923.

65. Joly S,Lange C,Thiersch M,Samardzija M,Grimm C (2008) Leukemia inhibitory factor extends the lifespan of injured photoreceptors in vivo. J Neurosci 28: 13765–13774.

66. Graham DR,Overbeek PA,Ash JD (2005) Leukemia inhibitory factor blocks expression of Crx and Nrl transcription factors to inhibit photoreceptor differentiation. Invest Ophthalmol Vis Sci 46: 2601–2610.

67. Sancho-Pelluz J,Alavi MV,Sahaboglu A,Kustermann S,Farinelli P,et al. (2010) Excessive HDAC activation is critical for neurodegeneration in the rd1 mouse. Cell Death Dis 1: e24.

68. Chen B,Cepko CL (2007) Requirement of histone deacetylase activity for the expression of critical photoreceptor genes. BMC Dev Biol 7: 78.

69. Hong SJ,Dawson TM,Dawson VL (2004) Nuclear and mitochondrial conversations in cell death: PARP-1 and AIF signaling. Trends Pharmacol Sci 25: 259–264.

70. Hiramatsu N,Joseph VT,Lin JH (2011) Monitoring and Manipulating Mammalian Unfolded Protein Response. Methods in Enzymology, Vol 491: Unfolded Protein Response and Cellular Stress, Pt C 491: 183–198.

CHAPTER 3

MODULATION OF CELLULAR SIGNALING PATHWAYS IN P23H RHODOPSIN PHOTORECEPTORS.

by

OLGA SIZOVA, VISHAL SHINDE, AUSTIN R. LENOX and MARINA S. GORBATYUK.

Cellular Signalling

Format adapted for dissertation

MODULATION OF CELLULAR SIGNALING PATHWAYS IN P23H RHODOPSIN PHOTORECEPTORS.

Abstract

We previously reported activation of the unfolded protein response (UPR) in P23H rhodopsin (RHO) retinas a model of autosomal dominant retinitis pigmentosa (ADRP). Knowing that the UPR can trigger Ca^{2+} release from the endoplasmic reticulum and regulate cellular signaling we examined the level of Ca^{2+}-regulated proteins. We also looked for changes in the expression of Bcl2 family proteins, autophagy proteins and the mTOR/AKT pathways, as well as for the induction of mitochondria-associated apoptosis in the P23H RHO retina. Our data demonstrated that the elevation of calpain and caspase-12 activity was concomitantly observed with a decrease in the BCL2-XL/BAX ratio and an increase in mTor levels in the P23H-3 RHO retina suggesting a vulnerability of P23H RHO photoreceptors to apoptosis. The translocation of BAX to the mitochondria, as well as the release of cytochrome *C* and AIF into the cytosol supports this conclusion and indicates the involvement of mitochondria-induced apoptosis in the progression of ADRP. The level of autophagy proteins in general was found to be decreased in the P21–P30 P23H RHO retina. Injections of rapamycin, however, protected the P23H RHO rod photoreceptors from experiencing physiological decline. Despite this fact, the downregulation of mTOR did not alter the level of autophagy proteins. Our results imply that in addition to activation of the UPR during ADRP progression, photoreceptors also experience alterations in major proapoptotic pathways.

Introduction

Retinitis pigmentosa (RP) is a heterogeneous group of eye disorders that result in irreversible blindness. Visual symptoms include night blindness, followed by photopia and decreasing visual fields, leading to tunnel vision and eventually legal blindness [1, 2]. Most frequently autosomal dominant RP (ADRP) is associated with mutations in rhodopsin (RHO), with such mutations accounting for approximately 25% of all ADRP cases [1]. Based on their biochemical and cellular properties, ADRP rhodopsin mutations have been classified into six groups, however most fall into the class I or class II categories [3]. Class I mutations can fold normally, but are not correctly transported to the outer segment. The S334ter RHO protein expressed in transgenic rats represents a Class I mutation. The substitution of proline for histidine at position 23 within the rhodopsin (P23H RHO) gene yields a Class II mutation. These RHO mutants are defective for proper folding. They are retained in the endoplasmic reticulum (ER) and are unable to form a functional chromophore with 11-cis-retinal [4].

In 1990 the P23H RHO mutant was proposed to cause ADRP [5]. Since then, the expression of P23H mutant rhodopsin (RHO) in photoreceptors has been studied in transgenic mice [6-8], rats [9- 11] and frogs [12-14]. Loss of photoreceptors and the course of visual decline have been previously described for rats expressing both the S334ter and P23H *RHO* transgenes (http://www.ucsfeye.net/mlavailRDratmodels.shtml) [15, 16]. However, molecular mechanism involved in the loss of vision in Class I and II mutations has not been studied in detail. Previously, we have demonstrated that activation of the unfolded protein response (UPR) occurs during retinal degeneration in both the S334ter

and P23H RHO rat models [11, 17, 18]. In the S334ter transgenic retina we have also determined that activation of the UPR is associated with increased expression of the JNK, Bik, Bim, Bid, Noxa, and Puma genes and cleavage of caspase-12 that, together with activated calpains, presumably compromise the integrity of the mitochondrial function in ADRP photoreceptors [18]. In P23H-3 *RHO* rats there have been no cellular signaling pathways identified as being involved in the mechanism underlying photoreceptor degeneration with the exception of the UPR [11, 17, 19]. Therefore, there is a critical need to describe any pathways that are modified concomitantly with the activated UPR in P23H-3 *RHO* photoreceptors in order to validate new therapeutic targets.

The UPR is initiated by the activation of three signaling pathways (PERK, ATF6 and IRE1) and is required for controlling ER protein folding capacity and reestablishing homeostasis in the cell. Upon acute or unresolved ER stress, the UPR also triggers apoptosis, which eliminates any cell that is incapable of restoring proper protein folding and orchestrating a coordinated adaptive downstream response. Previously, we demonstrated that P23H-3 RHO photoreceptors have an activated ER stress-induced caspase-7 [17] and a consistent increase in Bip and CHOP gene expression [11]. These results suggested that ER stress persists in P23H-3 RHO photoreceptors, which might stimulate apoptotic signaling in these animals. Subsequently the persistence of the UPR has been confirmed in our other study [11]. However, apart from the UPR, other signaling pathways have been found to originate from the ER and those pathways have not been properly investigated. For example, the Ca^{2+}-mediated signaling pathway could be triggered by the ER stress response leading to activation of calpains and caspase-12 [20, 21]. The Bcl2 family proteins are known to be upregulated during UPR activation via the transcriptional activity of ATF4

and CHOP (Puma, Noxa and Bim). They can also be upregulated by activated JNK, which phosphorylates the BCL-2/BCL-XL proteins and additionally, promotes autophagosome formation by releasing the active beclin-1/PI3K complex from the ER. This complex is known to regulate ATG12–ATG5 formation and to promote the LC3-II conversion during the formation of autophagosomes [22]. Therefore, autophagy, the major degradation pathway after UPR activation in neuronal cells, could also be induced by ER stress. Both the PERK/eIF2α and IRE1 arms of the UPR have been implicated in the regulation of autophagy [23].

mTOR/AKT signaling is another example of a pathway that is tightly regulated by the UPR. We have previously reported that a T17M RHO retina that experiences UPR activation also demonstrates an elevation of mTOR protein and a decrease in phosphorylated AKT [21]. It has been demonstrated that the UPR can activate mTOR via ATF6a signaling [24]. The ATF6 UPR pathway was found to be upregulated in both P23H and T17M RHO retinas [17], [21], thus implying that similar to T17M RHO, P23H RHO photoreceptors could also have modified mTOR/AKT signaling.

Thus, several signaling pathways have been identified that are mediated by the activation of the UPR, which is found in P23H-3 RHO photoreceptors [11, 17, 19]. They could be modified either by ER stress or independently altered to contribute to the mechanism of ADRP. In both scenarios, these signaling pathways could provide alternative therapeutic strategies in the P23H RHO retina in addition to gene therapy against mutant rhodopsin. Therefore, the major focus of this study is to identify whether UPR activation in P23H RHO photoreceptors is accompanied by changes in Ca^{2+}-induced signaling, autophagy,

and mTOR/AKT pathways during ADRP progression and whether alterations in mTOR cellular signaling could be responsible for slowing the rate of retinal degeneration.

Materials and methods

Animal use

All animal procedures conformed to the Association for Research in Vision and Ophthalmology Statement for the Use of Animals in Ophthalmic and Vision Research, and were approved by the Institutional Animal Research Committee of the University of Alabama at Birmingham. The P23H-3 RHO (line 3) rats were kindly provided by Dr. LaVail (UCSF). Rats were housed in specific pathogen-free (SPF) conditions with a 12-hour light and 12-hour dark cycle. Animals were sacrificed by thoracotomy, and retinas were rapidly excised (removal of the lens), placed on an ice-cold plate, and stored at − 80 °C.

RNA preparation and quantitative real-time PCR

Total RNA was isolated from individual SD and P23H-3 RHO (N = 4) retinas using an RNeasy Mini kit (Qiagen, Valencia, CA). We then used a high capacity cDNA reverse transcription kit (Applied Biosystems, Carlsbad, California, USA). Two cDNA reactions were prepared from each RNA sample and 10 ng cDNA was used for qRT-PCR using Applied Biosystems TaqMan assays that were validated for each selected gene on a One Step Plus instrument (Applied Biosystems, Foster City, CA). To analyze the samples, we compared the number of cycles (Ct) needed to reach the midpoint of the linear phase and

normalized all observations to the GAPDH housekeeping gene. The replicated RQ (Relative Quantity) values for each biological sample were averaged.

Retinal protein extract for western blot analysis

We obtained retinal protein extracts from dissected retinas that were sonicated in a buffer containing 25 mM sucrose, 100 mM Tris–HCl, pH = 7.8, and a mixture of protease inhibitors (PMSF, TLCK, aprotinin, leupeptin, and pepstatin). The total protein concentration from individual retinas was measured using a Bio-Rad protein assay, and 40 μg of total protein was used to detect individual proteins. The detection of proteins was performed using an infrared secondary antibody and an Odyssey infrared imager (Li-Cor, Inc.). Antibodies against PUMA (7467S), ATG5 (8540P), ATG7 (78558P), LC3 (#2775), mTOR (2983P), caspase-3 (9662P), caspase-9 (9507S) and caspase7 (9492P) were purchased from Cell Signaling (1:1000). Antibodies against AIF (sc5586), Cytochrome *C* (sc13156), NOXA (sc11718), and active BAX, which detects only the active form of the BAX protein (sc23959) were purchased from Santa-Cruz Biotechnology (1:1000). Anti-caspase-12 (ab62484) and anti-pAKT (ab66138), which detects phosphorylated AKT, were purchased from Abcam (1:1000). We used an anti-BAX antibody (B8429) and an anti-Lamp2 (L0668) antibody from Sigma-Aldrich (1:1000). B-Actin was used as an internal control and was detected using an anti-β-actin antibody (Sigma-Aldrich).

Intraperitoneal injection of rapamycin and ERG analysis

A 10 mg/kg dose of rapamycin was used for injections. A water solution of 5% ethanol, 5% tween-20 and 5% polyethylene glycol 400 was used to dissolve rapamycin and was also used in the vehicle-treated control injections. Starting at P15, daily intraperitoneal

injections (IPs) were performed in rats over the course of 10 days, during which no signs of weight loss were recorded. The *E*lectro*R*etino*G*rams (ERG) of treated and untreated animals were recorded as previously described [25] at P30 and P45, which correlate with 2 and 4 weeks post-treatment, respectively. Briefly, rats were dark-adapted overnight, then anesthetized with ketamine (100 mg/kg) and xylazine (10 mg/kg). Their pupils were dilated in dim red light with 2.5% phenylephrine hydrochloride ophthalmic solution (Akorn, Inc.). The KC UTAS-3000 Diagnostic System (Gaithersburg, MD) was used to perform scotopic ERGs. The measurements were conducted using a wire contacting the corneal surface with 2.5% hypromellose ophthalmic demulcent solution (Akorn, Inc.). The ERG was performed at different intensities including 0 dB (2.5 cd*s/m2), 5 dB (7.91 cd*s/m2), 10 dB (25 cd*s/m2), and 15 dB (79.1 cd*s/m2).

Calpain activity assay

The detection of calpain activity was performed using the Calpain Activity Assay kit from BioVision in accordance with the manufacturer's recommendations. The detection of the cleaved substrate Ac-LLY-AFC was performed using a fluorometer that was equipped with a 400-nm excitation filter and 505-nm emission filter.

Isolation of mitochondria from rat retinas

We separated the cytosolic fraction from the mitochondrial fractions from five individual P23H RHO and SD rats using the Mitochondria Isolation kit for Tissues (Thermo Scientific). The mitochondria were separated from the cytoplasm using the Dounce stroke method as recommended by the manufacturer. The protein concentration for each fraction was determined using a Bio-Rad protein assay. To confirm the absence of mitochondrial

contamination in the cytoplasmic fractions, western blot was done using a COXIV antibody (Abcam). To confirm the absence of cytosolic contamination in the mitochondrial fractions, western blotting with an anti-actin antibody was employed (Sigma-Aldrich).

Results

We previously described the activation of the ER stress response in P23H-3 RHO rat retinas at P30 [17]. For this reason, the modulation of the other cellular signaling pathways in the P23H RHO photoreceptor was primarily studied at P30 and P40.

The hallmarks of Ca^{2+}-induced signaling are upregulated in deteriorating P23H-3 RHO photoreceptors

We investigated the expression of Calpain 1 and 2, as well as Caspase-12, and found no differences in calpain 1 or 2 mRNA compared with controls. However, we did observe significant differences in the caspase-12 gene expression at P21, P30 and P40 (Fig. 1A). At each time point, caspase-12 mRNA was induced by more than 2-fold compared to SD. At P21, the relative caspase-12 expression was 3.67 ± 1.03 in P23H RHO vs. 1.60 ± 0.49 in arbitrary units (a.u.) in SD, $P < 0.05$. At P30 it was 3.76 ± 0.18 in P23H RHO vs. 1.38 ± 0.19 a.u. in SD, $P < 0.05$ and at P40 it was 2.36 ± 0.17 in P23H RHO vs. 1.04 ± 0.09 a.u. in SD, $P < 0.05$.

An analysis of activated calpain 1 and 2 demonstrated that at P30 and the activation of calpains was 30% higher in P23H RHO retinas compared to SD (0.45 ± 0.02 in P23H

RHO photoreceptors vs. 0.34 ± 0.02 in SD a.u., P = 0.01) (Fig. 1B). Cleavage of caspase-12 in P23H RHO retinas was 2.6-fold higher compared to SD (0.36 ± 0.06 in P23H photoreceptors vs. 0.14 ± 0.03 in SD a.u., P = 0.02) (Fig. 1C).

The expression of Bcl-2 family proteins is modulated in P23H-3 RHO retina We analyzed Bcl-2 family protein expression by western blot analysis (Fig. 2) and found that the level of anti-apoptotic BCL2-XL protein was decreased in transgenic retinas by 0.6-fold (0.15 ± 0.02 in P23H RHO photoreceptors vs. 0.24 ± 0.003 in SD a.u.) at P30 and by 0.4-fold (0.095 ± 0.01 in P23H RHO photoreceptors vs. 0.23 ± 0.07 in SD a.u., P < 0.05) at P40.

Alternatively, the expression of proapoptotic BH3-only proteins, such as BAX and PUMA, increased over time. The level of BAX was dramatically increased (136-fold) at P30 (0.68 ± 0.18 in P23H photoreceptors vs. 0.005 ± 0.002 in SD a.u., P < 0.0001). At P40, BAX protein levels were significantly decreased (0.003 ± 0.0002 in P23H RHO photoreceptors vs. 0.002 ± 0.0002 in SD a.u.). PUMA protein was not statistically different compared to SD at P30 (0.059 ± 0.01 in P23H RHO photoreceptorsvs. 0.060 ± 0.005 in SD a.u.), but at P40, its expression was significantly elevated by 1.7-fold (0.09 ± 0.004 in P23H photoreceptors vs. 0.05 ± 0.006 in SD a.u., P < 0.01). The level of NOXA protein decreased over time. However, this decrease was not statistically significant compared to SD at P30 (0.004 ± 0.0004 in P23H RHO photoreceptors vs. 0.005 ± 0.0007 in SD a.u.). At P40, the level of Noxa was reduced by 40% (0.003 ± 0.0002 in P23H photoreceptors vs. 0.005 ± 0.0007 in SD a.u., P < 0.05).

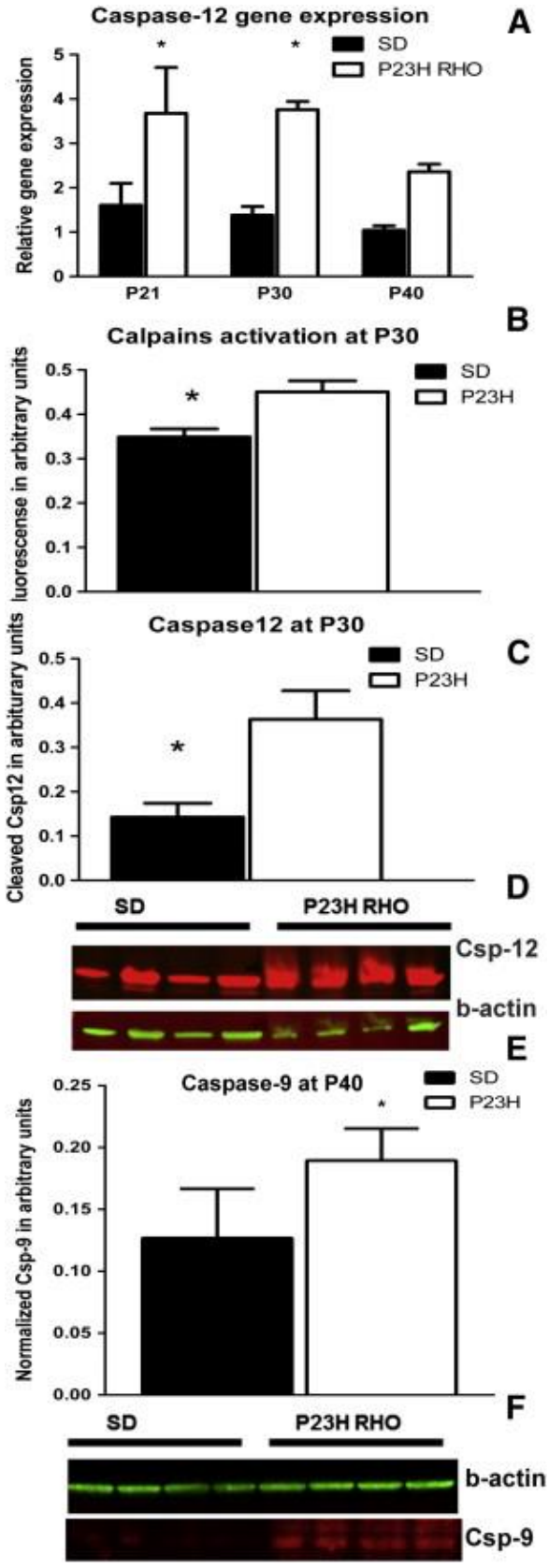
Caspase-12 gene expression
A
SD
P23H RHO
Relative gene expression
P21
P30
P40
B
Calpains activation at P30
SD
P23H
luorescense in arbitrary units
C
Caspase12 at P30
SD
P23H
Cleaved Csp12 in arbituary units
D
SD
P23H RHO
Csp-12
b-actin
E
Caspase-9 at P40
SD
P23H
Normalized Csp-9 in arbitrary units
F
SD
P23H RHO
b-actin
Csp-9

Fig.1.The activation of calpains, ER stress-induced caspase-12 and apoptotic protease activating factor-1-mediated caspase-9. (A) Relative caspase-12 gene expression in progressive P23H RHO retina. We analyzed caspase-12 gene expression by two-way ANOVA and found that at P21, P30 and P40 there was a greater-than 2-fold overexpression of caspase-12 mRNA in transgenic retinas ($P < 0.05$), N = 4. (B) We used the calpain μ and m activity assay, analyzed the results by a non-parametric t-test and found that the amount of the cleaved calpain substrate, Ac-LLY-AFC, was increased by 32% in transgenic retinas, N = 4. (C) The amount of cleaved caspase-12 was also elevated by 157% in P23H RHO retinas. (D) Images of western blots probed with anti-caspase-12 and anti-β-actin antibodies, N = 4. (A–C) These data suggest that calpain and caspase-12 are activated in the P23H RHO retina at P30 and point toward excessive cytosolic Ca^{2+} content that could perhaps result from persistent ER stress. (E) Detection of cleaved-9 in P40 transgenic retinas. We analyzed retinal protein extracts at P40 and found that the level of cleaved-9 was elevated in P23H RHO retina. The cleavage of caspase-9 was 40% higher in transgenic retina compared to SD ($P < 0.05$) and was coincided with the release of cytochrome C and AIF from the P23H RHO mitochondria. (F) Images of western blots probed with anti-caspase-9 and anti-β-actin antibodies, N = 4.

Initiation of mitochondria-induced apoptosis in P23H RHO photoreceptors

We separated the mitochondrial fraction of photoreceptor cells from the cytosol in order to analyze mitochondrial cytochrome C release and the translocation of AIF into the cytosol (Fig. 3). We found that as early as P21 there was accumulation of cytochrome C in the cytosol of P23H RHO retina photoreceptors (0.053 ± 0.011vs. 0.022 ± 0.005 in SD in a.u., P = 0.02). We also found the release of the AIF protein from mitochondria to cytosol. The cytochrome C and the AIF1 releases from the mitochondria were in agreement with elevation of the cleaved caspase-9 by 40% (0.19 ± 0.01 in P23H RHO photoreceptors vs. 0.12 ± 0.01 in SD in a.u., P = 0.03) at P40, (Fig. 1E, F.)

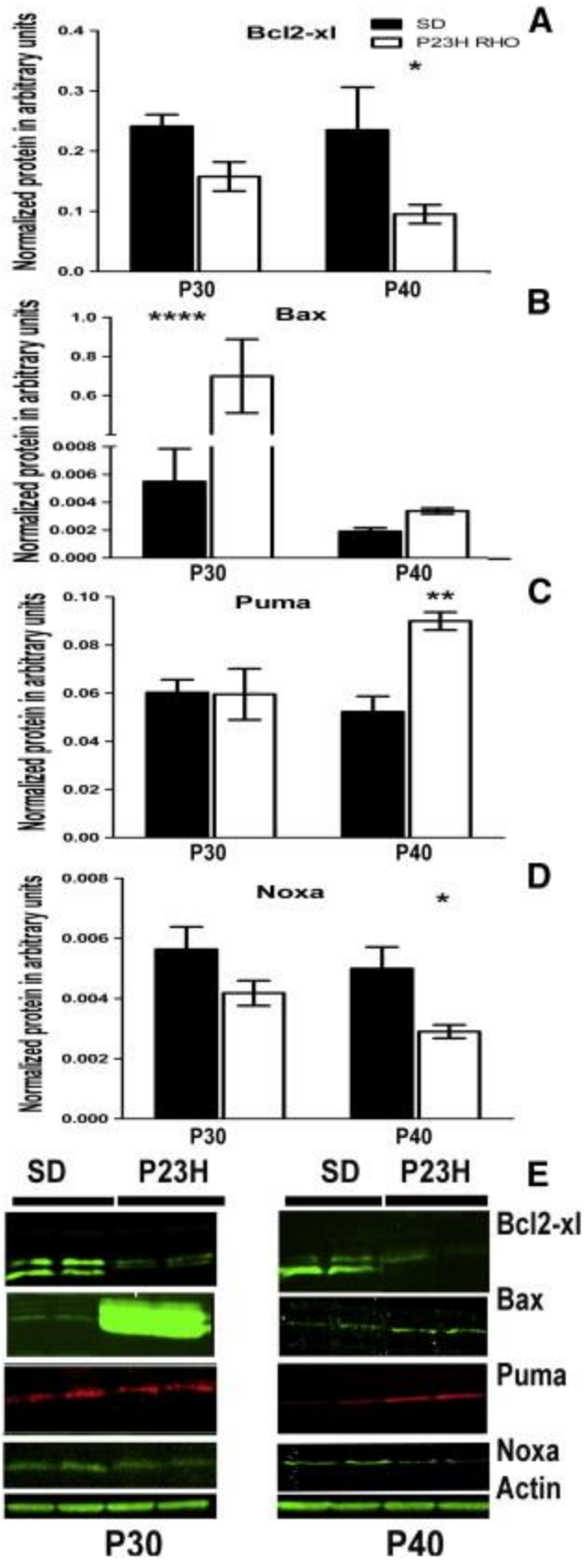
A
Bcl2-xl
SD
P23H RHO
*
Normalized protein in arbitrary units
0.4
0.3
0.2
0.1
0.0
P30
P40
B
Bax
****
1.0
0.8
0.6
0.008
0.006
0.004
0.002
0.000
C
Puma
**
0.10
0.08
0.06
0.04
0.02
0.00
D
Noxa
*
0.008
0.006
0.004
0.002
0.000
E
SD
P23H
Bcl2-xl
Bax
Puma
Noxa
Actin
P30
P40

Fig.2. Changes in the expression of Bcl2 family proteins in the progressive ADRP retina. (A) We analyzed retinal protein extracts from SD and P23H RHO rats by two-way ANOVA and found that the BCL2-XL protein was downregulated at P30 and P40 in P23H RHO photoreceptors. At P40, we observed a 59% reduction in the amount of BCL2-XL protein ($P < 0.05$), $N = 4$. (B) BAX protein was significantly elevated by 1270% ($P < 0.0001$) at P30 and by 73% at P30 in the P23H RHO retina, $N = 4$. (C, D) PUMA and NOXA proteins had a unique pattern of expression. (C) The PUMA protein was elevated by 73% at P40 ($P < 0.01$) and (D) NOXA was diminished by 41% at P40 ($P < 0.05$), $N = 4$. (E) Images of western blots probed with ant-Bcl2-xl, BAX, PUMA, NOXA and β-actin antibodies, $N = 4$.

We also found that BAX translocated to the mitochondria in P23H RHO photoreceptors at P40 and that the level of oligomerized BAX protein in the mitochondria of transgenic rats was 4.7-fold higher than in SD (0.047 ± 0.008 vs. 0.011 ± 0.005 in a.u., $P = 0.009$).

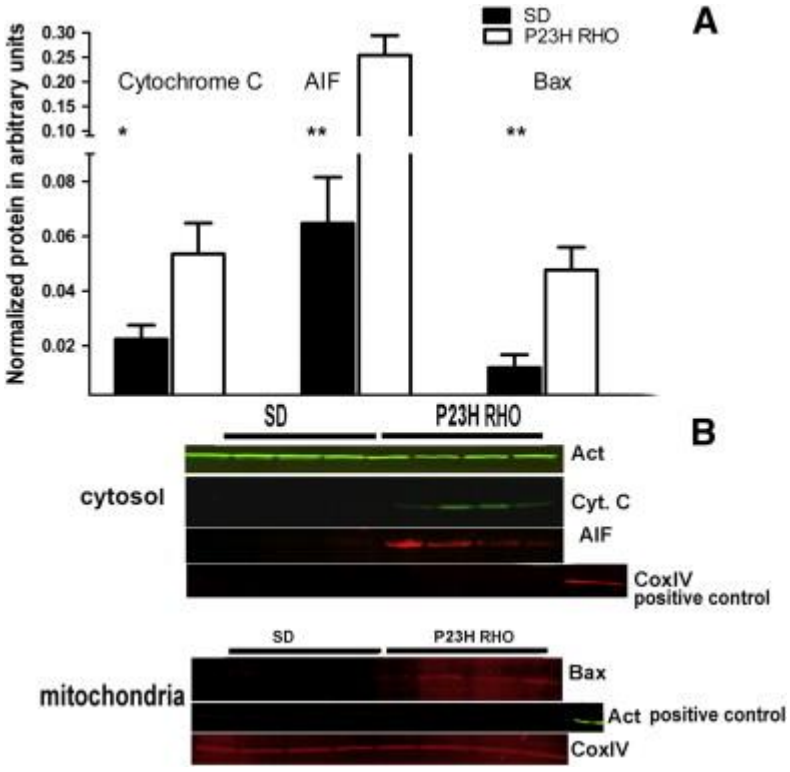

Fig. 3. Mitochondria-induced apoptosis in the P23H RHO retina. We separated the retinal cytosolic and mitochondrial fractions (N = 4) and analyzed the cytosolic fraction by probing western blots with antibodies against cytochrome C and cleaved AIF. (A) Using a non-parametric t-test, we found that at P21 there was a release of cytochrome C from the P23H RHO mitochondria to the cytoplasm. The observed density was 140% higher in transgenic cytosol samples compared to SD ($P = 0.02$). In addition, we observed a release of cleaved AIF from P23H RHO mitochondria The observed density for the corresponding band was 290% higher in P23H RHO rats compared to SD, ($P = 0.002$). At P40, we detected the translocation of BAX protein into the mitochondria of P23H RHO photoreceptors. The density for the corresponding band was 327% higher in transgenic photoreceptors than in SD ($P = 0.009$). The observed time point for this translocation (P40) does not exclude the possibility that BAX protein translocates to the mitochondria at earlier time points. (B) Western blot images for blots treated with anti-cytochrome C, AIF and BAX antibodies experiment with running anti-β-actin control for the mitochondrial fraction (two last lanes are positive controls) and COXIV control for the cytoplasmic fraction (two last gels are positive controls).

Autophagy is modified in the ADRP retina

The SD and P23H-3 RHO RNA extracts from P13, P21, P30, P40 and P60 retinas were analyzed to detect expression of the Atg5, Atg7, Lamp2 and Lc3 autophagy genes (Fig. 4A). The results of this experiment demonstrated that the pattern of autophagy gene expression was not uniform. For example, in P13 retinas expression of Atg7 and Atg5 genes was increased by 2.3 ± 0.14 and 1.6 ± 0.29 fold, ($P < 0.0001$ and $P < 0.5$), respectively while expression of the Lamp2 was only 0.43 ± 0.11, $P < 0.05$ of SD. At P21, expression of Atg5, LC3 and Lamp2 was significantly increased and was 3.18 ± 0.22, $P < 0.0001$, 2.33 ± 0.18, $P < 0.0001$ and 4.05 ± 0.39, $P < 0.0001$, respectively compared to SD, however, expression of Atg7 did not differ significantly from SD retinas. At P30, Atg7 and Lc3 gene expression remained elevated by 1.74 ± 0.19, $P < 0.01$ and 1.75 ± 0.19, $P < 0.01$, respectively while expression of the Lamp2 and Atg5 genes was downregulated. At P40 expression of all the genes, except Atg5, was significantly upregulated and was 1.6 ± 0.15, $P < 0.05$; 1.90 ± 0.30, $P < 0.05$ and 3.06 ± 0.27, $P < 0.0001$ fold higher than SD

for Atg7, Lamp2 and Lc3, respectively. By P60 expression of all genes was reduced, however only the decrease in Atg5 gene expression was significant. (0.5 ± 0.13 of SD $P < 0.05$).

We tested protein extracts from SD and P23H RHO retinas and found that the changes in the protein level of ATG5, ATG7, LAMP2 and LC3 did not correlate with alterations in the autophagy gene expression over the time (Fig. 4B). For example, all proteins with the exception of ATG5 at P30 and LC3 at P60 were either not significantly changed or significantly downregulated compared to SD. ATG5 was elevated by more than 3-fold (0.28 ± 0.023 in SD vs. 1.01 ± 0.078 in P23H-3 RHO, in a.u., $P < 0.0001$ at P30) and was downregulated by nearly 2-fold (0.45 ± 0.029 in SD vs. 0.247 ± 0.040 in P23H-3 RHO a.u., $P < 0.01$) at P60.

ATG7 was significantly diminished at both the P30 and P60 time points and was 0.45 ± 0.074 in SD vs. 0.22 ± 0.044 in P23H-3 RHO a.u., $P < 0.001$ and 0.25 ± 0.015 in SD vs. 0.058 ± 0.0128 a.u. in P23H-3 RHO, $P < 0.01$, respectively. LAMP2 was also downregulated at P30 by over 50% and was 1.17 ± 0.17 in SD vs. 0.59 ± 0.093 in P23H-3 RHO a.u., $P < 0.05$. In contrast, the LC3 protein showed an increase of 64% at P60 and was 1.88 ± 0.21 in SD vs. 3.03 ± 0.27 in P23H-3 RHO in a.u., $P < 0.01$

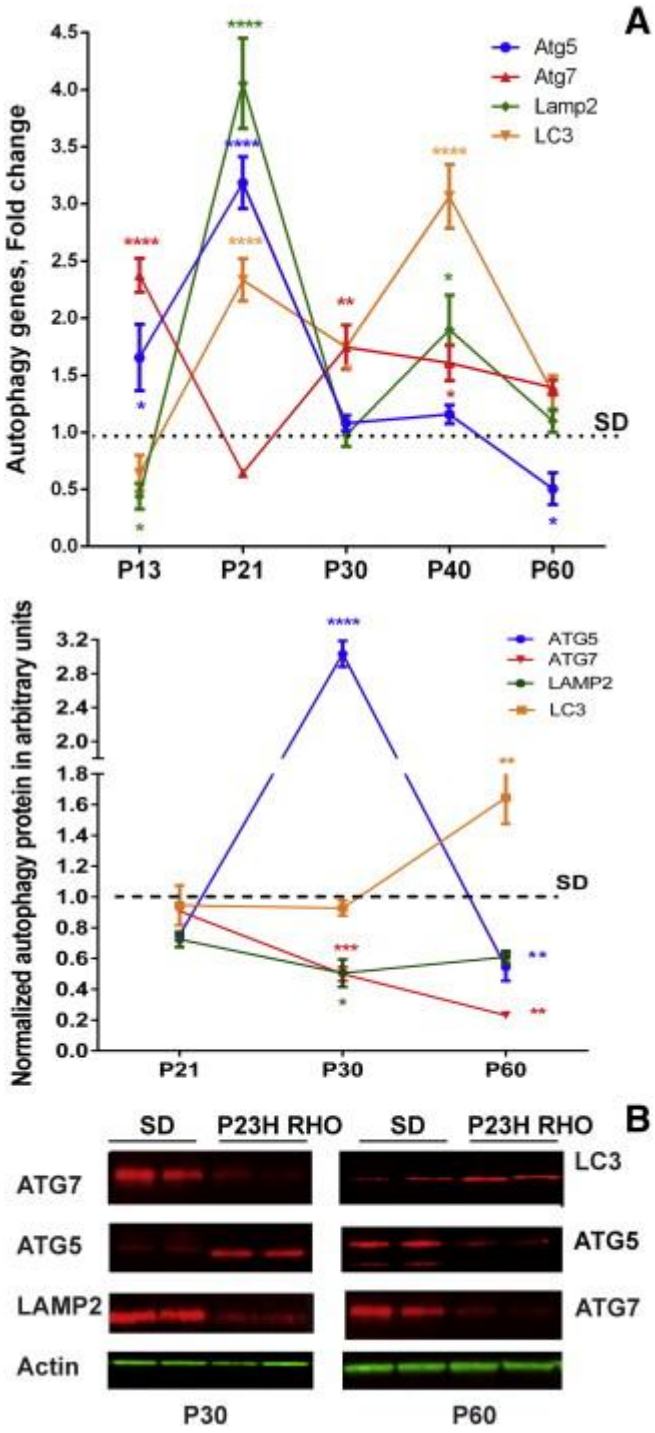

Fig. 4. Autophagy gene and protein expression are modified in P23H-3 RHO photoreceptors in a multiphasic manner. (A) Atg5, Atg7, Lamp2 and Lc3 gene expression in P13, P21, P30, P40 and P60 P23H RHO retinas (N = 4). At P13, expression of Atg5 and Atg7 was upregulated in ADRP photoreceptors by 1.6 and 2.4-fold respectively, while expression of Lamp2 was downregulated by 2-fold. At P21, expression of all genes, except Atg7, was upregulated by 3-, 4- and 2.3-fold for Atg5, Lamp2 and Lc3,

respectively. At P30, expression of ATG7 was the only one significantly higher compared with controls. At P40, Atg7, Lamp2 and Lc3 gene expression was significantly elevated by 1.6-, 1.9- and 3.0-fold. At P60, expression of all genes was similar to SD with the exception of Atg5, which was downregulated by 2-fold. (B) The level of ATG5, ATG7, LAMP2 and LC3 proteins was detected in P21, P30, P40 and P60 P23H-3 RHO retinas (N = 4) and the pattern of protein expression was found to be different from that of mRNA. At P21, no difference in ATG5, ATG7, LC3 and LAMP2 protein was observed in ADRP photoreceptors. At P30, we found that ATG5 protein levels were increased by 3.1-fold while levels of ATG7 and LAMP2 protein were decreased by 40% and by 50%, respectively. At P60, the level of LC3 protein was 60% higher in ADRP photoreceptors vs. SD photoreceptors, which was significant.

mTOR/AKT signaling is modified in progressive P23H RHO photoreceptors

We analyzed mTOR and phosphorylated AKT (pAKT) in P30 and P40 retinas and found that the level of mTOR protein was elevated in P23H RHO animals by 290% at P30 (0.029 ± 0.002 vs. 0.01 ± 0.009 in SD a.u.), $P < 0.05$ and by 430% at P40 (0.009 ± 0.003vs. 0.002 ± 0.0003 in SD a.u.) (Fig. **5**). In contrast, pAKT protein was significantly downregulated by 75% at P30 (0.013 ± 0.002 in P23H photoreceptors vs. 0.051 ± 0.009 in SD a.u.), $P < 0.001$ and by 44% at P40 (0.026 ± 0.04 in P23H photoreceptors vs. 0.046 ± 0.005 in SD a.u.), $P < 0.05$.

Injection of rapamycin decreases the level of mTOR and slows the rate of retinal degeneration

Knowing that rapamycin could modify mTOR signaling, we performed IP injections in P23H-3 RHO rats. Fig. 6 demonstrates results of the scotopic ERG analysis in RP-treated and V-treated rats. Analysis of scotopic ERGs revealed that a-wave amplitude was slightly increased in the RP-treated P23H-3 RHO rats at 2 weeks post-treatment (216 ± 8.8 in V-treated vs. 245 ± 11.98 in RP-treated retinas) and was increased by 40% in P23H-3RHO

rats at 4 weeks post-treatment compared with controls (176.4 ± 9.4 in V-treated vs. 249 ± 16.5 in RP-treated), $P < 0.05$. The b-wave amplitude of the scotopic ERG and the a-

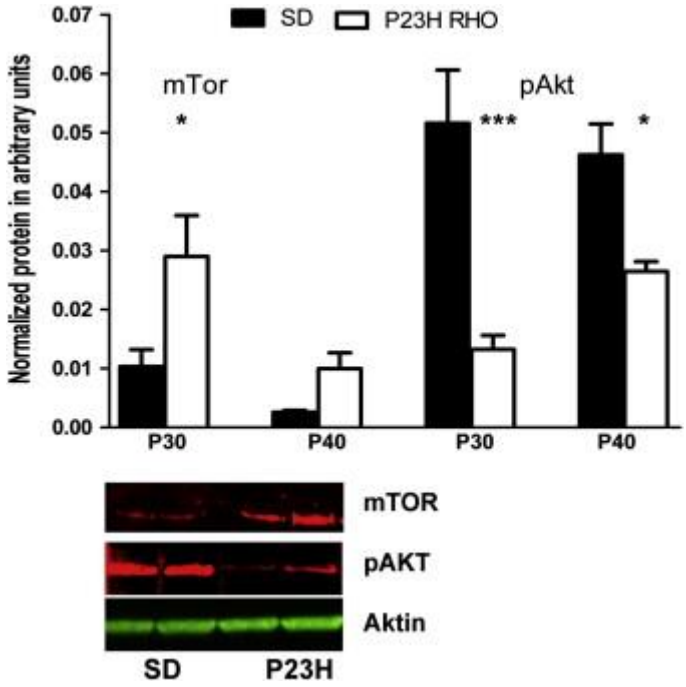

Fig. 5. The mTOR/AKT pathway is modified in the progressive ADRP retina. We analyzed retinal protein extracts from SD and P23H RHO rats by two-way ANOVA and determined that mTOR protein expression was significantly elevated in the P23H RHO retina at P30 (by 290%; $P < 0.05$), $N = 4$. The level of pAKT was reduced at P30 by 75% ($P < 0.001$) and at P40 by 44% ($P < 0.05$), $N = 4$. Bottom: Images of western blots for P23H-3 RHO and SD at P30 probed with anti-mTOR, pAKT and β-Actin antibodies.

and b-wave amplitudes of the photopic ERG did not change in the RP-treated P23H-3 RHO rats. Analysis of retinal protein extracts demonstrated that the mTOR protein was downregulated in RP-treated animals by nearly 2-fold (0.18 ± 0.02 in RP-treated rats vs. 0.34 ± 0.008 in V-treated animals, $P = 0.012$.)

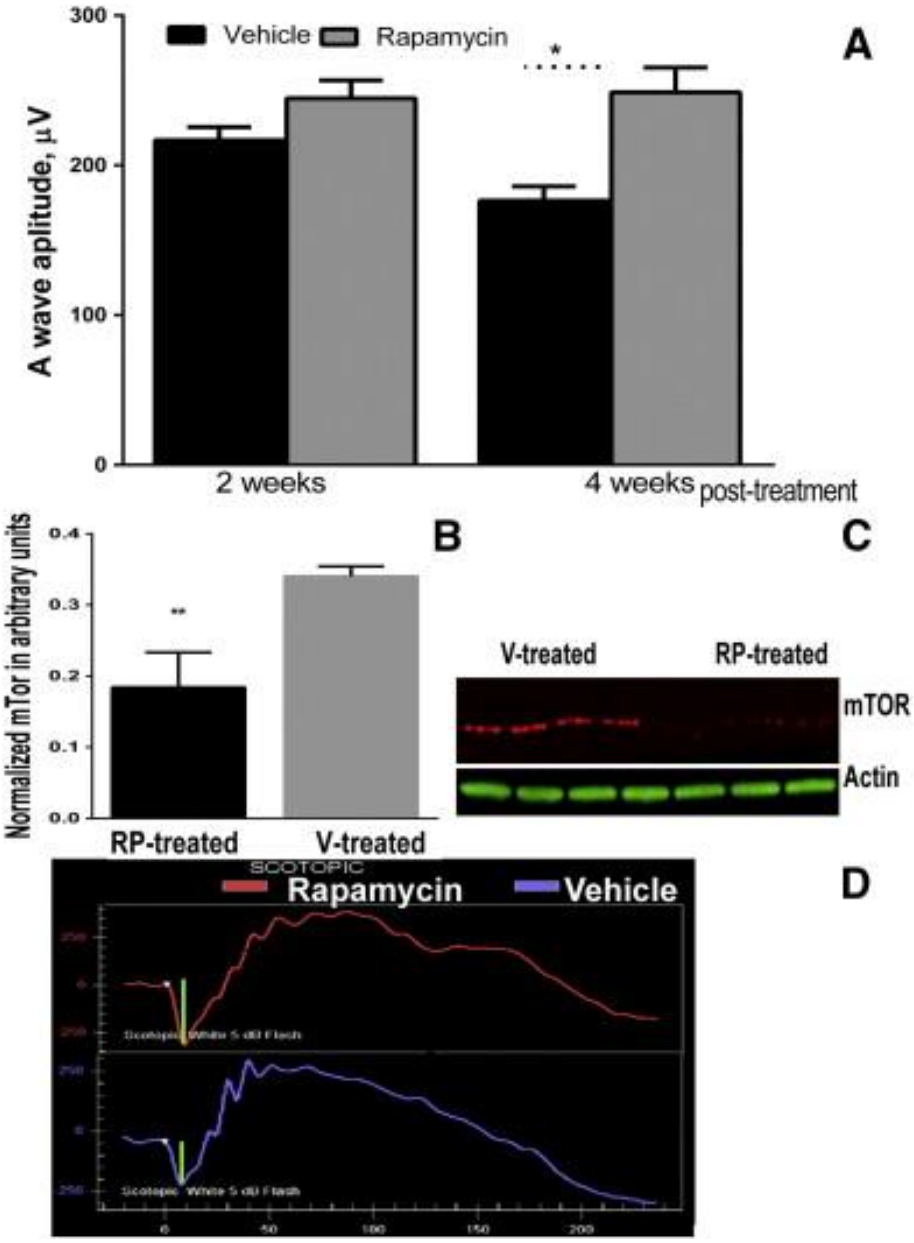

Fig. 6. Injection with rapamycin slows the decline of scotopic a-wave ERG amplitude. (A) A 40% increased in a-wave amplitude of scotopic ERGs was observed in P23H-3 RHO rats IP-injected with rapamycin (RP) (N = 8) vs. vehicle (V)-injected (N = 6) rats, $P < 0.05$. There was no difference between a-wave amplitudes in RP-treated animals at 2 and 4 weeks while V-treated rats demonstrated a continued decline in a-wave amplitude. The B-wave amplitude in rats treated with rapamycin was not changed (not shown). (B). IP-injected

rapamycin led to a decrease in mTOR levels in the P23H-3 RHO retina after 2 weeks post-treatment. Nearly a 2-fold decrease in the level of mTor was observed in RP-treated animals, P = 0.012. (C) Images of blots probed with anti-mTor and β-actin antibodies (D) Images of the scotopic ERG amplitudes registered at 0 dB or 2.5 $cd^{*}s/m^{2}$ in RP- and V-treated P23H RHO rats.

Discussion

Apoptosis has been shown to be the common pathway of photoreceptor cell death in several animal models of inherited retinal degeneration [26]. For example, in rd mice carrying mutant rod cGMP phosphodiesterase, the photoreceptors were found to die by apoptosis. In S334ter and P23H RHO rats, strong activation of calpain and poly-(ADP-ribose) polymerase (PARP), concomitant with calpastatin downregulation, increased oxidative DNA damage and accumulation of PAR polymers was strictly correlated with the temporal progression of retinal degeneration [27]. We have previously reported UPR activation in both mutant RHO transgenic rat models. Therefore, because the UPR might affect general signaling networks in photoreceptor cells, this study focused on some of the pathways that have been reported to be tightly controlled by the UPR.

Supporting the hypothesis of a persistent UPR in P23H-3 RHO photoreceptors, the induction of Ca^{2+} signaling was observed at P30. The observed activation of calpain and caspase-12 at P30 suggests that Ca^{2+} release from the persistent UPR may occur. Calpain activity is highly controlled in vivo by multiple mechanisms, including phosphorylation by PKA, which negatively regulates calpain activity, and an endogenous inhibitor, calpastatin [28]. Therefore, the activation of calpain in P23H-3 RHO photoreceptors implies either excessive cytosolic Ca^{2+} and/or downregulation of PKA. Neither of these phenomena has thus far been tested in the P23H RHO retina.

The level of Bcl2 family proteins was also altered during the activated UPR in P23H-3 RHO retina. For example, the anti-apoptotic BCL2-XL protein was reduced at P30 and

P40, which is indicative of the induction of transcriptional CHOP during UPR activation, as has been previously shown in P23H-3 RHO retinas [17] and [19]. Elevated CHOP may negatively regulate BCL2-XL gene expression [29]. In addition, p53 could be upregulated and, together with TATA binding protein, negatively control Bcl-2 gene expression by binding to the Bcl2 promoter TATA sequence [30]. Alternatively, the BAX protein was highly upregulated at P30, which suggests that the BAX/BCL2-XL ratio is significantly increased in transgenic rats. This in turn could determine the vulnerability of P23H-3 RHO photoreceptors to apoptosis that was confirmed in our experiments by detection of the cleaved caspase-12 and -9. In addition, we found that the BAX protein translocated to the mitochondria at P40 leading to disrupted mitochondrial activity. The observed time point for translocation (P40) does not exclude the possibility that BAX translocated at earlier time points. In line with this hypothesis, we observed the release of cytochrome C and AIF from the mitochondria to the cytosol of P23H RHO photoreceptors at P21. It is thus possible that this translocation could occur much earlier.

Other BH3-only proteins such as PUMA and NOXA also demonstrated altered expression at P30 and P40. Surprisingly, their changes in P23H-3 RHO photoreceptors were distinct. If the PUMA protein was increased at P40, then NOXA was decreased. Both proteins are well-known p53-inducible proapoptotic members and could participate in cell signaling differently [31]. For example, in normal cells, the disrupted MPTP induced by PUMA, but not NOXA, is mediated in part by a Ca^{2+} release from the ER [31]. However, upon expression of an oncoprotein such as E1A, induction of MPTP by NOXA occurs in cells in an ER-independent manner [31]. This fact provides additional evidence that the ER stress-induced release of Ca^{2+} to the cytosol occurs in the P23H RHO retina.

Autophagy has been implicated in various diseases including cancer, neurodegenerative diseases, pathogen invasion, as well as muscle and liver disorders. Interestingly, autophagy has been shown to be both beneficial and harmful [32]. In photoreceptor cell death, autophagy participates in the initiation of apoptosis [33] via a mechanism that in part depends on the Fas receptor. Autophagy has been shown to occur in photoreceptors as part of the basal processing of rod outer segments [34], as well as in animal models of hereditary retinal degeneration [35]. In our study we found that expression of autophagy-associated mRNAs was upregulated in the P23H-3 RHO retina and demonstrated a dynamic expression profile with a major increase in mRNA expression at P21. However, the UPR has been previously shown to be activated at P30 in P23H-3 RHO retina, and the PERK signaling pathway could perhaps be activated even earlier, leading to an upregulation of autophagy-related genes [36]. Regardless, by P60 a drop in the expression of autophagy-related genes was observed. However, the ER stress-induced Bip and CHOP mRNAs are significantly higher in P23H-3 RHOretinas at P60 as compared to SD [11]. That would suggest that a cellular mechanism other than the UPR controls autophagy gene expression in P23H-3 RHO photoreceptors.

Interestingly, protein levels of the corresponding autophagy genes did not mimic the dynamic alterations seen in the gene expression of the P23H-3 RHO retina. Recently, it was demonstrated that only 40% of the variation in protein concentration could be explained by knowing mRNA levels [37]. The remaining 60% of the variation in protein concentration could be determined by the rate of production and degradation of the participating molecules including the stability of mRNA. The role of miRNAs and RNA-binding proteins as potential mechanisms for regulating protein abundance was recently

highlighted [37] and the influence of miRNA deregulation on chaperone-mediated autophagy was also revealed [38]. In the P23H-3RHO retina we observed a significant increase in autophagy gene expression at P21 that did not result in elevated levels of autophagy proteins. Moreover, at P30 the downregulation of LAMP2 and ATG7 proteins was observed. The only exception was ATG5 that was elevated more than 3-fold compared to controls at P30. Perhaps, ATG5 translation was not as affected by posttranslational modifications compared to ATG7, LAMP2 and LCA3 proteins whose levels may have been inhibited by either RNA–protein binding or by protein–protein interactions. Therefore, the elevated ATG5 protein level at P30 is a consequence of an increase in its mRNA at P21. For example, it was recently proposed that β-catenin could negatively regulate autophagy by suppressing formation of the autophagosome and forming the β-catenin–LC3 complex [39]. Another example is p62 that binds directly to LC3 leading to degradation of p62- and LC3-positive bodies [40]. This could happen in addition to a well-known negative regulation of autophagy by mTOR, Bcl2, Beclin1 and p53 [41]. In agreement with these findings we found significant upregulation of mTOR protein at P30.

mTOR/AKt is known to be a negative regulator of autophagy [42], and its activity could attenuate autophagy and initiate lysosomal reformation. Recently, it has been found that during photoreceptor apoptosis in retinal degeneration in rd mice, the AKT survival pathway is inactivated [43]. In our ADRP rat model, we also observed downregulation of pAKT, which suggests that the inactivation of this pathway might have contributed to photoreceptor cell death. Thus, mTOR is highly upregulated in P30 P23H RHO retinas, which is in agreement with the activation of ATF6 [17]. With respect to the UPR, these data suggest that P30 is a critical time point for P23H-3 RHO photoreceptors, at which the

decision is made by the cell whether or not to prolong the UPR and to switch from pro-survival to pro-death UPR signaling. For this reason, we decided to modulate the mTOR protein using peritoneal injections of rapamycin. We found that the injections lead to an increase in the scotopic a-wave ERG response at 4 weeks after treatment. However, this treatment protected photoreceptors from further functional decline instead of rescuing vision in ADRP rats. It also needs to be mentioned that only the rod photoreceptor cells were sensitive to this treatment and that photopic ERG response, typical for cone photoreceptors was not altered. This would suggest that the major biochemical imbalance associated with an increase in mTOR occurs specifically in rod photoreceptors and that downregulation of mTOR benefits the ADRP rods expressing P23H RHO.

Surprisingly, we found that inhibition of mTOR in treated retinas did not lead to an increase in autophagy protein production and that the ATG5, ATG7, LAMP2 or LC3 proteins were not altered. This fact would suggest that while downregulation of mTOR is sufficient to protect the P23H-3 RHO photoreceptors from functional decline to some degree, proteins other than mTOR are also able to negatively regulate the level of autophagy in the P23H-3 RHO retina.

Conclusions

The current findings demonstrate that modulation of cellular networking occurs in P23H RHO photoreceptors concomitantly with the activation of the UPR. We demonstrated that during ADRP progression, mTOR/AKT and autophagy signaling, along with the expression of Bcl2-family proteins, was altered, and that these alterations coincided with changes in Ca^{2+}-regulated calpain and caspase-12 activation. In addition, we found that BAX translocated to the mitochondria and that this appeared to lead to mitochondria-induced apoptosis during ADRP progression. These data indicate the potential link between activation of the UPR and modulation of cellular signaling networks in P23H-3 RHO photoreceptors. However, additional experiments, including the modulation of UPR signaling by activating or inhibiting individual UPR arms in P23H-3 RHO retinas are necessary to uncover their relationships in the progressive ADRP retina. These results also point to a potential therapeutic target for blocking ADRP progression in P23H-3 RHO rats. Using mTOR inhibitors such as rapamycin that have been successfully tested in mice [44], [45] and [46], and now in rats, could be a promising therapeutic approach for treating ADRP.

Acknowledgements

This work was supported by National Institute of Health Grant RO1EY020905, The Foundation Fighting Blindness Grant and the VSRC Core Grant P30 EYoo3039.

References

[1]. Hartong DT, Berson EL, Dryja TP. Lancet. 2006; 368:1795–1809. [PubMed: 17113430]

[2]. Hamel C. Orphanet Journal of Rare Diseases. 2006:1.

[3]. Mendes HF, van der Spuy J, Chapple JP, Cheetham ME. Trends Mol Med. 2005; 11:177–185. [PubMed: 15823756]

[4]. Mendes HF, Zaccarini R, Cheetham ME. Adv Exp Med Biol. 2010; 664:317–323. [PubMed: 20238031]

[5]. Dryja TP, McGee TL, Reichel E, Hahn LB, Cowley GS, et al. Nature. 1990; 343:364–366. [PubMed: 2137202]

[6]. Goto Y, Peachey NS, Ripps H, Naash MI. Invest Ophthalmol Vis Sci. 1995; 36:62–71. [PubMed: 7822160]

[7]. Roof DJ, Adamian M, Hayes A. Invest Ophthalmol Vis Sci. 1994; 35:4049–4062. [PubMed: 7960587]

[8]. Olsson JE, Gordon JW, Pawlyk BS, Roof D, Hayes A, et al. Neuron. 1992; 9:815–830. [PubMed: 1418997]

[9]. LaVail MM. Proc Natl Acad Sci U S A. 2000; 97:11488–11493. [PubMed: 11005848]

[10]. Lewin AS, Drenser KA, Hauswirth WW, Nishikawa S, Yasumura D, et al. Nat Med. 1998; 4:967–971. [PubMed: 9701253]

[11]. Kroeger H, Messah C, Ahern K, Gee J, Joseph V, et al. Invest Ophthalmol Vis Sci. 2012; 53:7590–7599. [PubMed: 23074209]

[12]. Haeri M. PLoS One. 2012; 7:e30101. [PubMed: 22276148]

[13]. Tam BM, Moritz OL. J Neurosci. 2007; 27:9043–9053. [PubMed: 17715341]

[14]. Tam BM, Moritz OL. Invest Ophthalmol Vis Sci. 2006; 47:3234–3241. [PubMed: 16877386]

[15]. Chrysostomou V, Stone J, Valter K. Invest Ophthalmol Vis Sci. 2009; 50:2407–2416. [PubMed:19117918]

[16]. Pennesi ME, Nishikawa S, Matthes MT, Yasumura D, LaVail MM. Exp Eye Res. 2008; 87:561–570. [PubMed: 18848932]

[17]. Gorbatyuk MS. Proc Natl Acad Sci U S A. 2010; 107:5961–5966. [PubMed: 20231467]

[18]. Shinde VM, Sizova OS, Lin JH, LaVail MM, Gorbatyuk MS. PLoS One. 2012; 7:e33266. [PubMed: 22432009]

[19]. Lin JH, Li H, Yasumura D, Cohen HR, Zhang C, et al. Science. 2007; 318:944–949. [PubMed:

17991856]

[20]. Kitamura M. Am J Physiol Renal Physiol. 2008; 295:F323–F334. [PubMed: 18367660]

[21]. Choudhury S, Bhootada Y, Gorbatyuk O. Cell Death Dis. 2013; 4:e528. [PubMed: 23470535]

[22]. Rodriguez D, Rojas-Rivera D, Hetz C. Biochim Biophys Acta. 2011; 1813:564–574. [PubMed: 21122809]

[23]. Doyle KM, Kennedy D, Gorman AM, Gupta S, Healy SJ, et al. J Cell Mol Med. 2011; 15:2025–2039. [PubMed: 21722302]

[24]. Appenzeller-Herzog C, Hall MN. Trends Cell Biol. 2012; 22:274–282. [PubMed: 22444729]

[25]. Nashine S, Bhootada Y, Lewin AS. PLoS One. 2013; 8:e63205. [PubMed: 23646198]

[26]. Jomary C, Neal MJ, Jones SE. Mol Cell Neurosci. 2001; 18:335–346. [PubMed: 11640892]

[27]. Kaur J, Mencl S, Sahaboglu A, Farinelli P, van Veen T, et al. PLoS One. 2011; 6:e22181.

[PubMed: 21765948]

[28]. Wu HY, Tomizawa K, Matsui H. Acta Med Okayama. 2007; 61:123–137. [PubMed: 17593948]

[29]. McCullough KD, Martindale JL, Klotz LO, Aw TY, Holbrook NJ. Mol Cell Biol. 2001;

21:1249–1259. [PubMed: 11158311]

[30]. Wu Y, Mehew JW, Heckman CA, Arcinas M, Boxer LM. Oncogene. 2001; 20:240–251.

[PubMed: 11313951]

[31]. Shibue T, Suzuki S, Okamoto H, Yoshida H, Ohba Y, et al. EMBO J. 2006; 25:4952–4962.

[PubMed: 17024184]

[32]. Codogno P. Cell Death Differ. 2005; 12(Suppl. 2):1509–1518. [PubMed: 16247498]

[33]. Kunchithapautham K, Rohrer B. Autophagy. 2007; 3:433–441. [PubMed: 17471016]

[34]. Reme CE. Albrecht Von Graefes Arch Klin Exp Ophthalmol. 1977; 203:261–270. [PubMed:

303474]

[35]. Kunchithapautham K, Rohrer B. Autophagy. 2007; 3:65–66. [PubMed: 17102584]

[36]. B'Chir W, Maurin AC, Carraro V, Averous J, Jousse C, et al. Nucleic Acids Res. 2013; 41:7683–7699. [PubMed: 23804767]

[37]. Vogel C, Marcotte EM. Nat Rev Genet. 2012; 13:227–232. [PubMed: 22411467]

[38]. Alvarez-Erviti L, Seow Y, Schapira AH, Rodriguez-Oroz MC, Obeso JA, et al. Cell Death Dis.2013; 4:e545. [PubMed: 23492776]

[39]. Petherick KJ, Williams AC, Lane JD, Ordonez-Moran P, Huelsken J, et al. EMBO J. 2013; 32:1903–1916. [PubMed: 23736261]

[40]. Pankiv S, Clausen TH, Lamark T, Brech A, Bruun JA, et al. J Biol Chem. 2007; 282:24131–24145. [PubMed: 17580304]

[41]. Liang C. Cell Death Differ. 2010; 17:1807–1815. [PubMed: 20865012]

[42]. Yu L, McPhee CK, Zheng L, Mardones GA, Rong Y, et al. Nature. 2010; 465:942–946.[PubMed: 20526321]

[43]. Jomary C, Cullen J, Jones SE. Invest Ophthalmol Vis Sci. 2006; 47:1620–1629. [PubMed:16565401]

[44]. Kunchithapautham K, Coughlin B, Lemasters JJ, Rohrer B. Invest Ophthalmol Vis Sci. 2011;52:2967–2975. [PubMed: 21273550]

[45]. Zhao C, Yasumura D, Li X, Matthes M, Lloyd M, et al. J Clin Invest. 2011; 121:369–383.[PubMed: 21135502]

[46]. Zhao C, Vollrath D. Aging. 2011; 3:346–347. [PubMed: 21483039]

CHAPTER 4

UNFOLDED PROTEIN RESPONSE-INDUCED DYSREGULATION OF CALCIUM HOMEOSTASIS PROMOTES RETINAL DEGENRATION IN RAT MODELS OF AUTOSOMAL DOMINANT RETINITIS PIGMENTOSA.

by

VISHAL SHINDE, PRAVALLIKA KOTLA, CHRISTIANNE STRANG and MARINA S. GORBATYUK.

Submitted to Cell Death and Disease

Format adapted for dissertation

UNFOLDED PROTEIN RESPONSE-INDUCED DYSREGULATION OF CALCIUM HOMEOSTASIS PROMOTES RETINAL DEGENRATION IN RAT MODELS OF AUTOSOMAL DOMINANT RETINITIS PIGMENTOSA**.**

Abstract

The molecular mechanism of autosomal dominant retinitis pigmentosa (ADRP) in rats is closely associated with a persistently activated unfolded protein response (UPR). If unchecked, the UPR might trigger apoptosis, leading to photoreceptor death. One of the UPR-activated cellular signaling culminating in apoptotic photoreceptor cell death is linked to an increase in intracellular Ca^{2+}. Therefore, we validated whether ADRP retinas experience a cytosolic Ca^{2+} overload, and whether sustained UPR in the wild-type retina could promote retinal degeneration through Ca^{2+}mediated calpain activation. We performed an *ex-vivo* experiment to measure intracellular Ca^{2+} in ADRP retinas as wells as to detect the expression levels of proteins that act as Ca^{2+}-sensors. In separate experiments with the subretinal injection of tunicamycin (UPR inducer) and a mixture of calcium ionophore (A231278) and thapsigargin (SERCA2b inhibitor) we assessed the consequences of a sustained UPR activation and increased intracellular Ca^{2+} in the wild-type retina, respectively by performing scotopic ERG, histological, and western blot analyses. Results of the study revealed that induced UPR in the retina activates calpain-mediated signaling and increased intracellular Ca^{2+} is capable of promoting retinal degeneration. A significant decline in ERG amplitudes at 6 weeks post treatment was associated with photoreceptor cell loss that occurred through calpain-activated CDK5pJNK-Csp3/7 pathway. Similar calpain activation was found in ADRP rat retinas. A

2-fold increase in intracellular Ca^{2+} and up- and down-regulations of ER membrane-associated Ca^{2+}-regulated IP3R channels and SERCA2b transporters were detected. Therefore, sustained UPR activation in the ADRP rat retinas could promote retinal degeneration through increased intracellular Ca^{2+} and calpain mediated apoptosis.

Introduction

Rat models of autosomal dominant retinitis pigmentosa (ADRP), the S334ter and P23H RHO rats expressing truncated and mutant mouse rhodopsins, experience severe retinal degeneration. The ADRP progression in these animals is characterized by an activated unfolded protein response (UPR) and the mitochondrial dysfunction (1-3). Recent work conducted with ADRP mice models has revealed that the persistently activated UPR could be responsible for promoting retinal degeneration via the activation of an inflammatory response(4). However, in addition to modulated expression of interleukins IL-1b and IL-6 cytokines, the activated UPR may promote cytotoxicity through Ca^{2+} depletion from the ER, thus affecting the function of the mitochondria(5).

It is known that the ER serves as the primary store and regulator of Ca^{2+} in cells governing protein synthesis, gene expression, secretion, metabolism, and apoptosis(6). Therefore, the ER disturbance results in a release of Ca^{2+} into the cytosol, after which free Ca^{2+} can be either transported to the mitochondria or directly activate cytotoxic cellular pathways(7). The findings support the fact that Ca^{2+} transport from the ER to mitochondria plays a significant role in regulating cellular bioenergetics, the production of reactive oxygen species, the induction of autophagy, and apoptosis (8-10).

It has been found that in photoreceptors, different cellular compartments demonstrate a marked variation in Ca^{2+} concentrations, perhaps associated with their varying functions, including the transduction of photon energy into an electrical signal and transcriptional,

translational, metabolic, and synaptic properties (11). For example, the cGMP-regulated cyclic-nucleotide-gated cation channels (CNGCs) regulated by the phototransduction cascade and the voltage-gated calcium channels (VGCCs) regulated by light-induced cell membrane hyperpolarization. CNGCs and VGCCs are located on the outer segments (OS) and in the cell body and synaptic terminal, respectively. In addition, store-operated calcium entry (SOCE) channels in the plasma membrane, sarco/endoplasmic reticulum Ca^{2+}-ATPase transporters (SERCA), inositol triphosphate receptors (IP3), and ryanodine receptors in the ER, and the voltage dependent anion channels (VDAC) in the mitochondria have also been shown to contribute to the regulation of intracellular Ca^{2+}in photoreceptors(12, 13).

Thus, Ca^{2+}-induced cell death in addition to apoptotic cell death has been proposed to occur in the outer nuclear layer (ONL) of the retina of transgenic animals mimicking human retinal degeneration (14).

There are several studies supporting the hypothesis that Ca^{2+}-induced photoreceptor cell death plays a crucial role in ADRP pathogenesis. D-cis-diltiazem, the CNGC and VGCC Ca^{2+} channel antagonist, has been reported to delay the kinetics of rod degeneration in rd1 mice (15). An alternative therapeutic strategy inhibiting calpain activity has been also successfully applied to retard ADRP progression (16-18). Despite the fact that progress has been made in understanding the significance of Ca^{2+} overload in degenerating photoreceptors, direct evidence of Ca^{2+} overload in ADRP photoreceptors has not been provided. Importantly, the role of an activated UPR in promoting Ca^{2+}-mediated cytotoxicity in degenerating photoreceptors and has not been studied yet.

Therefore, we hypothesized that a persistently activated UPR contributes into an intracellular Ca^{2+}overload in ADRP retinas and a cytosolic Ca^{2+} overload triggers a loss of photoreceptor function, eventually leading to photoreceptor cell death in rat models of ADRP.

Materials and Methods

Ethics statement

The animal protocol was carried out with approval from the Institutional Animal Care and Use Committee at the University of Alabama at Birmingham and in accordance with the guidelines of the Association for Research in Vision and Ophthalmology statement for the use of Animals in Ophthalmic and Vision Research. All efforts were made to minimize the number and the suffering of the animals used.

Animal models

Homozygous S334ter RHO (line 4) and P23H RHO (line 3) transgenic rats were maintained in the UAB housing facility and were bred with wild-type (WT) Sprague-Dawley (SD) rats to generate heterozygous S334ter-4 RHO and P23H-3 RHO rats. Therefore, the SD rats were used as WT controls in our experiments. The animals were sacrificed on postnatal days (P) P13, P21, P30, P40, and P60 for RNA, protein analyses, calcium measurement, and photoreceptor isolation. All rats were maintained in specific pathogen-free (SPF) conditions with a 12-hour light and 12-hour dark daily cycle.

Measurement of cytosolic calcium concentrations in photoreceptors.

Retinas were harvested from S334ter, P23H, and SD rats under a dissecting microscope in dim red light. The retinas were incubated with Ca^{2+} indicator dye Fluo4 AM (Life technologies, F14201- 10uM) and Calcein redorange AM to detect viable cells (Life technologies C34851- 5 uM) for 90 minutes in Ames media at 36ºC (Sigma; pH 7.4, equilibrated with 95% O_2 and 5% CO_2) and Pluronic acid (Life Technologies P6866-10 uM). Retinas were flat mounted to orient the photoreceptor cell side upwards in the perfusion chamber (perfused 2–4 ml/min with oxygenated Ames media at 36ºC). Flat mounted retinas were imaged using infrared light on a Zeiss Axioskop microscope equipped with a 40X long working distance water-immersion objective. Fluo4 fluorescence was measured using a 488-nm excitation light from an Excite light source to detect fluorescence from free calcium. Viable cells were identified by Calcein fluorescence in response to a 577-nm excitation light, Fluorescence images were acquired with an Axiocam hRM camera and Axiovision 4.6 software. Fluorescence levels of individual photoreceptors from all rat strains were measured and quantified from the fluorescence images of flat mount retinas using Image J. Only individual viable photoreceptors with both Calcein AM and Fluo4 AM fluorescence were counted.

RNA preparation and real-time PCR analysis

Retinas from SD, S334ter-4 RHO, and P23H-3 RHO rats were isolated at P13, P21, P30, P40, and P60. Total RNA was isolated from the individual retinas from each strain using Trizol (N= 5). cDNA was prepared using a cDNA Reverse transcription kit (Applied Biosystems) from the RNA extracts of SD, S334ter-4 RHO, and P23H-3 RHO retinas. Each cDNA (20 ng) was subjected to qRT-PCR using Applied Biosystems TaqMan assays

(validated for each selected gene) on a One Step Plus instrument (Applied Biosystems, Foster City, CA) to compare the number of cycles (Ct) needed to reach the midpoint of the linear phase. All observations were normalized to the GAPDH housekeeping gene. The replicated RQs (Relative Quantity) values for each biological sample were averaged. Biological samples from each strain were used for the qPCR data analysis.

Retinal protein extract for Western blot analysis

Retinal protein extracts were obtained from dissected retinas by sonication in a buffer containing 25 mM of sucrose, 100 mM of Tris-HCl, pH = 7.8, and a mixture of protease inhibitors (PMSF, TLCK, aprotinin, leupeptin, and pepstatin). The total protein concentration in the right and left retinas from individual rat pups was measured using a Biorad protein assay, and 40 μg of total protein was used to detect individual proteins. The detection of proteins was performed using an infrared secondary antibody and an Odyssey infrared imager (LiCor, Inc.). Antibodies against phosphorylated (p) IP3R (#S1756), Calpastatin (#4146S), M-Calpain (#2556S), and P-SAPK/JNK (46668P) are from Cell Signaling Technology. Serca2b (#ab2861), Calcineurin (ab3673), antibodies were purchased from Abcam. Bax inhibitor 1 was obtained from Novus Biologicals (#NBP2-24912), antibodies against Bip (#sc-1050) and CDK5 (SC173) from Santa Cruz; and B actin from Sigma Aldrich (#A1978). All antibodies we used at a dilution of 1:1000.

Intravitral injection

Two different treatment groups were generated by intravitreal drug injections. In the 1st group, SD rats at P21 were injected intravitreally with UPR inducer Tunicamycin (2ug

Sigma T7765) and contralateral eyes were injected with vehicle. Retinas were extracted at postinjection days 1, 4, and 8 from injected eyes and compared for the protein expression of the markers of calcium-induced apoptosis with Western blot. In the next treatment, different groups of SD rats at P21 were injected intravitreally with calcium ionophore A23187 (500 ng Sigma #C7522) and Thapsigargin (100ng Sigma #T9033) together. Injected animals were analyzed for retinal functional testing (ERG) 2, 4, and 6 weeks following the injection as well as for the activation of calcium-induced apoptosis 36 hours after injection.

Scotopic ERG

Rats were dark-adapted overnight, then anesthetized with ketamine (100 mg/kg) and xylazine (10 mg/kg). The pupils were dilated in dim red light with 2.5% phenylephrine hydrochloride ophthalmic solution (Akorn, Inc.). Scotopic ERGs were recorded using a wire contacting the corneal surface with 2.5% hypromellose ophthalmic demulcent solution (Akorn, Inc.). The ERG was performed at the following light intensities: −20 dB (0.025 cd*s/m^2), −10 dB (0.25 cd*s/m^2), 0 dB (2.5 cd*s/m^2), 5 dB (7.91 cd*s/m^2), 10 dB (25 cd*s/m^2), and 15 dB (79.1 cd*s/m^2). Five scans were performed and averaged for each light intensity. The a-wave amplitudes were measured from the baseline to the peak in the cornea-negative direction, and the b-wave amplitudes were determined from the cornea-negative peak to the major cornea-positive peak. The signal was amplified, digitized, and stored using the LKC UTAS-3000 Diagnostic System (Gaithersburg, MD).

Calpain activity assay

The detection of calpain activity was performed using the Calpain Activity Assay kit from BioVision according to the manufacturer's recommendations. The activation of calpains in intravitreal drug-injected (calcium ionophore and thapsigargin) and vehicle-injected SD retinal tissues was compared. The detection of the cleavage substrate Ac-LLY-AFC was performed in a fluorometer that was equipped with a 400-nm excitation filter and 505-emission filter (Perkin Elmer 1420 multilabel counter Victor^3 V).

Caspase-3/7 activity assay

Caspase-3/7 activity was measured using Caspase-3/7-Glo assay system kit from Promega (# G8090) as per the manufacturer's instructions. The retinal protein extract of intravitreal drug- (calcium ionophore and thapsigargin) and vehicle-treated SD animals were compared for caspase-3/7 activity. The luminescent signal generated from caspase cleavage by substrate was measured in a luminometer (Perkin Elmer 1420 multilabel counter Victor^3 V).

Histological analysis

Rats were euthanized using a CO_2 chamber. The eyeballs were enucleated, affixed in 4% freshly made paraformaldehyde (Cat# S898-09 J.T.Baker, Phillipsburg, NJ, USA), and kept at 4 °C for 8 h. Then, the eyes were hemisected and the eyecups were transferred to fresh PBS to remove formaldehyde and then immersed in a 30% sucrose solution for cryoprotection. Eyecups were then embedded in a cryostat compound (Tissue TEK OCT, Sakura Finetek USA, Inc., Torrance, CA, USA) and frozen at −80 °C. Twelve-micron sections were obtained using a cryostat. To count the nuclei of photoreceptors, we stained cryostat-sectioned retinas with H&E using an H&E stain Kit (Cat#3490). Other slides

were used for immunohistochemistry. Digital images of the right and left retinas of individual rats were taken, and the outer segment length was analyzed in the central superior and inferior retinas, located equidistant from the ONH. Images were analyzed by an investigator blinded to the experimental conditions. All sections were examined on a microscope equipped with a digital camera (Carl Zeiss Axioplan2 Imaging microscope B000707, Carl Zeiss, Gottingen, Germany).

Immunohistochemical analysis

Twelve-micron sections were obtained and fixed on polylysine treated glass slides. Slides were warmed for 30 min at 37 °C and washed in 0.1 M PBS for 10 min three times. Slides were kept in blocking buffer with 10% normal goat serum and 0.3% Triton solution for 1 h at room temperature and washed with PBS three times. The sections were incubated with primary antibody for VDAC (cell signaling #4866S) at 4 °C overnight. The slides were then washed three times with PBS and incubated with secondary antibody for 1 h at room temperature. After washing, the sides were cover slipped using a mounting medium containing DAPI and allowed to dry for 1 h. Images were using a wide-field fluorescence microscope (Carl Zeiss Axioplan2 Imaging microscope B000707, Carl Zeiss, Gottingen, Germany).

Photoreceptor isolation

Petri dishes were incubated for 2 hours at 37^{o}C with 2.5ug/cm^{2} anti WGA directed against Wheat germ agglutinin (WGA) lectin (vector laboratories Burlingame California). Anti WGA was diluted in 25mM of bicarbonate buffer (pH 8), with 0.9% NaCl and 2 mg/ml of BSA. After 3 washes with warm bicarbonate buffer, the dishes were consequently

coated with 5 ug/cm^2 of WGA lectin (vector laboratories) diluted in bicarbonate buffer and incubated for 2 hours at 37^{o}C. After incubation, the petri dishes were washed with warm PBS and stored in 0.2% BSA in PBS until used.

The retinas from 30-day-old SD rats were harvested under dim red light, and the retinas were suspended in cold Hybernate A media (Life technologies). Each retina was transferred to a tube with 1 ml of HybA and warmed for 8 minutes at 37^{o}C in a water bath. The warmed HybA media was aspirated, and the retina was incubated with Papain (0.06 mg/ml Worthington biochemical, Lakewood, NJ) in HybA for 20 minutes at 37^{o}C in a water bath with gentle shaking every 10 minutes. Papain solution was aspirated and 1 ml of 2% FBS solution in HybA was added to the retina and incubated for 5 minutes at room temperature to stop the enzymatic reaction. FBS solution was aspirated and Neurobasal (NBA) media supplemented with 1:50 B27 and 0.5 mM of L-Glutamine was added to the tissue. For the dissociation of the retinal cells, the treated retinas were manually pipetted (gently 5–6 times) using 1000 µl and 200 µl tips. The retinal suspension containing dissociated cells was collected.

The retinal suspension was placed on lectin-coated petri dishes and incubated for 30 minutes at 37^{o}C with gentle swirling every 10 minutes. After incubation, non-adherent cells were removed by washing them with serum-free NBA media. The attached cells were dissociated with pipetting and seeded with 4 X 10^5 cm^2 in NBA media supplemented with B27 and Glutamine.

Semi-quantitative RT-PCR

Semi-quantitative RT-PCR was performed with cDNAs prepared from photoreceptors isolated from the WT rats. PCR products were detected using 1% agarose gel and UV light based imager (Life Technology).

MTT assay

Cell viability was assessed by a 3-(4, 5-dimethylthiazol- 2-yl)-2-5-diphenyl tetrazolium bromide (MTT) assay. Then, $1X10^5$ cells per well were seeded into 96-well micro-culture plates at 37°C with 5% CO2 and allowed to attach for 24 h. Cells were treated with designated doses of Tunicamycin for 48 hr and incubated with MTT at a final concentration of 0.5 mg/ ml for 4 h before the completion of the exposure time at 37°C. The formation of MTT to formazon crystals by viable cells was assessed using 200 μL/well of DMSO at room temperature for 15 min. Optical density was measured at 490 nm using a micro-plate reader model 680 (Bio-Rad, CA, USA). The reduction in viability of cells in each well was expressed as the percentage of control cells.

Statistical analysis

Two-way ANOVA comparisons were used to calculate the statistical significance of differences in fold-change of mRNA expression and levels of pIP3R protein in rats. A one-way ANOVA test was used to calculate the statistical significance of differences in levels of normalized proteins in P21 ADRP retinas and Ca^{2+} detection in ADRP photoreceptors. For comparisons of protein levels and Ca^{2+} detection in Tn-injected and controlled retinas we used the Student's *t*-test. To calculate the statistical significance of differences in the a- and b-wave ERG amplitudes, a two-way ANOVA was applied. For

all experiments, a P-value lower than 0.05 was considered to be significant (*P<0.05, **P<0.01, ***P<0.001, ****P<0.0001).

Results

Transgenic S334ter and P23H RHO rats experience a cytosolic Ca^{2+} increase in their photoreceptors.

Previous studies from our lab have shown that the S334ter and P23H Rho rats have retinal degeneration associated with persistently activated UPR and disrupted mitochondrial function resulting in calpain activation and the release of cytochrome C and AIF from mitochondria.(1, 2). However, it has been demonstrated that activation of the calpain system requires intracellular Ca^{2+} concentrations of at least tens of μM (19) while the intracellular Ca^{2+} concentrations in dark adapted photoreceptors range only from 300-500 nM (20). However, direct evidence of Ca^{2+} overload in photoreceptor cells has not yet been provided. Therefore, we started the ex-vivo study detecting free cytosolic Ca^{2+} in the photoreceptors of S334ter and P23H RHO rats.

However, before detection of the Ca^{2+} load in ADRP retinas with ongoing UPR, we validated the methods for Ca^{2+} measurement and provided proof of principle that the activated UPR causes cytosolplasmic Ca^{2+} overload. Initially, we performed subretinal injections of P30 SD rats with tunicamycin (Tn) in one eye and vehicle in contralateral eye and detected the level of cytoplasmic Ca^{2+} in the photoreceptors. Fig. 1 and Table S2 present the results of the study evidencing that the activated UPR provokes Ca^{2+} overload in the cytosol of photoreceptors.

Next, we measured the cytosolic Ca^{2+} level in the photoreceptors of both S334ter and P23H RHO retinas and demonstrated that both ADRP retinas shows elevated cytoplasmic

Ca2+ level compare to SD at P30 (Fig1). Therefore, after registering a free cytosolic Ca^{2+} increase, we decided to dissect the sources of such overload and performed experiments in which we tested the expression of Ca^{2+}signaling proteins specific for different compartments of photoreceptor cells

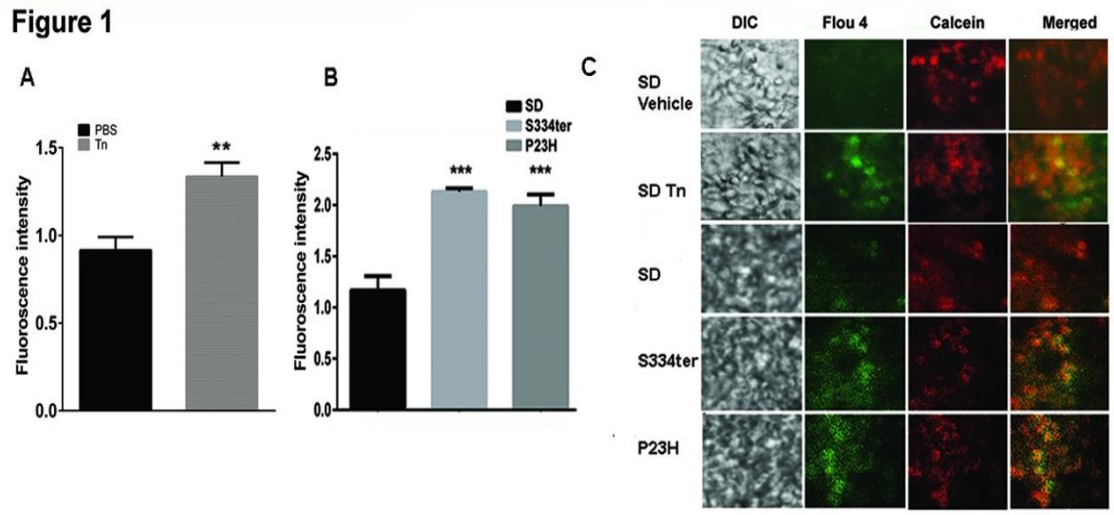

Figure 1. The Ca^{2+} cytosolic increase is detected in SD rat retinas injected with tunicamycin and in ADRP S334ter and P23H RHO rat retinas (N=4). **A**. A measurement of the fluorescent intensity in viable photoreceptors of SD retinas injected with Tn. Means of 45.78 ± 3.801 (N=5) and 66.79 ± 3.967 (N=5) were found by using the image J program and t-test. B. A measurement of the fluorescent intensity in viable photoreceptors of S334ter and P23H RHO rats (N=4). Means of 2.13 ± 0.032 and 1.99 ± 0.113 ($P< 0.001$ for both) were found by one-way Anova in S334ter and P23H Rho retinas, respectively, compared to SD retinas (1.16 ± 0.138). Data are shown as means ± SEM. **B**. Images of SD photoreceptors treated with Tn and vehicle (two upper panels) and naïve SD, S334ter and P23H RHO photoreceptors up-taking the Flou 4 AM dye. The isolated retinas were incubated in a mixture of the Flou4AM detecting free cytosolic Ca^{2+} and the calcein AM detecting viable photoreceptor cells.

Increased free cytosolic Ca^{2+} is linked to the over-expression of ER-membrane Ca^{2+}-channels and cytosolic Ca^{2+}signaling proteins. The diffuse accumulation of the cGMP and S334ter and P23H RHO rats has been previously shown in the ONL of the retina, suggesting a Ca^{2+} increase in S334ter and P23H RHO photoreceptors (14). The VGCC expression is known to reflect the modulation in Ca^{2+} concentration (23) so we tested the level of VGCC protein expression by western blot analysis and found no difference between control and experimental groups. These data suggested that the Ca^{2+} increase registered in transgenic photoreceptors is not generated by VGCC malfunctioning. Keeping that in mind, we then tested whether the source of the Ca^{2+} elevations was from intracellular compartments by measuring the expression levels of the cytosolic Ca^{2+} signaling proteins calpastatin and calcineurin, the ER resident calreticulin, and the mitochondrial VDAC protein.

The expression of cytosolic calpastatin (CAST), a Ca^{2+}-dependent cysteine protease inhibitor of calpains, was up-regulated in the retinas of both transgenic models. Both mRNA and protein levels were increased at P21 (Fig. 2A and B, Table S3 and S4). However, the highest upregulation in *Cast* mRNA and protein levels were found in P23H Rho retinas. Interestingly, the CAST overexpression in this experiment tightly correlated with previously detected calpain activity in these animals at P21 and P30 (1, 2), confirming calpain-mediated signaling in these retinas. In addition, cytosolic calcineurin (CN), a Ca^{2+}- and calmodulin-dependent serine-threonine phosphatase was also upregulated in the retinas of both transgenic models at P30 (Fig. 2C and Table S3 and S4). Increases in

calcium dependent calpastatin and calcineurin protein expression in ADRP retinas further serve as an additional evidence of cytoplasmic calcium overload.

Next, we analyzed the expression of the mitochondrial VDAC, a multifunctional protein know to participate in ER-mitochondria cross-talk, the transport of ROS, ATP, Ca^{2+}, metabolites, and apoptosis(24) and found that VDAC mRNA was significantly higher in both transgenic retinas at P21 and P30 (Fig. 2D and Table S3). The elevation of VDAC expression was then confirmed by immunohistochemical analysis of retinal cryostat sections treated with anti-VDAC antibody at P30 (Fig 2E). This analysis demonstrated an increase in the VDAC protein in both S334ter and P23H RHO inner segments of photoreceptors pointing out the perturbance in mitochondrial homeostasis these data support our previous finding of mitochondria-mediated apoptotic photoreceptor cell death in these animals.

The ER resident Ca^{2+} binding protein calreticulin (CRN) is known to be sensitive to changes in the concentration of Ca^{2+} in the ER lumen. For example, it has been demonstrated that its promoter encompassing 115-260 and 685-1736 regions and containing the CCAAT nucleotide motif is believed to be activated in response to Ca^{2+} depletion by increasing mRNA levels (25). Therefore, knowing about a persistently activated UPR, we were not surprised to learn that the *Crn* mRNA was dramatically (over 2-fold) elevated in both transgenic retinas at P21 and (over 4-fold) in S334ter retinas at P40 (Fig. 2F and Table S3). Interestingly, the CRN protein level was not elevated in these retinas.

To verify the ER's involvement in the elevation of free cytosolic Ca^{2+} (Fig.1), we analyzed the expression of ER resident Ca^{2+} sensing receptor proteins: phosphorylated (p) inositol

triphosphate receptor IP3R, SERCA2b and Bax inhibitor-1 (BI-1) (Fig. 3 and Tables S3 and S4). *Ip3*r mRNA and pIP3R protein was upregulated at both animal models, suggesting changes in the IP3 channel activity on the ER membrane (Fig. 3B). These changes tightly correlated with the observed elevation of BI-1 (Bax inhibitor-1) mRNA and protein (Fig. 3C and D). In general, BI-1 is known to be an IP3R-interacting protein, enhancing IP3R activity and resulting in lower steady-state Ca^{2+} within the ER (26). Consequently, cells over-expressing BI-1 are known to have a reduced luminal concentration of Ca^{2+} in the ER (27). In the retina, the link between BI-1 and the IP3 has not been demonstrated so far. Therefore, we performed a binding assay, immunoprecipitating IP3R in rat retinal protein extracts and running Western blot analysis for BI-1 (Fig. S1). Our data indicated that BI-1 is a binding partner of IP3R that could upregulate IP3R activity in the retina.

Another ER transmembrane protein, SERCA2b, transfers Ca^{2+} from the cytosol of the cell to the lumen of the ER using energy from ATP hydrolysis. Interestingly *Serca2b* mRNA was elevated in both transgenic retinas at P21 (Fig. 3E), while the SERCA2b protein was observed to diminish (Fig. 3E). Therefore, the abovementioned upregulation of pIP3R and BI-1 and the reduction of the SERCA2b in the ADRP rat models suggests Ca^{2+} dysregulation in the ER and the Ca^{2+} efflux to the cytosol in photoreceptors (Fig. 1).

We next wanted to verify whether induction of the UPR resulted in the modifications of the expression of ER Ca^{2+} channel proteins and the cytosolic Ca^{2+} sensing proteins similar to that shown for ADRP retinas.

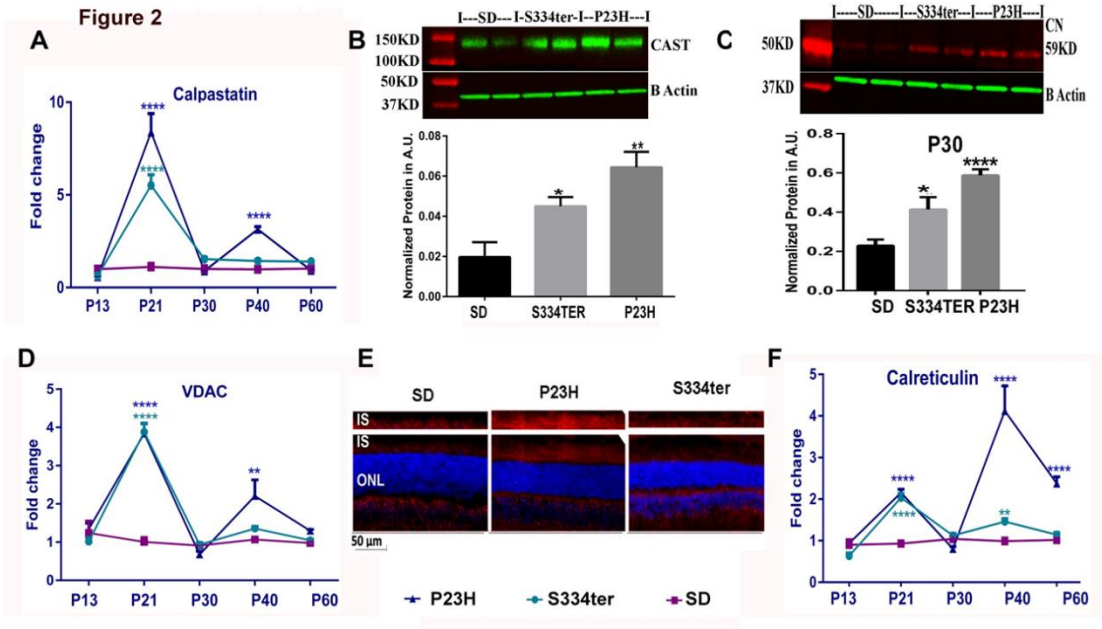

Figure 2 The expression of Ca^{2+}sensing genes and proteins in ADRP retinas measured by qRTPCR (N=4) and western blot (N=4) analyses. A. Analyzing data by two-way anova, calpastatin mRNA expression was found to be upregulated in ADRP retinas at P21 as compared to SD (P<0.0001). The same trend was observed at P40 (P<0.0001). B. Calpastatin protein expression was elevated in ADRP retinas at P21 vs. SD retinas (P < 0.05 and P < 0.01, respectively). C. At P30, both ADRP retinas demonstrated increases in calcineurin (P < 0.05 and P < 0.0001, respectively) compared to controls. D. The *Vdac* mRNA expression was found to be upregulated in both ADRP retinas at P21 (P < 0.0001 for both strains). At P40, only P23H Rho retinas demonstrated changes in *Vdac* mRNA expression as compared to control (P < 0.01). E. Immunohistochemical analysis of ADRP cryostat retinas stained against VDAC protein at P30 revealed an increase in the VDAC expression in the inner segments of photoreceptors. F. Dramatic upregulation in calreticulin expression was found in P21-P60 ADRP retinas (P < 0.0001). Data are shown as means ± SEM. Images of Western blots treated with a correspondent antibody are shown above the graphs for the calculation of individual proteins.

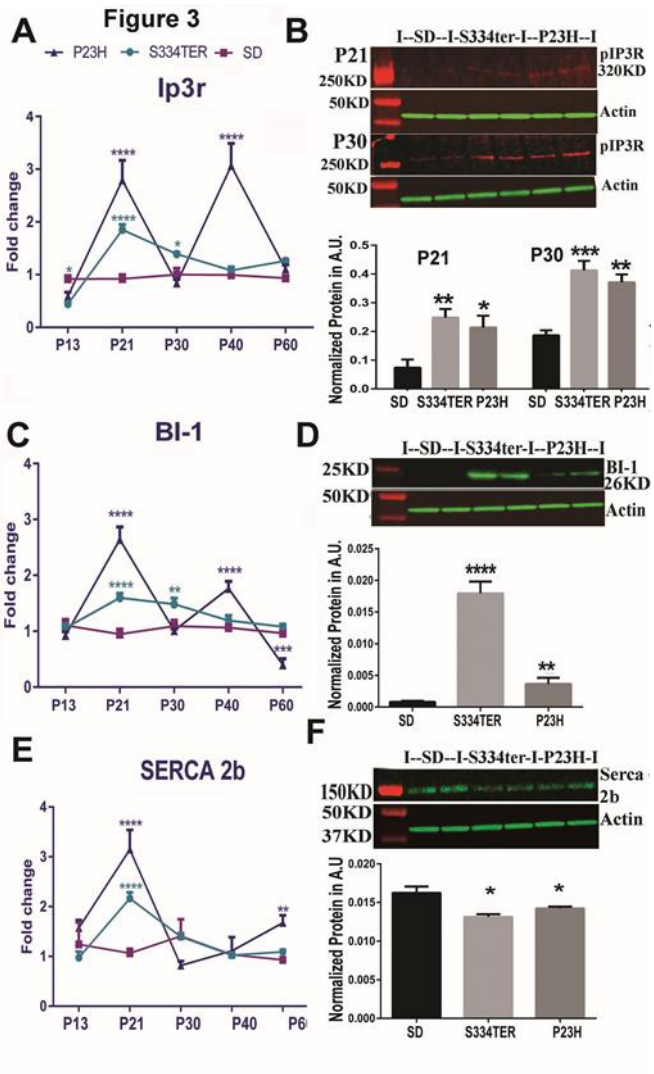

Figure 3. The expression of ER membrane Ca^{2+} channels in ADRP retinas detected by qRT-PCR and western blot analyses (N=4). A. Fold changes in *Ipr3r* mRNA expression in ADRP retinas were observed from P21 to P40 and analyzed by two-way ANOVA. **B**. The pIP3R protein expression in ADRP retinas at P21 and P30. **C.** The *Bi-1* mRNA expression in ADRP retinas from P13 to P60 is shown. **D.** The expression of the BI-1 protein in P21 ADRP retinas. The SS34ter retinas demonstrated a dramatic 56.66-fold over-production of the BI-1 protein compared to P23H Rho retinas, which had a 10-fold increase in BI-1 protein compared to SD ($P < 0.0001$ and $P < 0.01$, respectively). **E** and **F.** Interestingly, the SERCA2b gene and protein expression reflected an opposite pattern of changes. While at P21, the *Serca2b* mRNAs were up-regulated ($P < 0.0001$ for both strains) (E), the SERCA2b protein level was lower in both ADRP rat retinas (F). Data are shown as means ± SEM. Images of Western blots treated with a correspondent antibody are shown above the graphs for the calculation of individual proteins.

UPR activation in WT retinas and photoreceptors induces Ca^{2+} sensing protein expression, resulting in photoreceptor cell death. We isolated photoreceptors from SD retinas and cultured them to study the impact of the treatment with tunicamycin (Tn) on photoreceptor cell death (Fig. 4). First, we confirmed that the cultured retinal cells were not contaminated by other retinal cell types by detecting specific cell markers such as RPE65 (RPE), GNAT2 (cones), Green opsin (cones), Thy1 (ganglion cells) and rhodopsin by semi-quantitative PCR (Fig.4A). Then we tested different concentrations of tunicamycin (Tn) to identify the concentration necessary to induce the UPR in cultured rat photoreceptors and affect cell viability. Previously, we have used Tn and demonstrated that a persistently activated UPR is capable of inducing retinal degeneration (4). Using MTT assay, we measured the intensity of viable photoreceptor cells to identify a correlation between Tn dose and the number of surviving photoreceptors after 48 hr (Fig. 4B). Furthermore we confirmed that 2ug/ml Tn induces photoreceptor cell death within 18 hours which occurs through the upregulation of calpain activity. These results indicated that the ER homeostasis in cultured photoreceptors was compromised, leading to calpain-associated photoreceptor cell death (Fig. 4C).

*S*ubretinal injection with 0.02 μg/eye of Tn in WT retinas also resulted in calpain over-expression measured 4 days after the injection. In addition to calpain, we observed an increase in the pIP3R and the BI-1 proteins (Fig. 4D, E, and F). More surprising, SERCA 2b protein was significantly upregulated (over 8.25-fold) in Tn-treated retinas compared to ADRP retinas, suggesting that at this stage of the UPR, the retinal cells are attempting to recover the balance between Ca^{2+} efflux and influx. In addition, consistent with ADRP retinas, we also observed the upregulation of CN by 1.5-fold in Tn-treated retinas.

Together, these results mimic the situation with a persistently activated UPR in ADRP retinas and provide proof of principle that ER stress in the retina modulates expression of ER membrane Ca^{2+}-regulated proteins resulting in Ca^{2+}-induced calpain activation and Ca^{2+}-facilitated photoreceptor cell death. Therefore, we examined whether ER Ca^{2+} depletion and elevated cytoplasmic Ca^{2+} could reduce retinal function and promote retinal degeneration similar to that observed in ADRP retinas.

Increased cytosolic Ca^{2+} promotes the loss of photoreceptor function in the WT retinas.

Our data with Tn (Fig. 1) showed that injection with Tn results in increase in the cytosolic Ca^{2+} in photoreceptors. Previously, this treatment has been found to induce photoreceptor cell death in the mouse retina (4). In the current study we performed a single subretinal injection with mix of A23187 and thapsigargin (Tg), targeting the SERCA2b activity to create a new experimental rat model of retinal degeneration directly associated with increased cytosolic Ca^{2+} content. A23187, a divalent cation ionophore, is widely used in laboratories to increase intracellular Ca^{2+} in intact cells. The dose of A23187 (0.05μg per eye) was chosen based on a previously published *in vitro* study (28). Tg is a non-competitive inhibitor of the SERCA Ca^{2+} ATPase. Therefore, injecting the SD rat retinas with these drugs would be expected to result in increased cytosolic Ca^{2+}. Retinas were analyzed 2, 4, and 6 weeks after injection by ERG and protein analyses were performed to validate the effect of increased cytosolic Ca^{2+} on photoreceptor function and cellular signaling. All retinal cell types in this model would also be expected to have increased cytosolic Ca^{2+}. However, by registering the photoreceptor-originated scotopic a-wave ERG amplitudes we measured the direct effects of increased cytosolic Ca^{2+} specifically in

rod photoreceptors. Experimental data from Tg and A23187 injected retinas as compared to control retinas are presented in Fig.5A. These data demonstrated that injections led to a sustained decline in the scotopic ERG a- wave amplitudes at 2 and 6 weeks after drug administration (50% and 49%, respectively). This finding suggested that increase in intracellular Ca^{2+} results in retinal functional

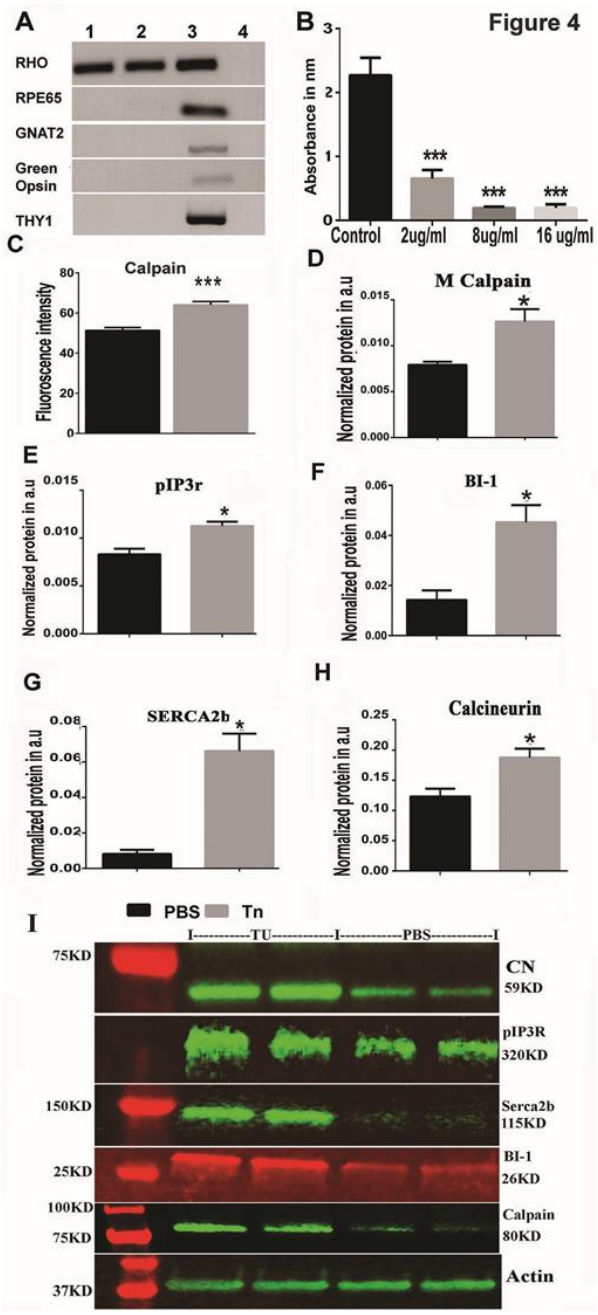

Figure 4. The tunicamycin treatment of primary photoreceptor cultures and the subretinal injection of tunicamycin in SD rats result in cell death by the activation of calpain-induced Ca^{2+}-signaling. **A, B,** and **C.** Primary photoreceptor cultured cells were confirmed to express rod photoreceptor markers such as rhodopsin (lines 1 and 2) and to lack cone and ganglia cell markers such as GNAT2 and Thy1 compared to whole retinal cell lysate (line 3) and negative controls (line 4) (A). **B.** Different concentrations of Tn were used to verify a dose of Tn at which a rod cell viability would be compromised measured by MTT assay (N=6). The read absorbance correlated with viable cells. **C**. The dose of 2 μg/ml Tn was used to test whether calpain activation occurred in Tn-treated rod photoreceptor cells

(N=3). Increase in calpain activity was found 18 hours after treatment with Tn ($P < 0.01$). **D, E, F, G, H** and **I** (N=4). The dose of 0.02 μg of Tn per eye was used to inject SD retinas and then rat retinas were analyzed 4 days after injection ($P < 0.05$ for all analyzed proteins compared to PBS injection). **D.** The Tn injection resulted in the elevation of the calpain level. **E.** Additionally, an increase in the IP3R protein level was associated with Tn injection vs PBS-injected retinas. **F**. This increase was in agreement with the elevated BI-1 protein and was opposite to the result of concomitant elevation of SERCA2b compared to PBS-treated retinas **(G). H.** Interestingly, the calcineurin protein level was also significantly increased in Tn-injected retinas. **I.** Images of Western blots treated with correspondent antibodies are shown. Data are shown as means ± SEM. Images of Western blots treated with a correspondent antibody are shown above the graphs for the calculation of individual proteins.

loss. The B-wave amplitude also declined in this model by 39% and 47% at 2 and 6 weeks, respectively.

To verify whether the decline in photoreceptor function was associated with photoreceptor cell loss, we further performed a histological analysis in which we stained retinal sections with H&E (Fig. 5B and C). The number of photoreceptor nuclei in drug-treated retinas was 36% lower than in vehicle treated retinas ($P<0.05$), suggesting that injections with A23187 and Tg resulted in Ca^{2+}-induced retinal degeneration in the experimental rat model.

To characterize the experimental rat model of retinal degeneration, we harvested injected (A23187 + Tg) retinas 36 hr. postinjection and attempted to highlight the cellular signaling involved in photoreceptor cell loss (Fig. 5D, E, F, and G). We found that injection with drugs resulted in a 43% up-regulation of calpain activity and 2.85-fold increase in calcineurin expression at 36 hours postinjection. Further we tested downstream calpain-activated target CDK5 and found that the CDK5 level was significantly higher in A23187+Tg– injected retinas than vehicle-injected retinas, pointing out the potential phosphorylation of the MEKK1 and activation of the JNK apoptotic pathway(29). To

validate this hypothesis, we tested the pJNK level and demonstrated that pJNK protein expression was 77% higher in drug-injected retinas. Altogether, these data indicate that the apoptotic pathway was elevated in treated retinas. Therefore, we then verified caspase-3/7 activity and found almost a 9-fold elevation of the caspase-3/7 activity in retinal extract treated with drugs. Our data demonstrated that subretinal injection with a drug mixture (A23187+Tg) in rats results in Ca^{2+}-induced retinal degeneration via upregulation of calpain-mediated cell death

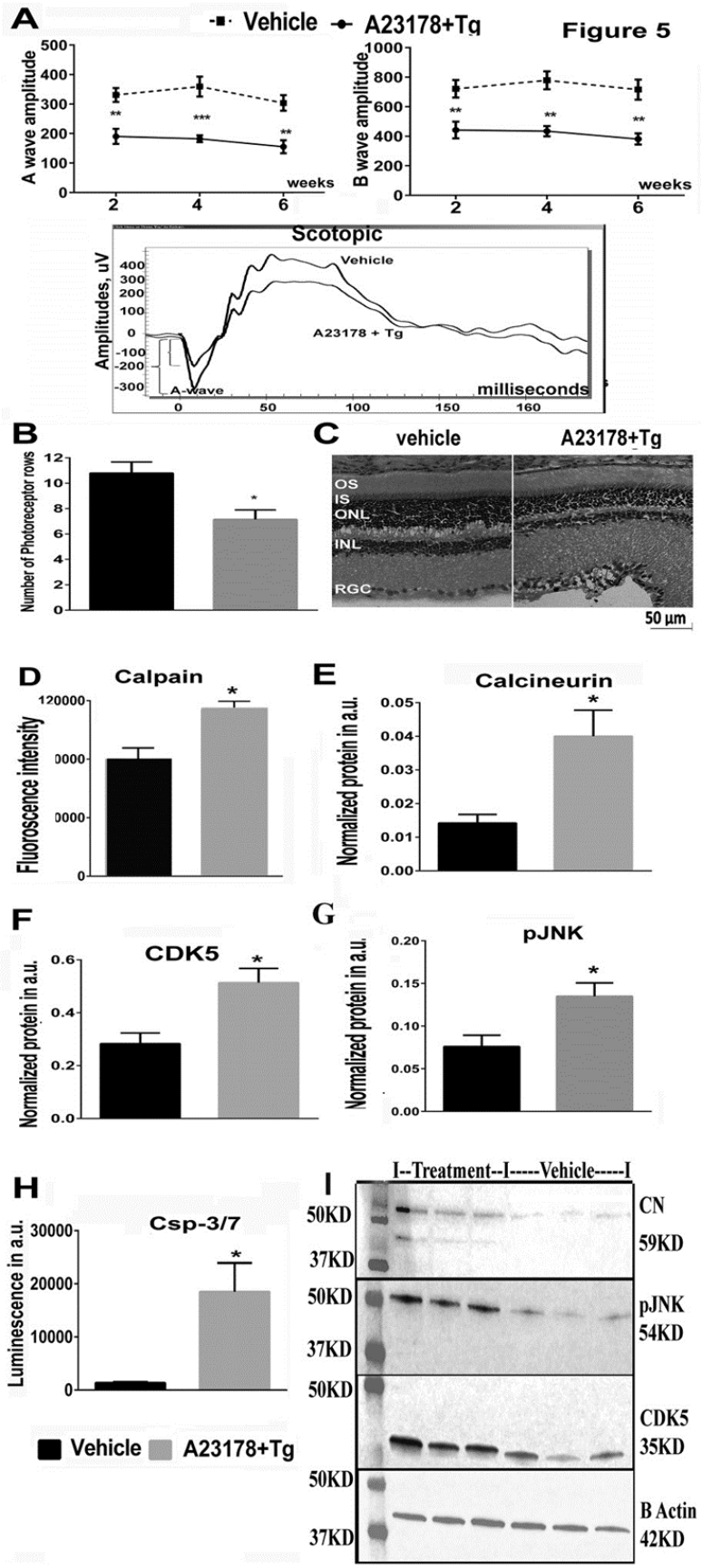
A
Vehicle
A23178+Tg
Figure 5
A wave amplitude
B wave amplitude
weeks
Scotopic
Amplitudes, uV
Vehicle
A23178 + Tg
A-wave
milliseconds
B
Number of Photoreceptor rows
C
vehicle
A23178+Tg
OS
IS
ONL
INL
RGC
50 µm
D
Calpain
Fluoroscence intensity
E
Calcineurin
Normalized protein in a.u.
F
CDK5
Normalized protein in a.u.
G
pJNK
Normalized protein in a.u.
H
Csp-3/7
Luminescence in a.u.
Vehicle
A23178+Tg
I
I--Treatment--I-----Vehicle-----I
50KD
37KD
CN
59KD
pJNK
54KD
CDK5
35KD
B Actin
42KD

Figure 5. Subretinal injection of the combined A23178 and Tg drugs promotes retinal degeneration via Ca^{2+}-mediated calpain activation. A: Scotopic ERG analysis was shown at 10 dB (25 cd*s/m^2). Analyzing by two-way anova, reduction of the a-wave amplitudes was observed at 2, 4 and 6 weeks postinjection, compared to vehicle-treated retinas ($P < 0.01$, $P < 0.001$, and $P < 0.01$, respectively) (N=4). The b-wave was also diminished compared to control-injected retinas ($P < 0.01$ for all time points) (N=4). Bottom: Images of the scotopic ERG amplitudes registered at 10 dB in two groups of animals are shown. B. Subretinal injection of the combined A23187+Tg results in photoreceptor cell loss (N=4). C. Images of H&E stained retinal cryosections injected with drugs and vehicle. D-H. Protein expression and activity assay performed 36 hr posttreatment (for all $P<0.05$) (N=4). I. Images of Western blots treated with correspondent antibodies are shown. B-actin served as a loading control. Data are shown as mean ± S.E.M.

Discussion

The presence of a Ca^{2+} overload in the nerve fiber layer (NFL) and the inner nuclear layer (INL) in P23H RHO rat retinas (line 1) has been reported recently (30). However, indirect indications of increased intracellular Ca^{2+} in degenerating S334ter and P23H RHO photoreceptors have been provided only by the therapeutic modulation of Ca^{2+} blockers or inhibitors in their retinas (21, 22). Our study is the first molecular genetic evidence demonstrating that in the retina of rat models of ADRP, ER Ca^{2+} depletion contributes to the mechanism of retinal degeneration. In our study, we first demonstrated an increase in intracellular Ca^{2+} during the ADRP progression in photoreceptors and linked this increase to a persistently activated UPR-induced ER Ca^{2+} depletion. Thus, we found that the modified expression of ER membrane Ca^{2+} channels and resident buffering proteins is associated with increased cytoplasmic Ca^{2+} and an elevation of mitochondrial VDAC, regulating the Ca^{2+} flow from the ER to mitochondria in ADRP photoreceptors. These events are in agreement with a previously reported cytochrome *C* and AIF1 release from the mitochondria in S334ter and P23H RHO retinas (1, 2, 31).

Both the S334ter and P23H RHO rats demonstrate the activation of the UPR at P21 and P30 (2, 30). Interestingly, although the rate of retinal degeneration in these two ADRP models differs, the level of the cytosolic Ca^{2+} increase in the P30 photoreceptors is similar. This suggests that the source of elevated intracellular Ca^{2+} in photoreceptors could be a result of malfunctioning ER in which modified expressions of the Ca^{2+} sensing

genes and proteins (pIP3R, BI-1, calreticullin) result in extensive Ca^{2+} outflow from ER lumen. It is worth mentioning here that if for the pIP3R and BI-1 both the mRNA and the protein level were upregulated, the calreticulin protein was not altered as compared to elevated *Crn* mRNA. Perhaps, discrepancy in a gene and protein expression in both groups can be easily explained by the recently reported correlation between the CRN over-production and the Ca^{2+} over-load within the ER. Thus, Michalak et al. has found that 50% of all Ca^{2+} stored in the ER binds to CRN, and therefore, CRN protein over-production indicates an elevation in the ER luminal Ca^{2+}(36). Moreover, Waser et al. have demonstrated that over-expression of *Crn* mRNA is a sign of ER Ca^{2+} depletion (25). Therefore, up-regulation of *Crn* mRNA expression and unaltered protein production indicate ER Ca^{2+} reduction in both ADRP retinas.

Concomitantly with activated UPR and upregulated calpain activity have been previously shown (1, 2, 31), in this study, we observed the upregulation of calpastatin and calcineurin levels. In general, CN is known to regulate the activity of AKT through dephosphorylation in degenerating retinas (23). Therefore, we were not surprised to observe a dramatic increase in the CN protein in P30 P23H Rho retinas that are known to experience an essential decrease in phosphorylated AKT and consequent up-regulation of mTOR signaling (1). All these data highlight a cellular defense mechanism activated in photoreceptors from P21 to P40 that is trying to cope with a launched mechanism of photoreceptor degeneration. However, the strength of such signaling seems to be insufficient to block Ca^{2+}-induced calpain activation and, consequently, intracellular Ca^{2+} affects the mitochondrial homeostasis in these animals. As proof of this hypothesis,

the observed VDAC elevation indicates a disrupted molecule flux across the outer mitochondrial membrane and suggests cross talk between these two organelles.

Next, we were interested in testing whether sustained UPR activation is capable of triggering photoreceptor cell death via Ca^{2+}-induced signaling. We have previously tested Tn *in vivo* and have demonstrated the activation of the UPR induces retinal degeneration in mouse retinas (4). In this study, we demonstrated sustained UPR-induced cytotoxicity in a primary photoreceptor culture and *in vivo* and analyzed a signaling responsible for cell loss. Both *in vitro* and *in vivo,* Tn induces a calpain activation that is associated with disrupted ER Ca^{2+} sensing receptor expression. This implies that UPR-induced photoreceptor cell death occurs via Ca^{2+} efflux from ER lumen and Ca^{2+}-mediated calpain signaling. However, in order to obtain direct evidence that the intracellular Ca^{2+} increase induced by persistently activated UPR in photoreceptors as seen in Fig. 1 promotes retinal degeneration we created an experimental rat model of Ca^{2+}-induced retinal degeneration.

Subretinal injection of the combined A23187 and Tg drugs triggers Ca^{2+}-induced photoreceptor cell death. The rod-derived a-wave amplitude of the scotopic ERG was significantly downregulated. In this model, the functional loss of photoreceptors is in agreement with a number of dying cells. Therefore, the findings from these experiments permit us to conclude that we created an experimental model of retinal degeneration triggered by Ca^{2+}-induced cytotoxicity. The experimental model mimics the inherited retinal degeneration occurring in rats, not only by the reduction of the scotopic ERG amplitudes and photoreceptor cell death, but also by the mechanism responsible for apoptotic photoreceptor cell death found in ADRP rat retinas. Perhaps the Ca^{2+}-calpain-

CDK5-JNK caspase-3/7 signaling activated by the injection of the mixture of A23187 and Tg is not the only mechanism by which the execution of photoreceptor cell death occurs. However, the fact of activated calpain suggests that this signaling also triggers apoptotic cell death. It also implies that a future experiment with photoreceptor-specific knockout or the overexpression of calpain is necessary to understand the role of calpain-activation in retinal degeneration. Despite existing limitations, such as the cell specificity of responses to drug injection in the retina, the importance of experimental models for the field of retinal cell biology can be appreciated by applying genetically modified animals with the modified expression of Ca^{2+} sensing genes involved in neurodegeneration.

Therefore, our study revealed the involvement of Ca^{2+}-activated cellular signaling in ADRP progression and indicated that manipulation with ER channels SERCA2b, IP3R, calpain, calpastatin, and CDK5 expression during the UPR-induced cytosolic Ca^{2+} increase might be beneficial for patients with retinal degeneration. As UPR and Ca^{2+} driven cell death mechanisms have been observed in several retinal dystrophies (37), the proposed therapeutic targets could be tested to treat these retinal degenerations.

Acknowledgement

This work was supported by the National Institute of Health Grant RO1EY020905 and VSRC Core Grant P30 EY003039

References

1. Sizova OS, Shinde VM, Lenox AR, Gorbatyuk MS. Modulation of cellular signaling pathways in P23H rhodopsin photoreceptors. Cellular signalling. 2014 Apr;26(4):665-72. PubMed PMID: 24378535. Pubmed Central PMCID: 4083739.

2. Shinde VM, Sizova OS, Lin JH, LaVail MM, Gorbatyuk MS. ER stress in retinal degeneration in S334ter Rho rats. PloS one. 2012;7(3):e33266. PubMed PMID: 22432009. Pubmed Central PMCID: 3303830.

3. Kaur J, Mencl S, Sahaboglu A, Farinelli P, van Veen T, Zrenner E, et al. Calpain and PARP activation during photoreceptor cell death in P23H and S334ter rhodopsin mutant rats. PloS one. 2011;6(7):e22181. PubMed PMID 21765948. Pubmed Central PMCID: 3134478.

4. Rana T, Shinde VM, Starr CR, Kruglov AA, Boitet ER, Kotla P, et al. An activated unfolded protein response promotes retinal degeneration and triggers an inflammatory response in the mouse retina. Cell death & disease 2014;5:e1578. PubMed PMID: 25522272.

5. Mekahli D, Bultynck G, Parys JB, De Smedt H, Missiaen L. Endoplasmic-reticulum calcium depletion and disease. Cold Spring Harbor perspectives in biology. 2011 Jun;3(6). PubMed PMID: 21441595. Pubmed Central PMCID: 3098671.

6.Bravo R, Parra V, Gatica D, Rodriguez AE, Torrealba N, Paredes F, et al. Endoplasmic reticulum and the unfolded protein response: dynamics and metabolic integration. International review of cell and molecular biology. 2013;301:215- 90. PubMed PMID: 23317820. Pubmed Central PMCID: 3666557.

7. Kaufman RJ, Malhotra JD. Calcium trafficking integrates endoplasmic reticulum function with mitochondrial bioenergetics. Biochimica et biophysica acta. 2014 Oct;1843(10):2233-9. PubMed PMID: 24690484.

8. Mallilankaraman K, Cardenas C, Doonan PJ, Chandramoorthy HC, Irrinki KM, Golenar T, et al. MCUR1 is an essential component of mitochondrial Ca2+ uptake that regulates cellular metabolism. Nature cell biology. 2012 Dec;14(12):1336-43. PubMed PMID: 23178883. Pubmed Central PMCID: 3511605.

9. Mallilankaraman K, Doonan P, Cardenas C, Chandramoorthy HC, Muller M, Miller R, et al. MICU1 is an essential gatekeeper for MCU-mediated mitochondrial Ca(2+) uptake that regulates cell survival. Cell. 2012 Oct 26;151(3):630-44. PubMed PMID: 23101630. Pubmed Central PMCID: 3486697.

10. Sancak Y, Markhard AL, Kitami T, Kovacs-Bogdan E, Kamer KJ, Udeshi ND, et al. EMRE is an essential component of the mitochondrial calcium uniporter complex.

Science. 2013 Dec 13;342(6164):1379-82. PubMed PMID: 24231807. Pubmed Central PMCID: 4091629.

11. Krizaj D. Calcium stores in vertebrate photoreceptors. Advances in experimental medicine and biology. 2012;740:873-89. PubMed PMID: 22453974. Pubmed Central PMCID: 3370389.

12. Molnar T, Barabas P, Birnbaumer L, Punzo C, Kefalov V, Krizaj D. Store-operated channels regulate intracellular calcium in mammalian rods. The Journal of physiology. 2012 Aug 1;590(Pt 15):3465-81. PubMed PMID: 22674725. Pubmed Central PMCID: 3547263.

13. Hoppe UC. Mitochondrial calcium channels. FEBS letters. 2010 May 17;584(10):1975-81. PubMed PMID: 20388514.

14. Arango-Gonzalez B, Trifunovic D, Sahaboglu A, Kranz K, Michalakis S, Farinelli P, et al. Identification of a common non-apoptotic cell death mechanism in hereditary retinal degeneration. PloS one. 2014;9(11):e112142. PubMed PMID:

25392995. Pubmed Central PMCID: 4230983.

15. Barabas P, Cutler Peck C, Krizaj D. Do calcium channel blockers rescue dying photoreceptors in the Pde6b (rd1) mouse? Advances in experimental medicine and biology. 2010;664:491-9. PubMed PMID: 20238051. Pubmed Central PMCID: 2921874.

16.Paquet-Durand F, Sanges D, McCall J, Silva J, van Veen T, Marigo V, et al. Photoreceptor rescue and toxicity induced by different calpain inhibitors. Journal of neurochemistry. 2010 Nov;115(4):930-40. PubMed PMID: 20807308.

17. Sanges D, Comitato A, Tammaro R, Marigo V. Apoptosis in retinal degeneration involves cross-talk between apoptosis-inducing factor (AIF) and caspase-12 and is blocked by calpain inhibitors. Proceedings of the National Academy of Sciences of the United States of America. 2006 Nov 14;103(46):17366-71. PubMed PMID: 17088543. Pubmed Central PMCID: 1859935.

18.Ozaki T, Nakazawa M, Yamashita T, Sorimachi H, Hata S, Tomita H, et al. Intravitreal injection or topical eye-drop application of a mu-calpain C2L domain peptide protects against photoreceptor cell death in Royal College of Surgeons' rats, a model of retinitis pigmentosa. Biochimica et biophysica acta. 2012 Nov;1822(11):1783-95. PubMed PMID: 228851

19. Sorimachi H, Ono Y. Regulation and physiological roles of the calpain system in muscular disorders. Cardiovascular research. 2012 Oct 1;96(1):11-22. PubMed PMID: 22542715. Pubmed Central PMCID: 3444232.

20. Krizaj D, Copenhagen DR. Calcium regulation in photoreceptors. Frontiers in bioscience : a journal and virtual library. 2002 Sep 1;7:d2023-44. PubMed PMID: 12161344. Pubmed Central PMCID: 1995662.

21. Ozaki T, Ishiguro S, Hirano S, Baba A, Yamashita T, Tomita H, et al. Inhibitory peptide of mitochondrial mu- calpain protects against photoreceptor degeneration in rhodopsin transgenic S334ter and P23H rats. PloS one 2013;8(8):e71650. PubMed PMID: 23951212. Pubmed Central PMCID: 3739725.

22.Bush RA, Kononen L, Machida S, Sieving PA. The effect of calcium channel blocker diltiazem on photoreceptor degeneration in the rhodopsin Pro213His rat. Investigative ophthalmology & visual science. 2000 Aug;41(9):2697-701. PubMed PMID: 10937585.

23. Park CH, Kim YS, Kim YH, Choi MY, Yoo JM, Kang SS, et al. Calcineurin mediates AKT dephosphorylation in the ischemic rat retina. Brain research. 2008 Oct 9;1234:148-57. PubMed PMID: 18703031.

24.Shoshan-Barmatz V, Ben-Hail D. VDAC, a multi-functional mitochondrial protein as a pharmacological target. Mitochondrion. 2012 Jan;12(1):24-34. PubMed PMID: 21530686.

25. Waser M, Mesaeli N, Spencer C, Michalak M. Regulation of calreticulin gene expression by calcium. The Journal of cell biology. 1997 Aug 11;138(3):547-57. PubMed PMID: 9245785. Pubmed Central PMCID: 2141645.

26. Michalak M, Groenendyk J, Szabo E, Gold LI, Opas M. Calreticulin, a multi-process calcium-buffering chaperone of the endoplasmic reticulum. The Biochemical journal. 2009 Feb 1;417(3):651-66. PubMed PMID: 19133842.

27. Kiviluoto S, Schneider L, Luyten T, Vervliet T, Missiaen L, De Smedt H, et al. Bax inhibitor-1 is a novel IP(3) receptor-interacting and -sensitizing protein. Cell death & disease. 2012;3:e367. PubMed PMID: 22875004. Pubmed Central PMCID: 3434651.

28.Sano R, Reed JC. ER stress-induced cell death mechanisms. Biochimica et biophysica acta. 2013 Dec;1833(12):3460-70. PubMed PMID: 23850759. Pubmed Central PMCID: 3834229.

29. Przygodzki T, Sokal A, Bryszewska M. Calcium ionophore A23187 action on cardiac myocytes is accompanied by enhanced production of reactive oxygen species. Biochimica et biophysica acta. 2005 Jun 10;1740(3):481-8. PubMed PMID: 15949718.

30. Kang MJ, Chung J, Ryoo HD. CDK5 and MEKK1 mediate pro-apoptotic signalling following endoplasmic reticulum stress in an autosomal dominant retinitis pigmentosa model. Nature cell biology. 2012 Apr;14(4):409-15. PubMed PMID: 22388889. Pubmed Central PMCID: 3319494.

31.Caminos E, Vaquero CF, Martinez-Galan JR. Relationship between rat retinal degeneration and potassium channel KCNQ5 expression. Experimental eye research. 2015 Feb;131:1-11. PubMed PMID: 25499209.

32. Gorbatyuk MS, Knox T, LaVail MM, Gorbatyuk OS, Noorwez SM, Hauswirth WW, et al. Restoration of visual function in P23H rhodopsin transgenic rats by gene delivery of

BiP/Grp78. Proceedings of the National Academy of Sciences of the United States of America. 2010 Mar 30;107(13):5961-6. PubMed PMID: 20231467. Pubmed Central PMCID: 2851865.

33. Sitaramayya A. Soluble guanylate cyclases in the retina. Molecular and cellular biochemistry. 2002 Jan;230(1-2):177-86. PubMed PMID: 11952093.

34.Blute TA, Velasco P, Eldred WD. Functional localization of soluble guanylate cyclase in turtle retina: modulation of cGMP by nitric oxide donors. Visual neuroscience. 1998 May-Jun;15(3):485-98. PubMed PMID: 9685201.

35. Ahmad I, Barnstable CJ. Differential laminar expression of particulate and soluble guanylate cyclase genes in rat retina. Experimental eye research. 1993 Jan;56(1):51-62. PubMed PMID: 8094339.

36. Saini AS, Shenoy GN, Rath S, Bal V, George A. Inducible nitric oxide synthase is a major intermediate in signaling pathways for the survival of plasma cells. Nature immunology. 2014 Mar;15(3):275-82. PubMed PMID: 24441790.

37. Gorbatyuk M, Gorbatyuk O. Review: retinal degeneration: focus on the unfolded protein response. Molecular vision. 2013;19:1985-98. PubMed PMID: 24068865. Pubmed Central PMCID: 3782367.

Conclusion and Discussion

Despite several different genes responsible for Retinitis Pigmentosa phenotype, they all eventually drive photoreceptor cell death and blindness. The number of studies, including ours, are dedicated towards the elucidation of molecular mechanisms causing photoreceptor cell death in autosomal dominant retinitis pigmentosa (ADRP). Although there have been significant advancements in the understanding of discrete molecular pathways culminating in photoreceptor cell death, a detailed investigation towards understanding the sequence, cross-talk and significance of these molecular pathways during specific stages of the disease is missing. In this study we have demonstrated that interplay of several cellular pathways leads to the demise of the photoreceptors in two independent models of ADRP. These findings have revealed several potential therapeutic targets, the modulation of which could potentially prevent ADRP progression. Furthermore, our studies also hint towards putative genes that could be used as diagnostic markers to track the progression of this disease.

Unfolded protein response in S334ter and P23H RHO retinas

Recently, many studies have examined the involvement of unfolded protein response (UPR) in retinal degeneration [1] [2]. In fact, this molecular alteration is a characteristic of the P23H RHO transgenic rats [3]. Another investigation in S334ter RHO transgenic rats has demonstrated that S334ter truncated rhodopsin accumulates in the cytoplasm. Considering the previous finding, we started our investigation by examining the status of UPR and pro-apoptotic gene expression in S334ter- Rho retina at postnatal days (P) 10, 12,

15 and 21. We specifically decided to examine earlier time points as the rate of retinal degeneration is aggressive during the initial period in S334ter RHO retinas.

We analyzed the expression pattern of ER resident chaperon responsible for general protein folding Bip, calnexin, and Hasp40. The expression of all these genes was dramatically altered in S334ter RHO retina, suggesting a high demand for general protein folding in the ER of S334ter RHO retinas. We then went on to examine the expression of additional UPR markers such as IRE1, PERK, ATF6 and CHOP. Expectedly, these markers were also overexpressed at both protein and mRNA levels during ADRP progression. The three UPR arms IRE1, PERK and ATF6 indirectly trigger apoptotic signaling through downstream effector molecule CHOP. We observed most potent up-regulation of these UPR markers at P15 time point, strongly suggesting the activation of UPR in S334ter-RHO rat retinas during this stage of disease progression. In a separate study, we have also demonstrated the activation of UPR in T17M-RHO mice, which is another transgenic mice model of ADRP [4].

In the light of these findings it is clear that UPR could be a key signaling mechanism which drives retinal cell death in the majority of the retinal dystrophies. These studies make UPR pathway an interesting candidate for therapeutic targeting. Considering the fact that prolonged stress on ER activates UPR, an approach which can reduce ER stress and reestablish ER homeostasis could prevent UPR activation. This could be achieved by accelerating the activity of ER chaperons BIP, Calnexin, HSP40 to reduce protein folding stress within the ER lumen and prevent the activation of UPR. Interestingly, in P23H RHO rat, overexpression of BIP has reduced the rate of retinal degeneration [3].

UPR could be modulated by targeting three UPR arms IRE, PERK and ATF6 which drive apoptotic signaling upon activation. Several classes of chemical compounds which can modulate UPR such as IRE alpha inhibitor, ERAD modulator, PERK inhibitors, chaperone modulators and chemical chaperones are available with the evidence of impressive therapeutic efficacy in several pathogenic conditions [5]. Therapeutic efficacy of these chemical UPR modulators has not been tested in retinal dystrophies, and could be an attractive avenue for further investigation for treating retinal dystrophies.

The downstream effector molecule of UPR, CHOP (C/EBP Homologous Protein) plays an important role in ER stress induced apoptosis. In fact, the disruption of CHOP gene has been suggested to be a protective strategy against ER stress induced cell death in diabetes, Alzheimer's disease and cardiac hypertrophy [6-8]. Despite the significant role of CHOP in accelerating apoptosis in several pathogenic conditions, CHOP is necessary for the survival of photoreceptors in ADRP retina and its ablation does not protect retinal degeneration [9]. Considering the vital role of CHOP in photoreceptor survival, a dose dependent modulation of CHOP is necessary for possible therapeutic rescue during retinal degeneration.

Activation of UPR has been demonstrated at P30 in P23H RHO retina [10] and at P15 in S334ter RHO retina. Because UPR tightly regulates several signaling pathways such as autophagy, inflammation, mitochondria dependent apoptosis and calcium signaling [11] [12], we further studied weather UPR activation in S334ter and P23H RHO retina is accompanied by the changes in other cellular pathways.

Modulation of autophagy pathway

Autophagy has been suggested to be pro-survival or pro-apoptotic based on specific cellular context. [13]. Autophagy plays a significant role in several pathological conditions such as cancer, neurodegenerative diseases, and muscle and liver disorders. In S334ter RHO retinas we did not notice any change in the mRNA expression of autophagy associated proteins (except LAMP 2). However, in case of P23H, a robust upregulation in autophagy associated genes ATG5, ATG7, LAMP2 and LC3 was detected during P21- P40 time points. Surprisingly, the protein expression of these proteins did follow the similar dynamics as gene expression in P23H retinas. Rather we found that ATG7 and LAMP2 proteins were downregulated at P30, despite having elevated mRNA levels at these time points. Activation of UPR was observed in P23H RHO at the same time suggesting that the regulation of autophagy is driven by alternative mechanisms and not by UPR.

Downregulation of autophagy- associated proteins drove our study towards the regulators of autophagy and mTOR/AKT pathway – well known negative regulator of autophagy pathway [14]. In P23H RHO retinas, we found elevated mTOR activity at P30, which correlates well with the kinetics of UPR activation. The P30 promises to be the most crucial time point for targeting retinal degeneration, since majority of cellular changes occurred at this time point. As mentioned before, autophagy is able to promote cell survival and consequently, we hypothesized that accelerating autophagy could reduce cellular stress and enhance photoreceptor survival. In order to activate autophagy, we modulated mTOR by intravitreal and intraperitoneal injection of rapamycin (mTOR inhibitor). Inhibition of mTOR in P23H retina resulted in modest reduction in functional decline of photoreceptors. However, we did not find any change in the expression of ATG5, ATG7, LC3 and LAMP2.

This data suggested that autophagy may be regulated by some other regulators than mTOR. Interestingly, only rod photoreceptors responded to this treatment and not cones suggesting that biochemical changes associated with mTOR specifically took place in rod photoreceptors. For targeting autophagy mechanism in P23H retinas a thorough investigation of other regulators of autophagy such as beclin, BCL2 and p53 [14] is necessary.

Role of calcium induced apoptosis in S334ter and P23H RHO retinas

Calcium- induced photoreceptor cell death is another mechanism regulated by UPR [11, 15]. Activated UPR can disturb the calcium homeostasis in ER, cytosol and mitochondria [11]. Since UPR was found to be active in both ADRP models, we decided to measure a cytosolic Ca^{2+} concentration in photoreceptors of S334ter and P23H RHO retinas. To our knowledge this was the first attempt to measure free Ca^{2+} in the photoreceptor by ex vivo retinal imaging. Ex-vivo retinal calcium imaging study demonstrated that in both ADRP rat retinas there is almost a two fold increase in free cytosolic calcium as compared to the control retinas. The calcium homeostasis in photoreceptors is controlled by several calcium channels. These include: cGMP regulated cation channels present on outer segment (OS), voltage gated calcium channels (VGCC) present on cell body and synaptic terminal, store operated calcium entry (SOCE) located on the cell body and intracellular calcium channels present on ER and mitochondria [16, 17]. Due to several possible sources for cytoplasmic Ca^{2+} overload, we extended our study towards understanding the exact source of elevated Ca^{2+} in the photoreceptors of ADRP retina. Through enzyme activity assays and expression pattern of Ca^{2+}channels in ADRP retinas, we observed a marked modulation in ER luminal

and membrane Ca^{2+} sensing proteins suggesting that elevated Ca^{2+} in the cytosol of the photoreceptors could be a result of malfunctioning of ER.

We found a significant upregulation in the IP3R channel activity which releases free calcium from ER to cytoplasm during several stages of retinal degeneration in S334ter and P23H RHO rat retinas. Interestingly, it has been previously suggested that the IP3R channel senses UPR and subsequently alters the calcium signaling to promote neuronal cell death in neurodegenerative diseases [18]. In addition to this, it has been shown that IP3R deficient cells are resistant to apoptosis [19] and robust inhibition of IP3R is an effective strategy for the prevention of the progression of Huntington's disease and atrial fibration [20, 21]. Along with IP3R, we also found a thirty fold overexpression of BI-1 which is known to be an ER membrane calcium channel promoting the release of Ca^{2+} from ER lumen to the cytosol and enhancing IP3R activity [22]. Also, cells overexpressing BI-1 are known to have reduced ER luminal Ca^{2+} concentration [23].

We have also noticed reduced protein expression of SERCA2b in both ADRP retinas, which is present on the ER membrane and transfers free calcium from the cell cytoplasm to the ER lumen at expense of ATP [21]. Interestingly, enhanced SERCA activity was found to be protective against ER stress in few cell types during pathogenic conditions [24] [25] [26]. Also, an approach using the activation of SERCA channel to reduce cytoplasmic calcium concentration has been attempted successfully [27] [28]. Together with ER membrane calcium channels, we have also studied the expression pattern of ER luminal calcium sensor calreticulin. Similar to this, the dramatic upregulation of calreticulin mRNA and unchanged protein levels suggest a definite depletion in the ER luminal Ca^{2+} concentration.

Overall this study has given substantial evidence of ER calcium depletion in S334ter and P23H RHO retinas. Depletion of ER Ca^{2+} is a pathogenic phenomenon which occurs in many diseases [29]. These findings provide a strong rationale for targeting IP3R and SERCA2b Ca^{2+} channels mediated calcium signaling. Inhibiting IP3R activity or accelerating SERCA2b activity will most likely reduce the cytoplasmic Ca^{2+} concentration and prevent the activation of calcium induced apoptotic pathway.

Elevation of cytosolic calcium usually results in the activation of a wide variety of Ca^{2+} sensing enzymes [12]. These enzymes potentiate the apoptotic signaling and recruit the mitochondria in apoptotic events. Calpains and calcineurin are the cytoplasmic targets of Ca^{2+} and both are directly connected to apoptotic events. Activated calpains cleave ER localized procaspases 12 [30] and activated caspases 12 cleaves procaspases 9 and caspase 9 activates the executioner caspase 3 [31]. We found elevated calpain and caspase 12 activity in both the ADRP rat retinas accompanying UPR. We have also demonstrated overexpression of calcineurin, a serine threonine phosphatase, which promotes translocation of proapoptotic protein Bad to the mitochondria. Calpain activation requires very high Ca^{2+} concentration (usually in tens of μM) [32] whereas Ca^{2+} concentration in photoreceptor ranges from 300- 500 μM [33]. Therefore, the activation of calpains together with calcineurin serves as an additional evidence of cytoplasmic calcium overload in S334ter and P23H RHO retinas.

UPR and ER Ca^{2+} depletion link

To demonstrate the existence of an active link between the activation of UPR, ER calcium depletion, and retinal cell death, we have generated two pharmacologically induced retinal degeneration models. In the first induced model, we have performed intravitreal injections

in the wild type (WT) rats with tunicamycin (UPR inducer) and demonstrated that activated UPR drives ER calcium depletion and calcium induced apoptosis. In the second induced model, we injected the WT rats with a combination of calcium ionophore (A23187) and thapsigargin (SERCA2b inhibitor) which induces ER calcium depletion driving photoreceptor cell death. Through these induced models, we have demonstrated that ER calcium depletion and cytoplasmic calcium overload are sufficient to induce retinal cell death, which occurs through calcium induced apoptotic pathway.

Involvement of mitochondria in S334ter and P23H RHO retinal degeneration

Cytoplasmic Ca^{2+} overload and BCL2 family proteins together or individually can affect the mitochondrial function as a result of UPR activation [12]. In a series of experiments, we have shown the modulation in these factors at transcription and translational levels in the ADRP retinas. These factors function to open the mitochondrial permeability transition pore (MPTP) which results in the release of cytochrome c and apoptosis inducing factor (AIF) from mitochondrial membrane to cytosol with further lead to caspase 3 activation. We have demonstrated the release of cytochrome c and AIF in the cytosol of S334ter and P23H RHO retinas. However, further investigation is necessary to determine the exact factor responsible for this event.

Activated calpains can trigger both mitochondrial-independent and mitochondrial-dependent apoptosis [34]. We observed elevated calpain activity in both the ADRP models. Accelerated calpain activity has also been found in few other retinal dystrophies. These events altogether make calpain as an ideal therapeutic candidate to prevent the retinal cell death. Since calpains belong to the family of cysteine proteases, it is necessary to develop specific pharmacological inhibitor of calpains, which will not target generic cysteine

proteases within the cell. However, such pharmacological inhibitors are not available. Germline calpain knockout is known to be embryonically lethal. So generating a photoreceptor specific calpain knockout will be an ideal strategy to examine the feasibility of calpains as a therapeutic target to treat retinal dystrophies.

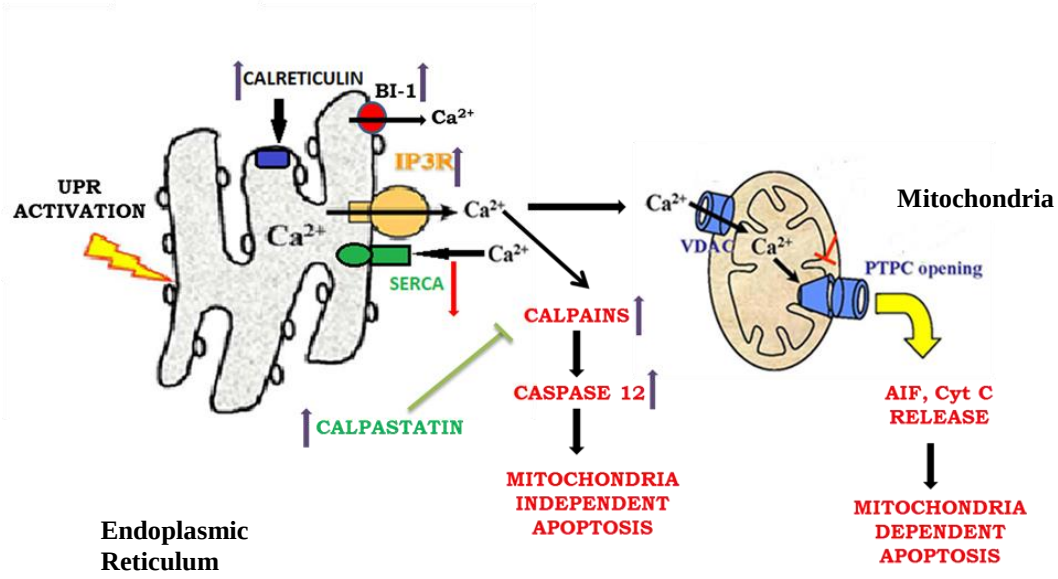

Summary of molecular events during the progression of retinal degeneration in S334ter RHO and P23H RHO retinas.

Significance

While dissecting the cellular changes during the course of retinal degeneration in ADRP retinas, we have successfully demonstrated that UPR, autophagy, mitochondria dependent and independent apoptosis are actively involved in the progression of disease in S334ter and P23H RHO retinas. We have also revealed several potential therapeutic targets which include UPR markers (BIP, CHOP, ATF4, and IRE1 alpha), SERCA2b, IP3R, BI-1, calpain and calreticulin and further investigation is necessary to test the efficacy of the therapy for retinal degeneration with these proteins.

During the investigation, we have successfully developed a novel method to measure the calcium concentration in the photoreceptors of live retina. This method can also be applied to measure the calcium concentration from the remaining retinal cell layers or from the other tissue samples with different types of cell population.

Our study has also successfully generated 2 pharmacologically driven retinal degeneration models including UPR induced retinal degeneration and calcium driven retinal degeneration models. UPR and calcium induced apoptosis are the major contributing factors in several neurodegenerative disorders and several retinal dystrophies. Therefore, these models could be useful to study the exact molecular and biochemical changes during retinal degeneration as well as to test the therapeutic effects of small molecules.

References

1. Ryoo, H.D., et al., Unfolded protein response in a Drosophila model for retinal degeneration. Embo j, 2007. 26(1): p. 242-52.
2. Wu, L.M., et al., [Endoplasmic reticulum stress proteins are activated in rd retinal degeneration]. Zhonghua Yan Ke Za Zhi, 2008. 44(9): p. 807-12.
3. Gorbatyuk, M.S., et al., Restoration of visual function in P23H rhodopsin transgenic rats by gene delivery of BiP/Grp78. Proc Natl Acad Sci U S A, 2010. 107(13): p. 5961-6.
4. Kunte, M.M., et al., ER stress is involved in T17M rhodopsin-induced retinal degeneration. Invest Ophthalmol Vis Sci, 2012. 53(7): p. 3792-800.
5. Hetz, C., E. Chevet, and H.P. Harding, Targeting the unfolded protein response in disease. Nat Rev Drug Discov, 2013. 12(9): p. 703-19.
6. Prasanthi, J.R., et al., Silencing GADD153/CHOP gene expression protects against Alzheimer's disease-like pathology induced by 27-hydroxycholesterol in rabbit hippocampus. PLoS One, 2011. 6(10): p. e26420.
7. Thorp, E., et al., Reduced apoptosis and plaque necrosis in advanced atherosclerotic lesions of Apoe-/- and Ldlr-/- mice lacking CHOP. Cell Metab, 2009. 9(5): p. 474-81.
8. Fu, H.Y., et al., Ablation of C/EBP homologous protein attenuates endoplasmic reticulum-mediated apoptosis and cardiac dysfunction induced by pressure overload. Circulation, 2010. 122(4): p. 361-9.
9. Nashine, S., et al., Ablation of C/EBP homologous protein does not protect T17M RHO mice from retinal degeneration. PLoS One, 2013. 8(4): p. e63205.
10. B'Chir, W., et al., The eIF2alpha/ATF4 pathway is essential for stress-induced autophagy gene expression. Nucleic Acids Res, 2013. 41(16): p. 7683-99.
11. Filadi, R., et al., Endoplasmic Reticulum-mitochondria connections, calcium cross-talk and cell fate: a closer inspection, in Endoplasmic Reticulum Stress in Health and Disease, P. Agostinis and S. Afshin, Editors. 2012, Springer Netherlands. p. 75-106.
12. Schroder, M. and R.J. Kaufman, The mammalian unfolded protein response. Annu Rev Biochem, 2005. 74: p. 739-89.
13. Codogno, P. and A.J. Meijer, Autophagy and signaling: their role in cell survival and cell death. Cell Death Differ, 0000. 12(S2): p. 1509-1518.

14. Yu, L., et al., Termination of autophagy and reformation of lysosomes regulated by mTOR. Nature, 2010. 465(7300): p. 942-6.

15. Peters, L.R. and M. Raghavan, Endoplasmic reticulum calcium depletion impacts chaperone secretion, innate immunity, and phagocytic uptake of cells. J Immunol, 2011. 187(2): p. 919-31.

16. Molnar, T., et al., Store-operated channels regulate intracellular calcium in mammalian rods. J Physiol, 2012. 590(Pt 15): p. 3465-81.

17. Hoppe, U.C., Mitochondrial calcium channels. FEBS Lett, 2010. 584(10): p. 1975-81.

18. Kiviluoto, S., et al., Regulation of inositol 1,4,5-trisphosphate receptors during endoplasmic reticulum stress. Biochim Biophys Acta, 2013. 1833(7): p. 1612-24.

19. Jayaraman, T. and A.R. Marks, T cells deficient in inositol 1,4,5-trisphosphate receptor are resistant to apoptosis. Mol Cell Biol, 1997. 17(6): p. 3005-12.

20. Xiao, J., et al., 2-Aminoethoxydiphenyl borate, a inositol 1,4,5-triphosphate receptor inhibitor, prevents atrial fibrillation. Exp Biol Med (Maywood), 2010. 235(7): p. 862-8.

21. Bauer, P.O., et al., Genetic ablation and chemical inhibition of IP3R1 reduce mutant huntingtin aggregation. Biochem Biophys Res Commun, 2011. 416(1-2): p. 13-7.

22. Kiviluoto, S., et al., Bax inhibitor-1 is a novel IP(3) receptor-interacting and -sensitizing protein. Cell Death Dis, 2012. 3: p. e367.

23. Sano, R. and J.C. Reed, ER stress-induced cell death mechanisms. Biochim Biophys Acta, 2013. 1833(12): p. 3460-70.

24. Park, S.W., et al., Sarco(endo)plasmic reticulum Ca2+-ATPase 2b is a major regulator of endoplasmic reticulum stress and glucose homeostasis in obesity. Proc Natl Acad Sci U S A, 2010. 107(45): p. 19320-5.

25. Fu, S., et al., Aberrant lipid metabolism disrupts calcium homeostasis causing liver endoplasmic reticulum stress in obesity. Nature, 2011. 473(7348): p. 528-31.

26. Zhang, J., et al., Enhanced endoplasmic reticulum SERCA activity by overexpression of hepatic stimulator substance gene prevents hepatic cells from ER stress-induced apoptosis. Am J Physiol Cell Physiol, 2014. 306(3): p. C279-90.

27. Tupling, A.R., M. Asahi, and D.H. MacLennan, Sarcolipin overexpression in rat slow twitch muscle inhibits sarcoplasmic reticulum Ca2+ uptake and impairs contractile function. J Biol Chem, 2002. 277(47): p. 44740-6.

28. Yamasaki-Mann, M. and I. Parker, Enhanced ER Ca2+ store filling by overexpression of SERCA2b promotes IP3-evoked puffs. Cell Calcium, 2011. 50(1): p. 36-41.

29. Mekahli, D., et al., Endoplasmic-reticulum calcium depletion and disease. Cold Spring Harb Perspect Biol, 2011. 3(6).

30. Nakagawa, T. and J. Yuan, Cross-talk between two cysteine protease families. Activation of caspase-12 by calpain in apoptosis. J Cell Biol, 2000. 150(4): p. 887-94.

31. Rao, R.V., et al., Coupling endoplasmic reticulum stress to the cell death program. An Apaf-1-independent intrinsic pathway. J Biol Chem, 2002. 277(24): p. 21836-42.

32. Sorimachi, H. and Y. Ono, Regulation and physiological roles of the calpain system in muscular disorders. Cardiovasc Res, 2012. 96(1): p. 11-22.

33. Krizaj, D. and D.R. Copenhagen, Calcium regulation in photoreceptors. Front Biosci, 2002. 7: p. d2023-44.

34. Takano, J., et al., Calpain mediates excitotoxic DNA fragmentation via mitochondrial pathways in adult brains: evidence from calpastatin mutant mice. J Biol Chem, 2005. 280(16): p. 16175-84.

APPENDIX

INSTITUTIONAL ANIMAL CARE AND USE COMMITTEE APPROVAL

THE UNIVERSITY OF ALABAMA AT BIRMINGHAM

Institutional Animal Care and Use Committee (IACUC)

NOTICE OF APPROVAL

DATE: September 10, 2014

TO: MARINA GORBATYUK, Ph.D.
VH -443
(205) 934-6762

FROM:

Robert A. Kesterson, Ph.D., Chair
Institutional Animal Care and Use Committee (IACUC)

SUBJECT: Title: Gene Therapy for Autosomal Dominant Retinitis Pigmentosa Based on the Over-expression of Molecular Chaperone GRP78
Sponsor: Foundation Fighting Blindness
Animal Project_Number: 141109792

As of November 5, 2014 the animal use proposed in the above referenced application is approved. The University of Alabama at Birmingham Institutional Animal Care and Use Committee (IACUC) approves the use of the following species and number of animals:

Species	Use Category	Number In Category
Rats	A	40
Rats	B	170

Animal use must be renewed by November 4, 2015. Approval from the IACUC must be obtained before implementing any changes or modifications in the approved animal use.

Please keep this record for your files, and forward the attached letter to the appropriate granting agency.

Refer to Animal Protocol Number (APN) 141109792 when ordering animals or in any correspondence with the IACUC or Animal Resources Program (ARP) offices regarding this study. If you have concerns or questions regarding this notice, please call the IACUC office at (205) 934-7692.

Institutional Animal Care and Use Committee (IACUC)
CH19 Suite 403
933 19th Street South
(205) 934-7692
FAX (205) 934-1188

Mailing Address:
CH19 Suite 403
1530 3rd Ave S
Birmingham, AL 35294-0019